SOME DIELECTRIC BREAKDOWN PROPERTIES OF OXYGEN WITH 3.2 cm RADIATION

by

JOHN GEORGE SKINNER

A THESIS

submitted to

OREGON STATE UNIVERSITY

in partial fulfillment of
the requirements for the
degree of

DOCTOR OF PHILOSOPHY

June 1962

APPROVED:

[redacted]

Professor of Physics

In Charge of Major

[redacted]

Chairman of Department of Physics

[redacted]

Chairman of School Graduate Committee

[redacted]

Dean of Graduate School

Date thesis is presented Nov. 28TH, 1961.

Typed by Elaine Anderson

ACKNOWLEDGMENTS

The author wishes to express his gratitude to his research director, Professor James J. Brady, for proposing the problem and for the many enlightening discussions regarding all phases of this work. He would like to thank Dr. E. A. Yunker for his continued interest and support, Dr. D. S. Burch for many interesting discussions concerning the problem, Mr. W. Linder of Boeing Airplane Company for his general assistance, Mr. E. Geller of the Mechanical Engineering Department O.S.U. for his assistance concerning dynamics of gas flow and Mr. J. Darrah for his assistance in taking the data. This work was performed under the auspices of the Antenna and Radomes Unit, Electronic Sciences Section, Boeing Airplane Company.

TABLE OF CONTENTS

TABLE OF FIGURES

SOME DIELECTRIC BREAKDOWN PROPERTIES OF OXYGEN WITH 3.2 cm RADIATION

This thesis consists of two parts. Part one describes the measurement of the net frequency of ionization of oxygen and part two is a study of the effect of a directed gas flow on a microwave discharge in oxygen. Part one was developed from the experimental work of part two and was carried out to help interpret the results of part two.

PART ONE

1) PURPOSE

The purpose of this investigation is to describe what is believed to be a new microwave method for determining the net frequency of ionization and to apply the technique to oxygen gas.

2) INTRODUCTION

The net frequency of ionization is the number of new electrons produced per electron per unit time and is an important parameter in a microwave discharge. It is defined as the time average of the difference between the frequency of ionization ν_i and the frequency of electron attachment ν_a to neutral molecules and atoms. In a certain region of operation the value of $(\nu_i - \nu_a)$ is constant with time and we may write $\nu = \nu_i - \nu_a$. This point is discussed in Section 3e, and for simplicity we will assume here that $(\nu_i - \nu_a)$ is constant with time.

Several experimental methods have been developed

to measure the net frequency of ionization. One of these is due to Herlin and Brown (21) who equated the rate of production of electrons to the rate of loss by diffusion in the limit of zero electron density. Their investigation yielded a new term called the high frequency ionization coefficient $= \nu/DE^2$ (ionization/volt^2), where D is the electron diffusion coefficient and E is the applied electric field. Later MacDonald (30) used Herlin and Brown's published values of the high frequency ionization coefficient for air (23) and determined the net frequency of ionization by using a calculated value of the diffusion coefficient for a given set of conditions.

A similar method was used by Varnerin and Brown (54) for hydrogen; but by using both ac and dc techniques with the same apparatus they were able to experimentally determine and D/μ, where μ is the mobility of the electrons. Their results are expressed in terms of the dc parameter, the first Townsend ionization coefficient. The general method of Herlin and Brown has also been used by MacDonald and Brown with helium (31) and hydrogen (32); also by MacDonald and Matthews with neon-argon mixtures (33).

A different microwave method has been presented by Madan et al (34) in which the time required for the electron density to build up from an initial value of 1 electron/cm^3 to some critical value is measured. The electron density goes through a wide range and the diffusion coefficient changes from free electron diffusion to ambipolar diffusion throughout the experiment. This has to be compensated for in the final results.

The method to be described uses a pulsed microwave source. The net frequency of ionization is determined from the measurement of the rate of change of the formation time of a microwave discharge with the time between pulses, and a knowledge of the rate of decay of the electron density in the afterglow of a microwave discharge. The method is applied to oxygen gas because the net frequency of ionization does not appear to have been determined for this gas by a microwave technique, but the necessary dc parameters are available to enable this value to be calculated for comparison purposes. Furthermore, the loss of electrons in a microwave afterglow in oxygen can be made to be primarily due to electron attachment to neutral molecules and atoms by selecting a suitable range of gas pressure and size

of discharge chamber, the electron decay rate for this process having already been determined by other workers.

3) THEORY

3a Definition of a Microwave Discharge

One of the parameters to be measured in this experiment is the period of time taken for an electron density to build up from some initial value to some convenient large value, the increase in the electron density being produced by an applied microwave signal. It is observed experimentally that when the electron density reaches a critical value the transmitted portion of the incident microwave signal is abruptly attenuated and the reflected signal increased. At this point a microwave discharge is said to have formed. The value of this critical density is dependent upon the frequency of the microwave signal; so the term "discharge" has rather a broad definition. However, since we are concerned only with radiation of 3.19 centimeter wavelength, in this investigation, the term discharge is more restrictive. The reflectivity R from a medium whose refractive index is η' is given by (7, p. 617)

$$R = \frac{|\eta' - 1|^2}{|\eta' + 1|^2} = \frac{(\eta - 1)^2 + \eta^2 x^2}{(\eta + 1)^2 + \eta^2 x^2}$$

where $\eta' = \eta (1 + jX)$ when the refractive index is complex, and X is called the attenuation index. For the "ideal" discharge the value of R is 1; therefore, $\eta' = 0$. In order to evaluate the critical electron density it is necessary to determine the refractive index of a gaseous medium containing a large number of electrons and positive ions. It will be assumed for simplicity that the number of electrons and positive ions are equal so that the net charge in the medium is zero. The refractive index may be evaluated through the relation $[\eta']^2 = \epsilon_c$ where ϵ_c is the complex dielectric constant of the medium.

The dielectric constant of a medium may be determined by considering the "average electron". Following Lorentz (15) the equation of motion of an electron in an applied electric field, $E = E_o \exp(-jwt)$ of angular frequency w, is given by

$$m \frac{d^2x}{dt^2} + m \nu_c \frac{dx}{dt} = - e E$$

where m is the mass of the electron, e is the magnitude of the charge of the electron, x is the electron's displacement and ν_c is the collision frequency between the electrons and the molecules.

Solving this equation for dx / dt we obtain

$$\frac{dx}{dt} = -\frac{eE}{m(\nu_c - jw)}$$

The conductivity σ of the system is given by

$$\sigma = \frac{J}{E} = \frac{-ne}{E}\frac{dx}{dt} = \frac{ne^2(\nu_c + jw)}{m(\nu_c^2 + w^2)} \qquad (1)$$

where J is the current density and n is the electron density. This equation has been derived more generally by Desloge et al (15) from the electron energy distribution function.

From Maxwell's equations we can obtain the one dimensional wave equation

$$\frac{\partial^2 E}{\partial z^2} - \mu\sigma\frac{\partial E}{\partial t} - \mu\epsilon\frac{\partial^2 E}{\partial t^2} = \frac{\partial^2 E}{\partial z^2} + K^2 E = 0 \qquad (2)$$

where $K^2 = jw\mu\sigma + w^2\mu\epsilon = \frac{w^2}{u^2}\left[1 + \frac{j\sigma}{w\epsilon}\right]$

$$= \frac{w^2}{u^2}\epsilon_c \ , \qquad (3)$$

u is equal to $(\mu\epsilon)^{-1/2}$ and is the velocity of the electromagnetic wave in the medium when the conductivity is zero, and ϵ_c is the complex dielectric constant for the ionized medium. Therefore

$$(\eta')^2 = \eta^2(1 + jX)^2 = \epsilon_c = 1 + \frac{j\sigma}{w\epsilon}$$

$$\eta^2(1-X^2)+2j\,\eta^2 X = 1 - \frac{ne^2}{m\epsilon(\nu_c^2+w^2)} + j\,\frac{ne^2\nu_c}{mw\epsilon(\nu_c^2+w^2)} \qquad (4)$$

Equating the real and imaginary parts we can solve for η and X, and hence R. At low gas pressures the collision frequency is small and the complex term may be neglected. The condition for 100% reflection from the medium is then given by

$$n = \frac{m\epsilon(\nu_c^2 + w^2)}{e^2}$$

The critical electron density n_{co} is defined as the value of n evaluated in the limit of zero gas pressure (i.e. the collision frequency term may be ignored) and for a volume of gas in free space (i.e. $\epsilon = \epsilon_o$), therefore

$$n_{co} = \frac{m\epsilon_o w^2}{e^2} = \frac{1.12 \times 10^{13}}{\lambda^2} = 1.1 \times 10^{12}\ \frac{\text{electrons}}{\text{cm}^3}$$

for $\lambda = 3.19$ cm

where λ is the wavelength (cm) of the incident radiation. When the gas is enclosed in a waveguide, the permittivity of the space is given by an effective ϵ and not ϵ_o. The ratio ϵ/ϵ_o may be

expressed as a wavelength ratio by use of the relation

$$\frac{\epsilon}{\epsilon_o} = \frac{\epsilon \mu}{\epsilon_o \mu_o} = \frac{c^2}{u^2} = \frac{\lambda_o^2}{\lambda_g^2}$$

where it is assumed that the permeability μ of the space is the same as that of free space, c and u are the velocities of propagation in free space and in the waveguide respectively, λ_o and λ_g are the wavelengths of the incident radiation in free space and in the waveguide respectively. Therefore, the critical electron density in the limit of zero gas pressure and with the gas enclosed in a waveguide is given by

$$n_c = \frac{1.12 \times 10^{13}}{\lambda_g^2} = 0.56 \times 10^{12} \frac{\text{electrons}}{\text{cm}^3} \text{ for}$$

$$\lambda_g = 4.46 \text{ cm}, \qquad (5)$$

where $\lambda_g = 4.46$ cm is the waveguide wavelength, for the dominant TE_{01} mode of propagation in a standard size X-band waveguide, when $\lambda_o = 3.19$ cm.

A plot of the reflectivity R of a low pressure discharge ($\nu_c \ll w$) as a function of the electron density ratio $r = n/n_c$ is given in Figure 1. It is quite evident that the reflected microwave signal

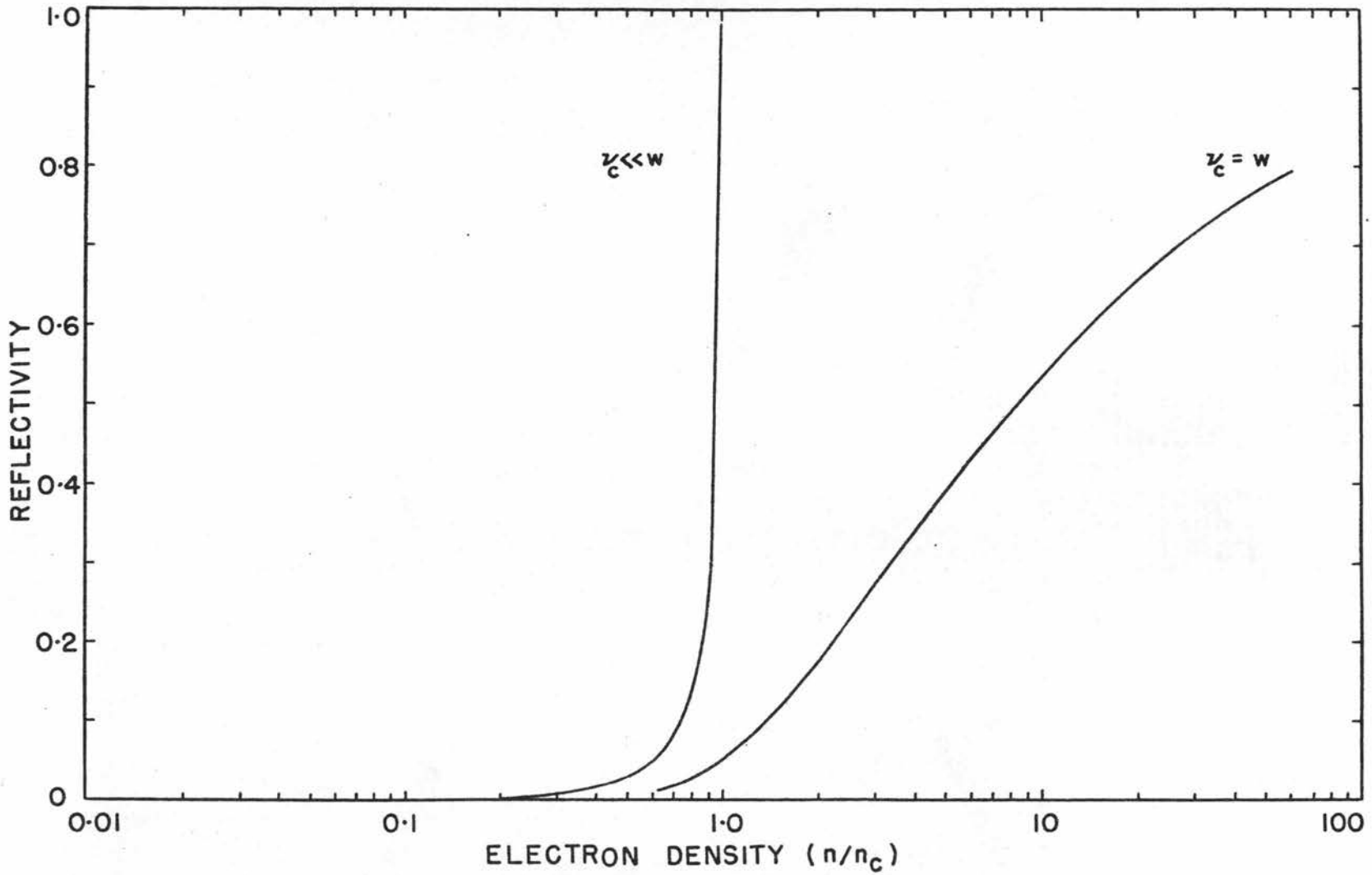

FIGURE 1. REFLECTIVITY — Vs — ELECTRON DENSITY

gives a clear indication when the critical electron density is attained. The effect of increasing the gas pressure is to spread out this "demarcation point". The reflectivity for a gas pressure such that $\nu_c = w$ is also shown in Figure 1. Experimentally it is more convenient to measure the time up to the point where the transmitted microwave signal is abruptly attenuated, rather than the point where the reflection suddenly increases. In the limit of zero gas pressure these two points occur at the electron density n_c. However, the pressures used in this experiment are such that the collision frequency is of the same order of magnitude as the angular frequency of the incident microwaves and, as explained earlier, this causes the "demarcation point" to be spread over a range of electron densities about the value n_c. Therefore the electron density at the point when the time is measured is not necessarily equal to n_c but is some value close to it. For this reason it is convenient to introduce another electron density term n_b which is arbitrarily defined as the electron density at which the transmitted microwave signal is abruptly attenuated. In the limit of zero gas pressure $n_b = n_c$, but at higher pressures it will be slightly different from

n_c. In line with this definition we also define the "formative time" of the discharge as being the period of time from the arrival of the microwave pulse in the discharge region (i.e. the beginning of the microwave pulse on an oscilloscope trace) to the point where the transmitted microwave signal is abruptly attenuated. The microwave power transmitted through the discharge region is attenuated by the factor $\exp(-4\pi\eta \times z/\lambda_g)$, where z is the length of path traversed through the discharge. This point is discussed further in Section 7c, and a plot of the expected attenuation for a given set of conditions is given in Figure 19.

3b. Production of Electrons in a Microwave Discharge

In a microwave discharge secondary electrons are produced by ionizing-collisions between the primary electrons and the gas molecules. The primary electrons, which are usually produced by an external radioactive source, gain their energy from the microwave field by having their normal oscillatory motion changed to a random motion by collisions (9, vol. 22, p. 531).

During the production period of the electrons, electrons are also being "lost" by several mechanisms

which include:

1) Attachment of electrons to neutral atoms and molecules,
2) Recombination of electrons with positive ions,
3) Diffusion of electrons from the discharge region.

In a gas with an electron affinity, such as oxygen, the attachment process is always an important loss mechanism. The recombination process is important when the electron density is large and the electron energy is small. The diffusion loss is, of course, dependent on the size of the discharge chamber and the gas pressure, and by selecting suitable parameters this loss mechanism can be made negligible.

Assuming that only the above mentioned processes are present, then the equation for the rate of change of the electron density is given by

$$\partial n/\partial t = \nu_i n - \nu_a n - \alpha n^2 + \nabla^2 (Dn) \qquad (6)$$

where t is the time parameter during the formation of the discharge and t = 0 is at the beginning of the microwave pulse; n is the electron density; ν_i is the frequency of ionization per electron; ν_a is the frequency of electron attachment to neutral

molecules; α is the recombination rate of electrons and positive ions, and D is the electron diffusion coefficient. By writing the rate of recombination as αn^2, it is assumed that the positive ion density is the same as the electron density. There appears to be very little information concerning the recombination of electrons and ions during the formation of a discharge, and due to the relatively low electron density and the high electron energy it is common practice to neglect this mechanism when the gas molecules have an electron affinity (17, 22, 35).

The frequency of ionization and the frequency of electron attachment may be combined to give the net frequency of ionization, given by $\nu = \nu_i - \nu_a$. Combining the above two factors into Equation 6 gives:

$$\partial n/\partial t = \nu n + \nabla^2 (Dn) \qquad (7)$$

The solution of this equation is dependent upon the boundary conditions and for this case the simplest appropriate geometry is that of two infinite parallel plates separated by a distance d. (NOTE. The actual discharge chamber in this experiment is a section of X-band waveguide. In one case where the diffusion losses are important the cross section of the

waveguide is approximately 2.2 cm x 0.1 cm, and this may certainly be represented by a set of parallel plates to a first approximation. In the other case the cross section is approximately 2.2 cm x 1.0 cm and, although this can be represented by a set of parallel plates of a given separation, it will be shown that the diffusion term is generally negligible and hence the geometry of the container is unimportant.)

The diffusion coefficient D is a slowly varying function of the electron energy and in the case of non-uniform electric fields it should be retained within the ∇^2 sign. However, with the consideration given in the above paragraph the value of D may be considered to be a constant and the term ∇^2 (Dn) may be replaced by D ∇^2 n. For a parallel plate geometry $\nabla^2 n$ can be replaced by $-n/\Lambda^2$, to a first approximation (10, p. 48), where Λ is the characteristic diffusion length given by d/π for a parallel plate geometry. Combining this step into Equation 7 we obtain

$$\partial n/\partial t = \nu n - Dn/\Lambda^2$$

whose solution is given by

$$\frac{1}{t} \ln \frac{n(t)}{n_o} = \nu - \frac{D}{\Lambda^2}$$

where n_o is the initial electron density and n(t) is the density after time t. When n(t) equals the critical electron density n_b, then $t = \tau$ is the formative time of the discharge; therefore

$$\frac{\ln (n_b/n_o)}{\tau p} = \frac{\nu}{p} - \frac{(Dp)}{(p\Lambda)^2} \qquad (8)$$

The equation has been expressed in terms of the proper variables ν/p, Dp and $p\Lambda$ (9, vol. 22, p. 536). Equation 8 is obtained on the assumption that the net frequency of ionization remains constant throughout the formation of the discharge. However, the presence of a large number of electrons, as the electron density approaches n_b, produces an increase in the effective electric field which increases the value of ν . Further consideration is given on this point in Section 7c where it is shown that the effect is negligible.

3c. Electron Loss Mechanisms in the Decay of a Microwave Discharge

When the microwave power is removed from the discharge, the average electron energy falls very rapidly to thermal energy due to the collisions between the electrons and the molecules. The electron density also decays rapidly due to the same loss mechanisms that are present during the formation

of the discharge. The equation for the decay of the electron density is therefore the same as that for the production of electrons except that the ionization term is missing. Thus

$$\partial n/\partial T = - \nu_a n - \alpha n^2 + \nabla^2 (D'n)$$

where T is the time parameter during the decay period of the electron density and T = 0 is at the end of the microwave pulse (i.e. the beginning of the decay period). Note that the value of the diffusion coefficient D' is different from that involved in the formation of the discharge because of the different values of the electron energy. Using the same approximations for $\nabla^2 (D'n)$ as used in Section 3b yields

$$\partial n/\partial T = - \nu_a n - \alpha n^2 - D'n/\Lambda^2 \qquad (9)$$

The recombination term is predominant when the electron density is large but its effect diminishes as the density decreases. Under these conditions Equation 9 becomes

$$\partial n/\partial T = (- \nu_a - D'/\Lambda^2)n \qquad (10)$$

If the geometry of the discharge chamber and the value of the gas pressure is such that the diffusion term is negligible then Equation 10 becomes

$$\partial n/\partial T = - \nu_a n \qquad (11)$$

Equations 9, 10 and 11 may be expressed by the general equation

$$\frac{\partial n}{\partial T} = -n\ \beta(T)$$

where $\beta(T)$ is a general decay constant which includes recombination, attachment and diffusion. Therefore

$$\ln \frac{n(T')}{n_f} = -\int_0^{T'} \beta(T)\, dT \qquad (12)$$

where $n(T')$ is the electron density at time T', and n_f is the electron density at time $T = 0$ (i.e. $T = 0$ is when the microwave power is removed and the electron density has built up to some final value n_f). In the initial portion of the decay period of the electron density, $\beta(T)$ will vary with time because of the rapid decay of the higher order electron diffusion modes (10, p. 48) and because of the recombination losses which depend on the square of the electron density. When these loss mechanisms are negligible, the decay constant is obtained from Equation 10 and is given by

$$\frac{\beta(T)}{p} = \frac{\beta}{p} = \frac{\nu_a}{p} + \frac{D'p}{(p\Lambda)^2} \qquad (13)$$

Hence, the value of β should remain constant providing the attachment and diffusion losses remain

constant with time. The pressure p has been introduced to express the equation in terms of proper variables. If the diffusion losses are negligible, then from Equation 13 we obtain

$$\frac{\beta}{p} = \frac{\nu_a}{p} \qquad (14)$$

Experimental work by Biondi (5) and Sexton et al (51, vol. 1, p. IA94), on the rate of decay of the electron density in the microwave afterglow in oxygen, show that although the density initially decays in a somewhat arbitrary manner a condition is obtained after a millisecond or so where the density decays exponentially with time. In the initial decay period all three decay mechanisms may be operative and the decay constant is given by $\beta(T)$. However, when the conditions are such that the decay rate is exponential then $\beta(T)$ is a constant and is given by Equation 13 or 14.

Biondi used his measured value of the electron decay rate to determine the attachment coefficient of thermal electrons to neutral molecules. The results were independent of pressure over a range of 8 to 25 mm Hg; so presumably the diffusion loss was negligible in his experiment and the decay rate is given by Equation 14. However, the value obtained

for the attachment coefficient was about 100 times smaller than that obtained by other workers (11, 19) and also later by Biondi himself (6, vol. 1, p. IA72) when using techniques not employing a microwave discharge. Although Biondi's microwave technique has been criticized, the method was used recently by Sexton et al to, once again, measure the attachment coefficient. Their results were approximately the same as the "microwave value" obtained by Biondi.

It has been suggested (13, p. 203-214) that the low value obtained for the attachment coefficient in the microwave afterglow studies is the result of a near balance between attachment and detachment resulting from collisions of the negative ions with vibrationally excited neutral molecules, which are formed during the microwave discharge. This means that the decay constant is given by

$$\frac{\beta}{p} = \frac{\nu_a - \nu_d}{p} \qquad (15)$$

where ν_d is the frequency of detachment. Whatever the explanation it is evident that there is a period in the decay of the electron density when the decay rate is exponential and β is a constant. From the published results of Sexton et al the average value

of β/p is 69.1 (sec mm Hg)$^{-1}$, for a pressure range of 5 to 20 mm Hg, providing the diffusion loss is negligible. The results also show that with their equipment, in which the characteristic diffusion length was 0.3 cm, the decay constant obtained a steady value in about 2.5 milliseconds at 5 mm Hg pressure and in less than 1 millisecond at 20 mm Hg pressure. Use of these facts will be made later.

3d. Method of Determining the Net Frequency of Ionization

The technique to be described implies the use of pulsed microwave power. The discharge is assumed to have reached a steady state condition where the electron density builds up from some value n_o at the arrival of the microwave pulse, attains the critical density n_b after a time τ (defined as the formative time of the discharge), reaches a density n_f by the end of the microwave pulse and then decays in the period between pulses to n_o. The cycle is repeated with each microwave pulse.

The decay of the electron density in the period between the microwave pulses is given by Equation 12. If T' is the time between pulses then $n(T') = n_o$. Substituting this into Equation 12 and combining the result with Equation 8 yields

$$\ln(n_b/n_f) + \int_0^{T'} \beta(T)dT = p\tau \left[\frac{\nu}{p} - \frac{Dp}{(p\Lambda)^2} \right] \qquad (16)$$

It should be noted here that the diffusion term on the right is the diffusion loss during the period of electron production. The loss of electrons by diffusion in the decay period, if present, is included in $\beta(T)$.

Differentiating Equation 16 with respect to time T' we obtain

$$\frac{d}{dT'} \ln (n_b/n_f) + \beta(T') = p \frac{d\tau}{dT'} \left[\frac{\nu}{p} - \frac{Dp}{(p\Lambda)^2} \right] + p\tau \frac{d}{dT'} \left[\frac{\nu}{p} - \frac{Dp}{(p\Lambda)^2} \right] \qquad (17)$$

The first term on the left contains the ratio of the critical electron density for breakdown to the final electron density in the discharge, as a function of the repetition rate of the microwave pulses. Since the repetition rate determines the electron density remaining at the beginning of the next pulse (i.e. it determines where the next discharge begins on the electron decay curve) it also determines the formative time of the discharge and hence determines the length of time remaining for the discharge to reach its final condition. By working in a range of operating conditions so that the formative time is small

compared to the length of the microwave pulse then there is a greater probability that the discharge will attain an equilibrium condition before the end of the microwave pulse; hence small variations in the formative time should not effect the final electron density n_f. For simplicity it will be assumed that n_f is constant with changing repetition rate; therefore, the first term on the left of Equation 17 will be neglected in the following discussion. Further discussion on this point is given in Section 7a.

The last term in Equation 17 is controlled solely by the electron production parameters; and the only term affected by the initial electron density, and hence the repetition rate, is the diffusion coefficient D. When the electron density approaches the critical density for breakdown, the value of D is given by the ambipolar diffusion coefficient. However when the initial electron density is small, D is first given by the free-electron diffusion coefficient and then later by the ambipolar diffusion coefficient. The variation in D with repetition rate can be made negligible by operating in a range which ensures that D is always given by the ambipolar diffusion coefficient.

(NOTE. This requires that the initial electron density be large which means that formative time of the discharge will be small. The short formative time is in agreement with our requirement that is necessary to assume that n_f remains constant.) The other possibility is to make the discharge chamber large enough so that the diffusion loss is negligible; hence its variation with repetition rate will be negligible. Further discussion on this point is given in Sections 3g and 3h.

The second term on the left of Equation 17 is the decay constant at time T'. As described in Section 3c there is a period in the decay curve of the electron density when $\beta(T)$ is a constant, the value of which can be determined from the results of other workers. If we therefore limit our operating conditions to T' greater than about 2 milliseconds (i.e. to microwave pulse repetition rates of less than 500 pps) and use relatively small formative times then Equation 17 reduces to

$$\frac{\nu}{p} = \frac{\beta}{p} \frac{1}{d\tau/dT'} + \frac{Dp}{(p\Lambda)^2} \qquad (18)$$

where β is given by Equation 13. By selecting a value of p so that the diffusion losses are

negligible then Equation 18 reduces to

$$\frac{\nu}{p} = \frac{\beta}{p} \frac{1}{d\tau/dT} = \frac{69.1}{d\tau/dT} \text{ (sec. mm Hg)}^{-1} \qquad (19)$$

where β is given by Equation 14 or 15 depending on the interpretation of the decay constant; in either case the numerical value of β is 69.1 (sec mm Hg)$^{-1}$ (see Section 3c). The value of $d\tau/dT$ may be obtained from a series of plots of the formative time of the discharge versus the reciprocal of the repetition rate of the microwave pulses at a constant energy per pulse. From a knowledge of the length of the microwave pulse, the microwave power can be expressed in terms of an effective electric field E_e. One can then obtain a plot of the net frequency of ionization ν/p as a function of E_e/p.

3e. The Effective Electric Field

In order to correlate the results from microwave and dc discharges it is necessary that the ac electric fields encountered in the microwave work be expressed by an effective field E_e which will produce the same net ionization as a dc field of the same magnitude (1, vol. 21, p. 395). If the period of relaxation of the electron energy is long compared to the rf period, the effective electric field is defined by

$$E_e^2 = E_{rms}^2 \frac{\nu_c^2}{\nu_c^2 + w^2} \qquad (20)$$

where E_e is the effective electric field,

E_{rms} is the rms of the microwave electric field,

w is the angular frequency of the microwave field and

ν_c is the electron-molecule collision frequency and is given by 3.5×10^9 p for oxygen (9, vol. 22, p. 568),

where p is the gas pressure in mm Hg. If the gas pressure is high, however, the relaxation time of the electron energy is comparable with or shorter than the rf period and account must be taken of the effect of the electron energy modulation (17). The immediate effect is that the net frequency of ionization varies over each rf cycle. It is under these circumstances that the effective net frequency of ionization is a time average of $(\nu_i - \nu_a)$. The overall effect may be expressed by using an equivalent electric field that is slightly larger than the effective field, as defined above, and is given by

$$\frac{E_{eq}}{p} = \frac{E_e}{p} + \Delta$$

where E_{eq} is the equivalent field and Δ represents the energy modulation effect. The value of Δ has been determined for air by Gould and Roberts for a pressure range of zero to infinity. The results show that when using 3.19 cm radiation, the value of Δ is approximately 0.013 volts/cm per mm Hg up to a pressure of 300 mm Hg. Since the results should be very similar for oxygen and because the maximum pressure used in this experiment is only 20 mm Hg, then the effect of energy modulation is negligible. The equivalent and effective electric field is therefore given by Equation 20.

3f. Calculation of the Net Frequency of Ionization from dc Parameters

The net frequency of ionization for oxygen may be evaluated from the first Townsend ionization coefficient α, the attachment coefficient η and the electron drift velocity v_d, all evaluated under dc electric field conditions (9, vol. 22, p. 566)

$$\nu = \nu_i - \nu_a = (\alpha - \eta)\, v_d$$

The net ionization coefficient $(\alpha - \eta)$ for oxygen has been determined by several groups of workers (19, p. 1; 42, p. 385-398; 48, vol. 1, p. IB127)

over a range of E_{dc}/p of 25 to 65 volts/cm mm Hg, and a pressure range p from a few mm Hg to 600 mm Hg. The results are in very good agreement differing by only about 12%. Since the results of Harrison and Geballe (19) have been tabulated (29, p. 413) they will be used when required for comparison purposes.

The electron drift velocity in oxygen has been determined as a function of a dc electric field by Healey and Kirkpatrick (29, p. 324), Bradbury and Nielsen (29, p. 230), Brose (8, p. 536-546), Herreng (24, p. 6-16) and Goodwin (16). The published results are plotted on Figure 2 for convenience. The following remarks are of interest when making a comparison of the different results. Loeb (29, p. 233) expresses the belief that the general results of Bradbury and Nielsen are probably the most consistent because of the agreement with their results, for certain gases, by other workers. Bradbury and Nielsen's results are currently used to evaluate the electron-molecule collision frequency (10, p. 186) (see Section 3e). The values obtained by Goodwin are for $E_{dc}/p < 20$ and agree very closely with those of Bradbury and Nielsen (14, p. 473-483). Loeb

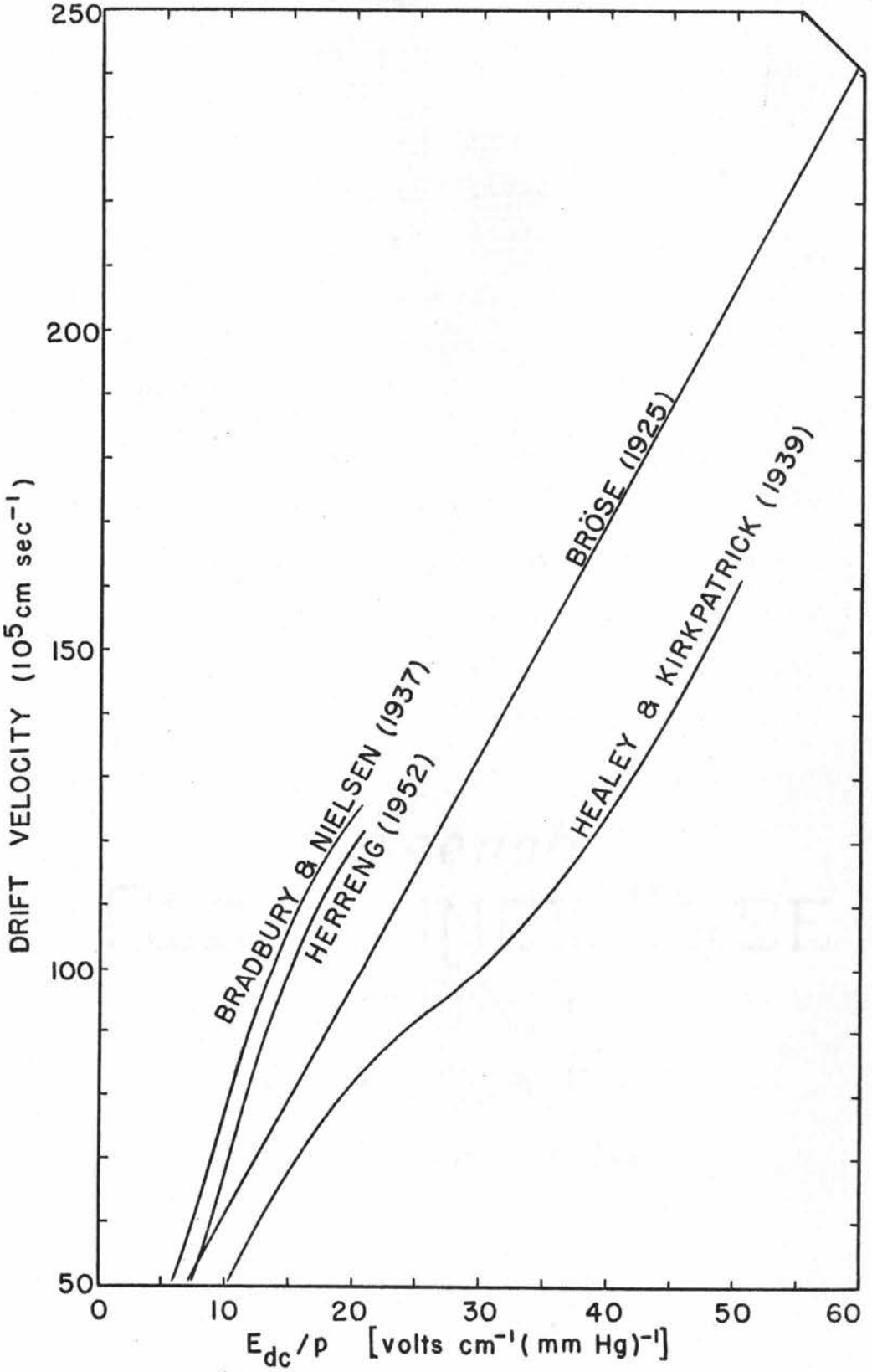

FIGURE 2 . DRIFT VELOCITY OF ELECTRONS IN OXYGEN

also states (29, p. 322) that Healey and Kirkpatrick's results for oxygen should be reliable even though their results for the inert gases may be in doubt. Loeb makes the general statement (29, p. 320) that results obtained before 1936 should be regarded with caution, especially for the inert gases, because the techniques of purity control were not adequately developed before this date. The question of gas impurity was considered by Prasad and Craggs (42, p. 385-398) when measuring the net ionization coefficient of oxygen. They used tank-oxygen of 99.5% purity for their general experiments and spectroscopically pure oxygen for a comparison experiment; no apparent differences were noted due to the different levels of gas impurities. The results by Bröse were obtained before 1936; however, his results for the mean energy of electrons in oxygen, which were obtained at the same time as the results of the drift velocity of electrons in oxygen, were used by Harrison and Geballe in 1953 (19) in their calculations for the cross-section for electron attachment.

It is apparent from the above remarks that there is no clear cut reason for using any particular set

of results for the electron drift velocity. Therefore, since the results of Bröse cover the largest range of E_{dc}/p these will be used when required for comparison purposes.

Gould and Roberts (17) calculated the net frequency of ionization for air from the above dc parameters and obtained good agreement with the values obtained by MacDonald (30) who used the value of the high frequency ionization coefficient, obtained by microwave methods, and a calculated value for the diffusion coefficient. This gives some confidence in the correspondence equations.

3g. The Diffusion Term

The purpose of this section is to obtain numerical values for the various diffusion coefficients so that an estimate may be made of the error involved if the diffusion term is neglected, and also for comparison purposes with experimental results. Two sets of conditions must be considered: one is during the formation of the discharge when the electron energy is much larger than that of the ions, and the other is during the decay period when the electron energy is approximately equal to that of the ions. There are transition regions in between these periods

particularly at the beginning of the decay period. However, in the decay period we are only concerned with conditions that occur about two milliseconds after the cessation of the discharge, and it is estimated by Loeb (29, p. 511) that the electrons attain near thermal energies in less than 100 microseconds after the cessation of a microwave discharge. An estimate of the time taken for the electron energy to decrease from a value of 7ev (see Section 3g-1) to thermal energies may be made by assuming the electron loses 2m/M of its energy per collision (m is the mass of the electron and M the mass of a molecule) and that the collision frequency is constant over the given energy range. The calculations yield a value of approximately 20 microseconds.

In addition to the high and low electron energy ranges the two regions of high and low electron density must be considered. For example, Madan et al (34) measured the formative time of a discharge starting with an electron density of unity and building up to a density of about 10^{11} electrons/cm^3. Throughout this density range the diffusion coefficient changes from "free electron" to

"ambipolar" and calculations were made to allow for this, based on the theory of the transition from free to ambipolar diffusion by Allis and Rose (2). In the present experiment a steady state pulsed discharge is used and the electron density at the beginning of each discharge period will probably be quite large. [According to the electron density decay curves by Sexton et al (51, vol. 1, p. IA94) n_o will be about $10^6/cm^3$ or greater.] It would therefore be convenient if a single value of the diffusion coefficient could be used.

The transition between free and ambipolar diffusion is controlled by the relative values of the characteristic diffusion length of the discharge chamber and a distance called the Debye length. The Debye length h is the separation between the average electron and ion when the mean kinetic energy equals the potential energy. This is given by (52, p. 17)

$$h = 6.9\ (T/n_e)^{1/2}\ \text{cms} \qquad (21)$$

where T is the kinetic temperature of the electrons in ^oK, and n_e is the number of electrons per cm^3. When the Debye length equals the characteristic diffusion length, the diffusion coefficient is about

twice the value of the ambipolar diffusion coefficient (2, p. 84). Using a characteristic diffusion length of Λ = 0.16 cm (see Section 3h) and an electron energy value of 7ev (see Section 3g-1), the diffusion coefficient is given approximately by the ambipolar diffusion coefficient during the discharge period when the electron density is greater than $10^8/cm^3$. During the afterglow period the electron density must be greater than $6 \times 10^5/cm^3$ in order for the diffusion to be ambipolar. It should be noted that in a recent paper by Kelly and Margenau (25) the ambipolar diffusion coefficient was used for the value of D during the discharge period, for a range of electron densities of from $3 \times 10^3/cm^3$ to the critical value for breakdown.

3g-1. Free Electron Diffusion Coefficient

The free electron diffusion coefficient D_e is given by (54, p. 946)

$$D_e = 2/3.\ \bar{u}\ \mu_e$$

where $\bar{u}$ is the average electron energy in electron volts, μ_e is the electron mobility = $e/m\ \nu_c$ where e is the electron charge in coulombs, m is the electron mass in kilograms and ν_c is the

electron-molecule collision frequency. The factor 2/3 is for a Maxwellian distribution, while for a Druyvesteyn distribution the factor is 0.763; the results are relatively insensitive to the distribution function used. For electrons with thermal energy this equation yields the value

$$D_e p = 8 \times 10^3 \text{ mm Hg cm}^2/\text{sec.}$$

There is a wide range of values obtained for D_e during the discharge period by the various authors due to the different values used for the average energy of an electron in a microwave discharge. Gould and Roberts (17) and MacDonald (30) used the value $\bar{u} = 0.036\ E_e/p$ which was obtained from the work by Healey and Reed (20, p. 79). (NOTE. The value given is for air but according to the reference it applies equally well for oxygen.) Kelly and Margenau (25, p. 1617) used the relation $D_e = l\,\bar{v}/3$, where l is the mean free path and $\bar{v}$ is the average speed of the electron, and determined that $\bar{v} = 3/4\ v_i$ where $1/2mv_i^2 = u_i = 12.5$ ev, the ionization energy for molecular oxygen. This yields the value $\bar{u} = 7$ev. Other values for the average electron energy as a function of E_e/p are given by Healey and

Kirkpatrick (29, p. 324) and Bröse (8, p. 536-546). Using the value of $\nu_c = 3.5 \times 10^9$ p and $E_e/p = 40$ volts/cm mm Hg gives the following values for the free electron diffusion coefficient during the discharge period,

$D_e p = 0.5 \times 10^6$ mm Hg cm^2/sec, using the results of Healey & Reed,

$D_e p = 1.0 \times 10^6$ mm Hg cm^2/sec, using the results of Healey & Kirkpatrick,

$D_e p = 1.6 \times 10^6$ mm Hg cm^2/sec, using the results of Bröse,

$D_e p = 2.3 \times 10^6$ mm Hg cm^2/sec, using the results of Kelly & Margenau.

3g-2. Ambipolar Diffusion Coefficient

When electrons are "lost" from the discharge region at the same rate as the positive ions, the ambipolar diffusion coefficient D_a is defined by (29, p. 208)

$$D_a = \frac{D_i \mu_e + D_e \mu_i}{\mu_e + \mu_i} \qquad (22)$$

where the subscripts i and e refer to the positive ions and electrons respectively. The value of $p\mu_i$ for positive, and negative, oxygen ions is

given by Varney (55) and Burch and Geballe (11) as approximately 2×10^3 mm Hg cm^2 (sec volt)$^{-1}$.

During the discharge period the average electron energy is very much larger than the average ion energy, and under this condition Equation 22 reduces to $D_a = D_e \mu_i/\mu_e = D_e/250$. By comparison, Kelly and Margenau (25) used a value of $D_a = D_e/40$ for the discharge period. During the afterglow period when the electrons have near thermal energies, Equation 22 simplifies to $D_a = 2D_i$; therefore the value of $D_a p$ equals 66 mm Hg cm^2/sec.

When the predominant electron loss mechanism is electron attachment to neutral molecules, then many negative ions are formed. If x is the fraction of electrons which remain unattached and (1-x) is the ratio of the negative to positive ions, the ambipolar diffusion coefficient is given by (29, p. 209)

$$D_a = \frac{x(\mu_+ D_e + \mu_e D_+) + (1-x)(\mu_+ D_- + \mu_- D_+)}{\mu_+ + \mu_e x + \mu_- (1-x)} \qquad (23)$$

where the subscripts + and - refer to the positive and negative ions respectively. During the discharge period the attachment rate will not be very large and we may assume that the ambipolar diffusion coefficient

is given by Equation 22. However, in the afterglow period the attachment rate is very large and Equation 23 applies. In the limit when x equals 1 we obtain the value $D_a=2D_+$; in the limit when x equals zero we obtain $D_a=D_+$. Therefore in the afterglow period the value of $D_a p$ is between 33 to 66 mm Hg cm^2/sec.

3h. Minimum Waveguide Height Necessary for the Diffusion Losses to be Neglected

The published results by Sexton et al (51, vol. 1, p. IA94) on the decay of the electron density in the afterglow of a microwave discharge in oxygen show that in the region where the decay is exponential then the decay rate is independent of pressure over a range of 5 to 20 mm Hg. The characteristic diffusion length in their experiment was 0.3 cm. This means that the diffusion losses in the afterglow in the present experiment may be neglected providing $p\Lambda > 1.5$ cm mm Hg.

The discharge chamber in this experiment consists of a length of X-band waveguide of standard width (2.20 cm) and of a suitable height. Standing waves are set up in the microwave field by totally reflecting the incident signal at a suitable point. Since the height of the waveguide will have to be quite large in order to neglect the diffusion losses,

the electric field distribution in the discharge region will be non-uniform. This means that the geometry of the chamber cannot be considered as a set of infinite parallel plates with a separation equal to the height of the waveguide. In the case of the parallel plate geometry with a separation d, and a uniform electric field between them, the characteristic diffusion length is given by d/π . The effect of bounding a given volume between these two parallel plates is to produce a non-uniform electric field, in the enclosed volume, which in turn tends to isolate the region of ionization to that where the electric field is large. Isolating the discharge in this manner has the effect of reducing the characteristic diffusion length. A variational-method for the solution to non-uniform electric field problems has been given by Platzman and Solt (40). The method is to determine an effective separation of an equivalent parallel plate geometry for an X-band rectangular cavity. The calculations, which require the aid of a computer, are given for air in a cavity, 0.900 inch x 0.961 inch x 0.400 inch high. Let us consider the standard X-band waveguide (0.900 inch x 0.400 inch)

as a trial size for the discharge chamber in the present experiment. The standing waves in the microwave field will have the effect of limiting the length of the discharge chamber to approximately 0.9 inches, so that the size of the chamber will be similar to that used by Platzman and Solt. Since the results for air and oxygen should be approximately the same, we may use the results of Platzman and Solt to determine the plate separation of an equivalent parallel plate geometry. The results yield a minimum effective parallel plate separation of d = 0.5 cms (Λ = 0.16 cms) for the above trial size chamber. In order for the diffusion losses in the afterglow period to be negligible it is necessary to satisfy the condition that the value of $p\Lambda$ be greater than 1.5 cm mm Hg; this requires that the pressure be 10 mm Hg or higher.

In order for the diffusion losses during the formation of the discharge to be negligible, we see from Equation 18 that we require

$$\frac{Dp}{(p\Lambda)^2} \ll \frac{\beta/p}{d\tau/dT} = \frac{69.1}{d\tau/dT} \quad (\text{sec mm Hg})^{-1}$$

The minimum experimental value of the right hand side for a gas pressure of 10 mm Hg is 5×10^5.

Using the free electron diffusion coefficient as an extreme value for D and using the value of $D_e p = 1.6 \times 10^6$ mm Hg cm^2/sec, then with $\Lambda = 0.16$ cm we obtain the value

$$\frac{Dp}{(p\Lambda)^2} = 6 \times 10^5$$

Therefore under these extreme conditions the value of ν/p at the low values of E_e/p will only be about one-half its correct value if the diffusion losses are neglected during the discharge period. However using the results of Allis and Rose (2) as a guide, the effective diffusion coefficient is about one-tenth of the free electron diffusion coefficient at an electron density of about $10^6/cm^3$ (i.e. the minimum expected value) and will, of course, decrease as the electron density increases. This indicates that the error introduced by neglecting the diffusion losses will only be about 10% at low values of E_e/p and considerably less at higher values of E_e/p.

In conclusion, by using a standard X-band waveguide for the discharge chamber, it should be possible to neglect the diffusion losses in the formation of the discharge and in the decay period

providing the gas pressure is 10 mm Hg or greater. This statement can be verified experimentally by noting any change in the results with pressure. The above discharge chamber will be referred to as the "1 cm chamber" in the future sections. The experiment was also performed in a "shallow" chamber, about 0.1 cm high, in which the diffusion losses will be important.

4) APPARATUS

The microwave technique used to produce the discharges is essentially the same as that used by Oskam (37). The method is to set up standing waves in the discharge region and to locate the nodes of the standing waves at the "weak points" in the system, such as at the microwave window, so that unwanted discharges may be avoided. Oskam found that the electric field required to produce electrical breakdown of the gas increased with increasing voltage standing wave ratio (VSWR) up to a value of VSWR of about 3. He attributed this as being partly due to the effective diffusion length decreasing as the standing wave ratio is increased (i.e. the length of the discharge decreases as the shape of the standing wave gets steeper). The shape

of the standing wave pattern is essentially constant for a VSWR greater than 3; therefore the breakdown field is constant. For this experiment it has been shown (Section 3h) that the diffusion losses may be neglected when a 1 cm high chamber is used. In the experiment using a shallow chamber the height of the chamber will effectively determine the characteristic diffusion length, so the length of the discharge will have negligible effect. For this reason, and because of experimental simplicity, the voltage standing wave is produced by 100% reflection of the incident power.

4a. Discharge Chamber

The 1 cm discharge chamber is constructed from standard X-band brass waveguide (0.900 inch x 0.040 inch), is 88 mm long and has a choke flange at each end (see Figure 3). The chamber is sealed off at one end with a flat brass plate and at the other end with a microwave window (Microwave Associates type MA 1430). The gas inlet is located in the center of the length of the chamber and on one of the broad faces of the waveguide. The length of the chamber, including the thickness of the window flange, is approximately equal to two waveguide wavelengths.

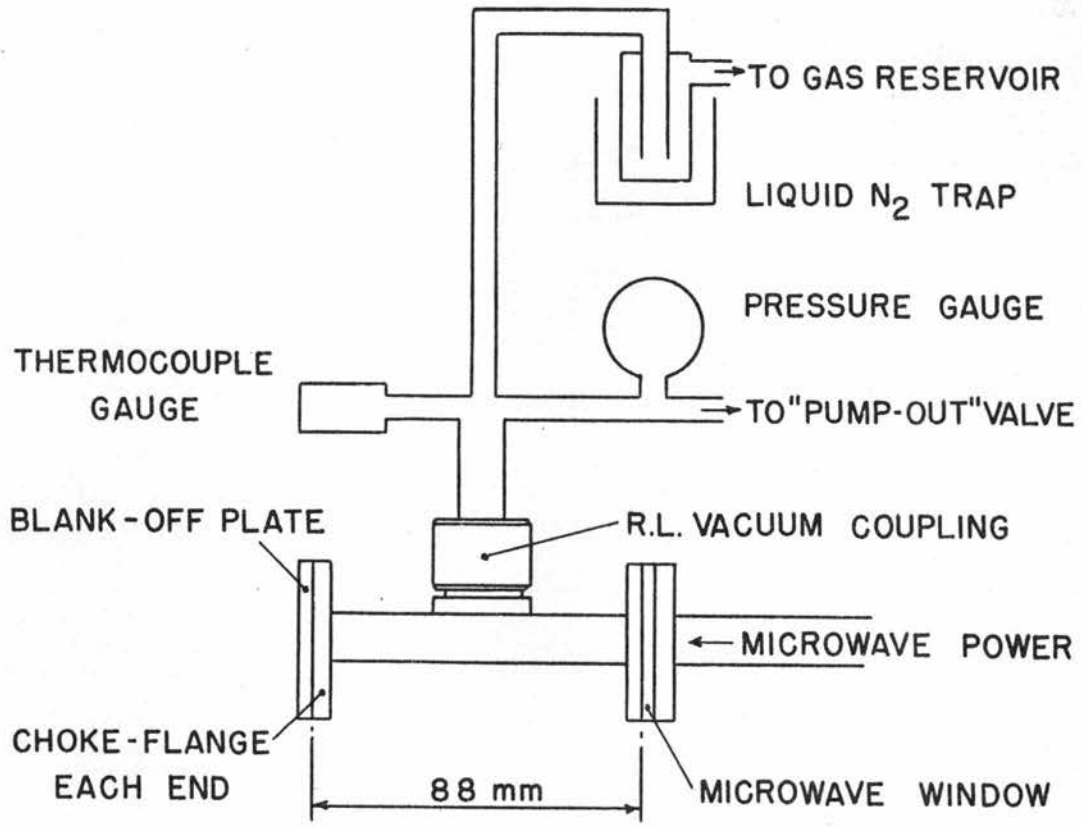

1cm DISCHARGE CHAMBER ASSEMBLY

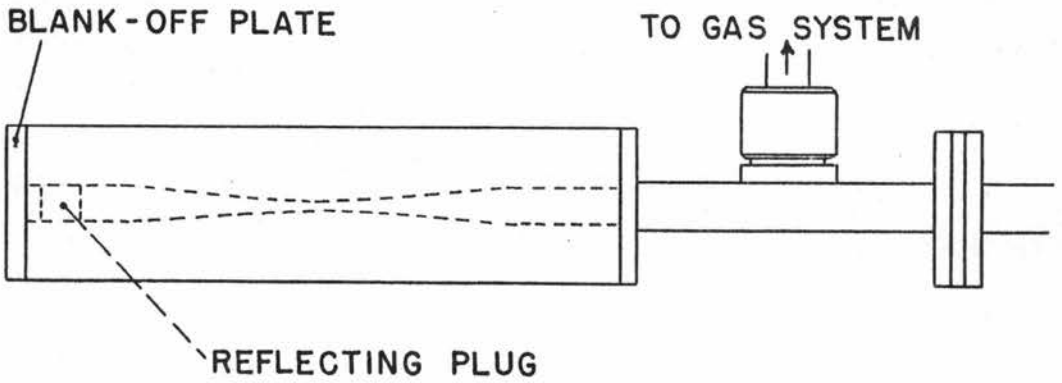

CONTOUR ASSEMBLY

FIGURE 3. DISCHARGE CHAMBER & GAS SYSTEM ASSEMBLY

This places the gas inlet hole and the microwave window at a node in the standing wave. The inside of the chamber was carefully finished to eliminate any irregularities where the tube and the flanges were joined. The interior surface was finished with 400 grit carborundum to remove any surface irregularities. The chamber was scrubbed well with soap and water to remove the carborundum grit, then washed in acetone to remove any grease. It was then boiled in distilled water and finally washed with ethyl alcohol.

A special contoured waveguide assembly was made for the study of the effect of a gas flow on a microwave discharge (see part two) and this was used in the present experiment as a "shallow" discharge chamber. The contour-assembly is described in full in part two and it is sufficient to say here that the contoured waveguide tapers down from a standard waveguide dimension to a small gap width, then opens up again to the standard waveguide size. Three gap widths of 0.114, 0.164 and 0.214 centimeters are available. Only the height of the waveguide varies, not the width. The purpose of the contoured waveguide is to ensure that the discharge occurs at

the point where the waveguide height is the smallest. This, therefore, requires that the antinode of the microwave standing wave also be located at this point; the setting-up procedure is described in part two. The long flow-tube used in conjunction with the contour-assembly in the gas flow experiment was omitted in the present experiment for convenience.

4b. Microwave Circuit

A schematic of the microwave circuit is shown in Figure 4. The 3.19 cm pulsed-power is obtained from an APS-4 radar unit. A power-divider next in line to the transmitter provides a coarse adjustment for the amount of power supplied to the main waveguide, the surplus power being absorbed in a matched terminating load. A 0-50 db precision variable attenuator provides a fine adjustment for the useable power. Next in line is a 20 db directional-coupler which is used to monitor the useable power. A small fraction of the power is coupled into the side arm where, after further attenuation, it is measured with the aid of a thermistor mounted in a suitable detector mount. The thermistor constitutes one arm of a balanced bridge, the remainder of which is part of the power meter (Hewlett Packard Model 430C).

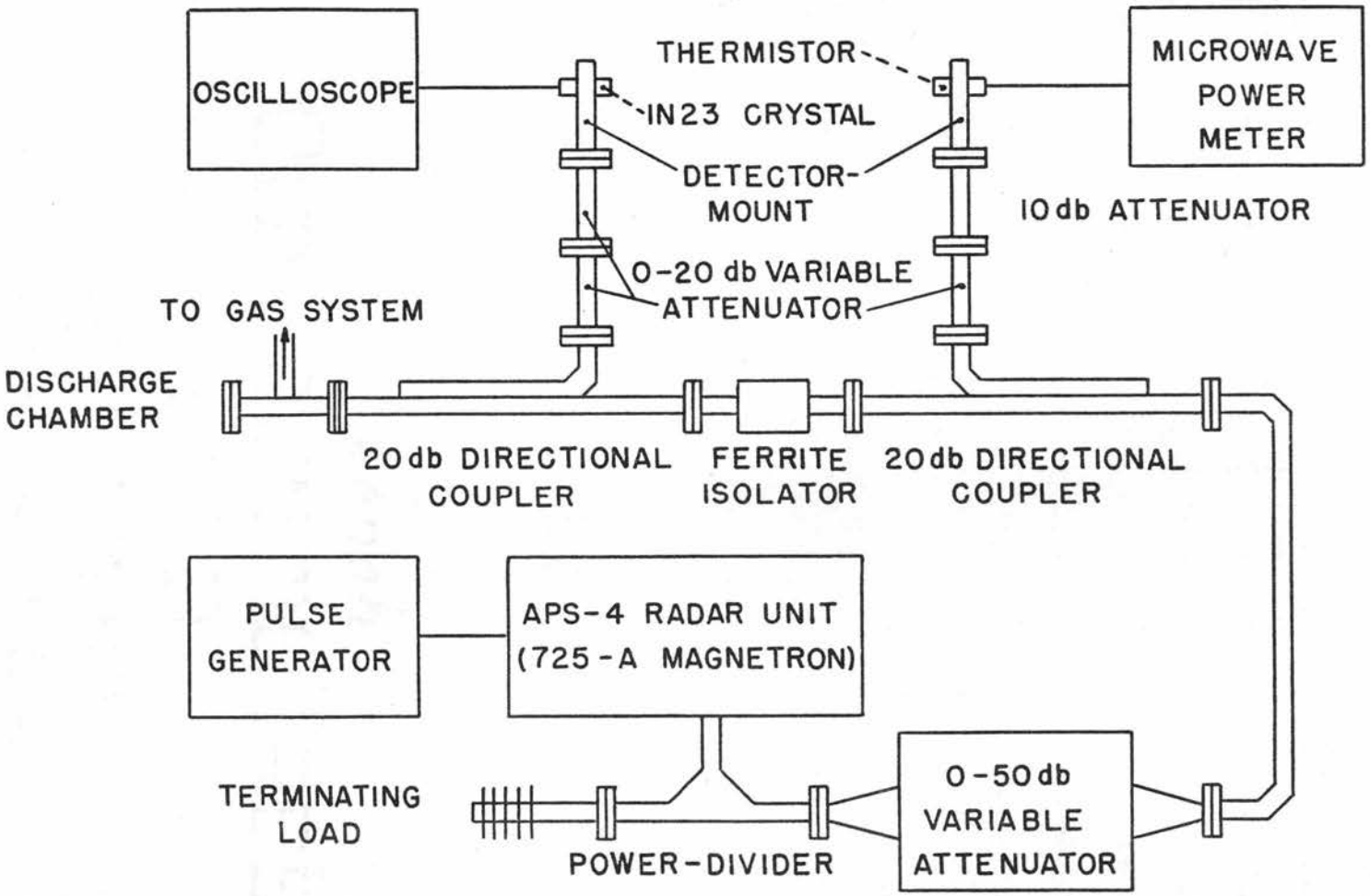

FIGURE 4. MICROWAVE CIRCUIT

A 0-20 db variable attenuator is mounted in the detector arm to enable the power meter to be easily zeroed. The power in the main waveguide then passes through a ferrite isolator (Cascade Research Model X126) whose function is to absorb the power reflected from the discharge chamber and so avoid damaging the magnetron. The microwave power then goes to the discharge chamber at the end of which it is reflected to set up standing waves in the chamber. The reflected power is monitored by means of a second 20 db directional coupler; the reflected power is rectified by means of a 1N23 crystal, and the resultant pulse shape displayed on an oscilloscope (Tektronix, Model 581).

Two modifications were made to the APS-4 radar unit to improve its stability and operating range. One was to replace the 1B22 spark-tubes, which are used to initiate the microwave pulse, with a 5C22 thyratron. The change was made because of the frequent miss-firing of the spark-tubes and the subsequent loss of time changing tubes. The necessary modifications are shown schematically in Figure 5. The other modification was a replacement of the multivibrator in the pulse repetition circuit with an

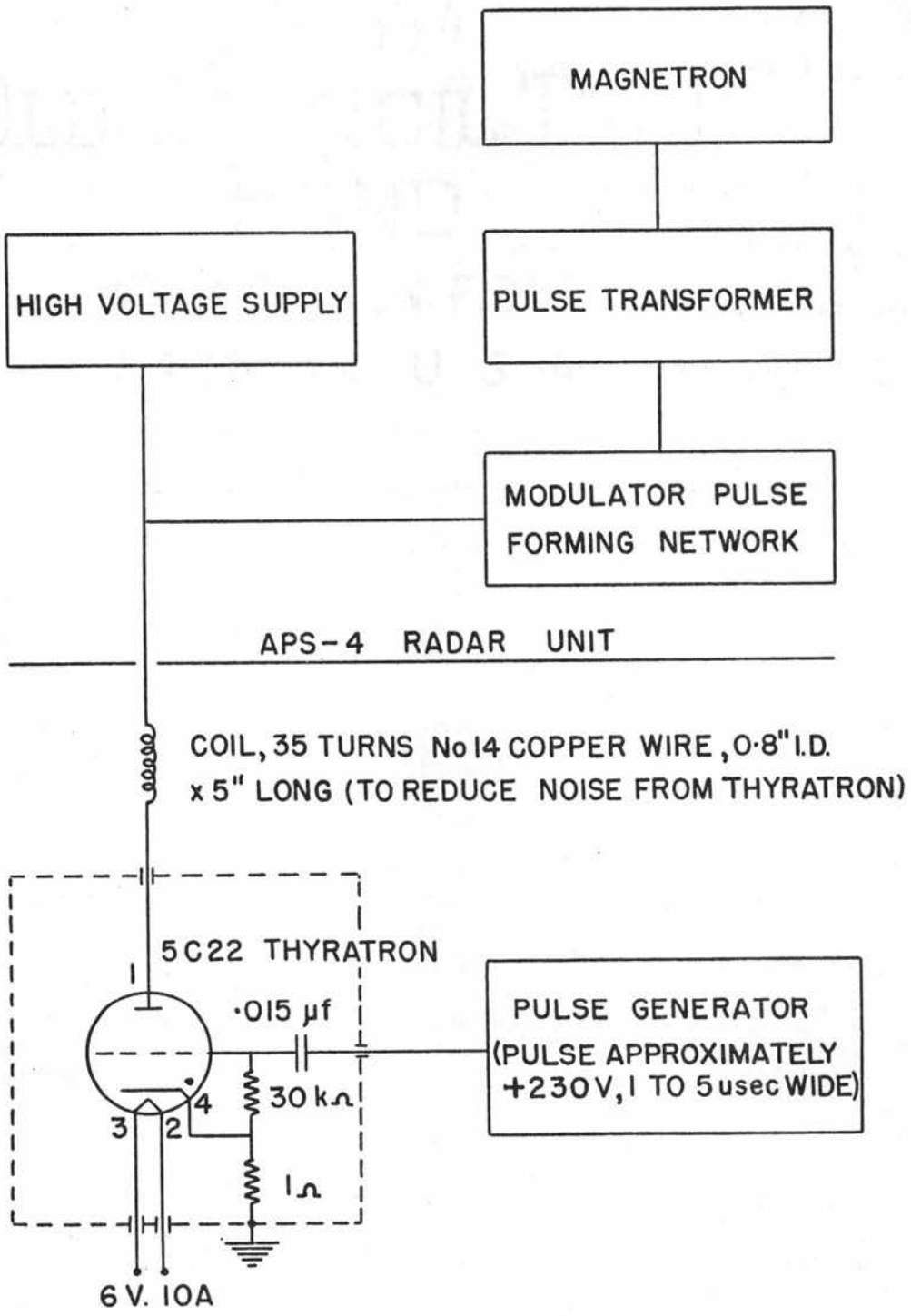

FIGURE 5. THYRATRON CIRCUIT FOR RADAR UNIT

external pulse generator (Measurements Corp. Model 74-B). This enabled the microwave pulse rate to be varied continuously over a range of from about 150 to 1000 pps, depending on the microwave pulse width being used. For trouble-free operation for more than several minutes the useable repetition rate with the 2.1 microsecond pulse is between about 250 to 450 pps. Outside of this range the duty cycle of the magnetron is either too small or too large and the magnetron operation becomes very intermittent or the high voltage circuit overloads. The radar unit has two microwave pulse lengths, listed as 0.6 and 2.1 microseconds.

4c. Gas System

The gas handling system was designed and built for the gas flow experiment and is described fully in part two. As far as this experiment is concerned the gas is obtained from a standard gas cylinder, it is passed through a solid CO_2 and acetone cold trap and then through a liquid nitrogen trap to remove the water vapor. The system is pumped out with an Edward's model ISC-450B mechanical vacuum pump whose base-pressure is of the order of several microns of mercury. The low pressure in the discharge chamber

is measured with a thermocouple type gauge with a Bon-De model BD-20R reading unit. The operating gas pressure in the discharge chamber is measured with a Wallace and Tiernan absolute pressure indicator, type FA-160. The pressure range of the gauge is 0 to 50 mm Hg with a listed accuracy of reading of 1/300 full scale reading. The gauge was checked against an oil manometer, filled with Dow Corning 702 silicon diffusion-pump oil, because the gauge did not zero correctly. The accuracy of setting and repeatability was found to be 0.25 mm Hg. The accuracy of the oil manometer was estimated to be 0.1 mm Hg.

5. EXPERIMENTAL PROCEDURE

5a. Method of Measuring Formative Times

As stated in Section 3a, the presence of a microwave discharge is detected by the large attenuation in the microwave signal. A large reflection coefficient is also associated with the large attenuation factor. The presence of the discharge is best illustrated by removing the metal reflector plate from the back of the discharge chamber and replacing it with a second microwave window and a terminating load. When there is no discharge present

the reflected microwave signal is very small and is similar to trace C in Figure 6. The discharge is initiated either with the aid of an external radioactive source, to provide a copious supply of primary electrons, or by increasing the microwave power until "breakdown" occurs. If the high power method is used then the reflected signal rises very rapidly as soon as the microwave pulse begins. This is shown in trace A, Figure 6. When the power level is reduced the reflected microwave signal first appears at the same height as that observed when there was no discharge present, but then rises rapidly after a measurable delay time indicating that a discharge has formed (see trace B Figure 6). This delay between the beginning of the microwave pulse and the point where the reflection suddenly increases is interpreted as the formation time of the microwave discharge. It should be noted that once the discharge has started it is self substaining and the external source may be removed without effecting the properties of the discharge. The oscilloscope traces shown in Figure 6 were taken using the 0.6 microsecond microwave pulse and the contoured waveguide assembly. The reflection from the tapered waveguide

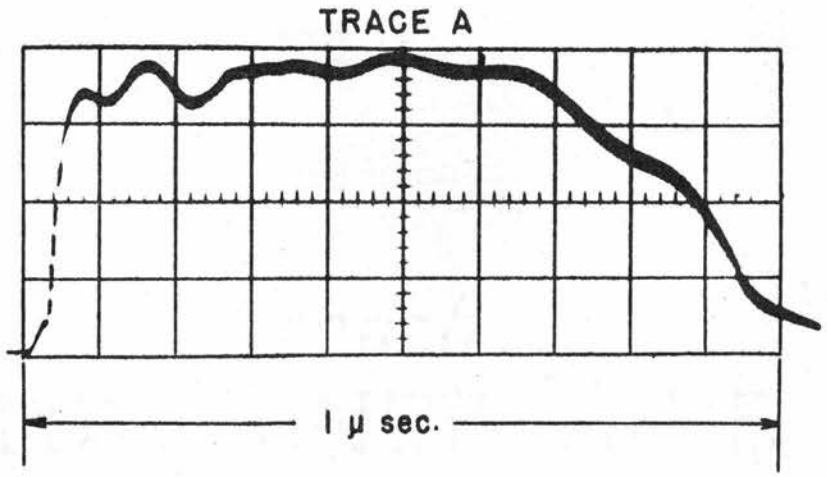

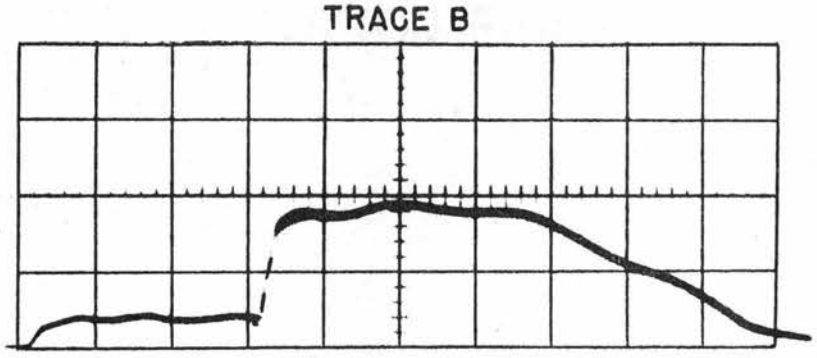

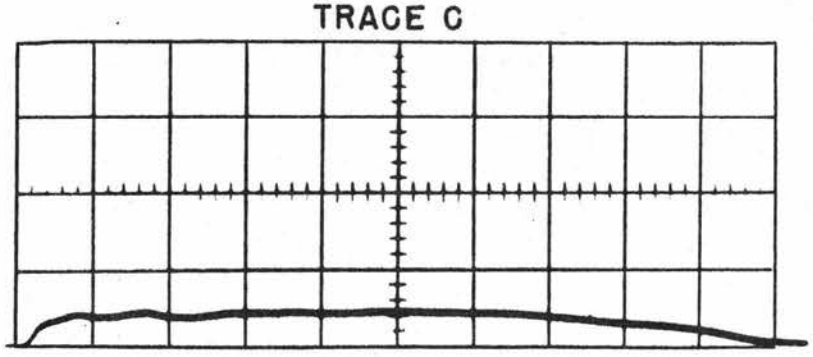

FIGURE 6. REFLECTED MICROWAVE PULSE.

is responsible for the relatively large reflected signal observed in trace C. Furthermore, the rectifying 1N23 crystal was operating in a very non-linear region. The particular discharge shown in these three traces was across one of the microwave windows. In several photographs part of the trace has been "dotted-in" because of the difficulties of reproduction.

When the metal plate is replaced at the back of the discharge chamber, to produce the voltage standing waves and to prevent discharges occurring at the microwave windows, the presence of the discharge is detected by a decrease of the reflected signal (i.e. a portion of the incident power is absorbed by the discharge); this is illustrated by the oscilloscope traces shown in Figure 8.

5b. Preliminary Experiments with the 1 cm Discharge Chamber

The length of the 1 cm discharge chamber is such that there are four antinodes of the voltage standing wave along the length of the tube and presumably there is equal probability of the discharge starting at any one of these antinodes. A check was made to ensure that the discharge

characteristics did not depend on the location of the discharge. A second 1 cm chamber was made which was identical to the first one except there was a 0.02 inch slot x 2 inches long along the center of the broad face of the chamber. This was covered with a glass plate (a standard 3 inch microscope slide) which was secured with Apiezon W wax. Observing the discharges visually it was found that at about 5 mm Hg pressure there was a greater tendency for the discharge to occur at the antinode nearest the radar source. At 10 mm Hg pressure there was a greater tendency for the discharge to occur at any one of the four antinodes; the probability of the discharge occurring at any one of the antinodes increased with increasing gas pressure. Using a pressure of 15 mm Hg, it was found that the formative time of the discharge for a given set of conditions was independent of the location of the discharge, within the accuracy of measurement.

A series of photographs were taken of the light pulse from the discharge and the associated transmitted microwave pulse (see Figure 7). The photographs were taken at a gas pressure of 12.5 mm Hg, and using the 2.1 microsecond microwave pulse at a repetition rate of 300 pps; the discharge was located at the second antinode from the microwave

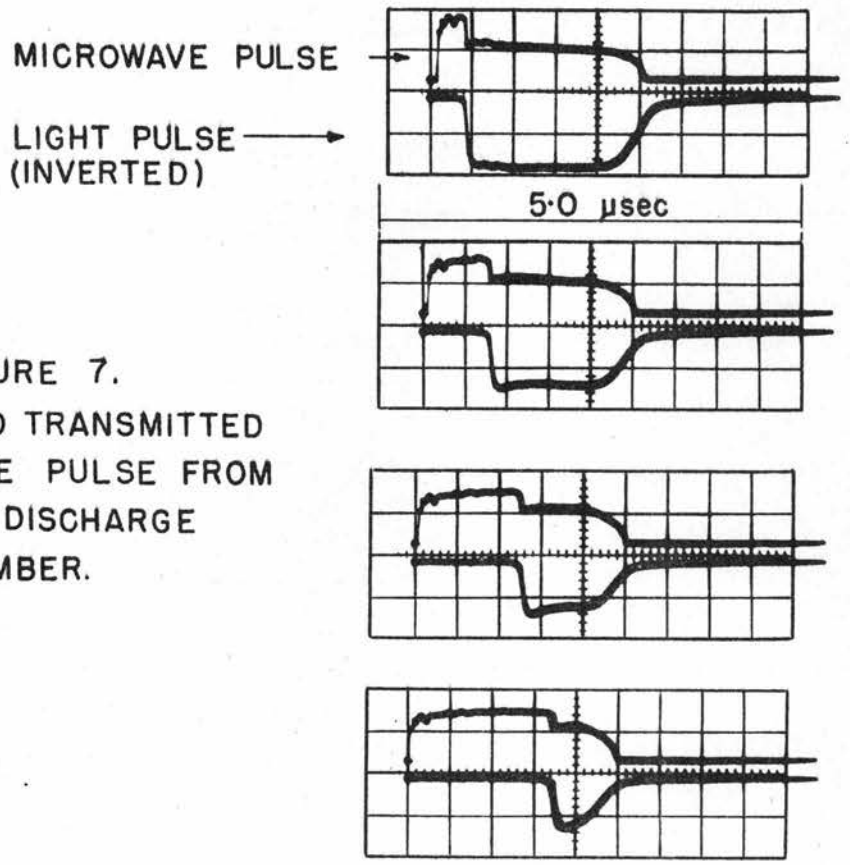

FIGURE 7.
LIGHT AND TRANSMITTED MICROWAVE PULSE FROM THE 1cm DISCHARGE CHAMBER.

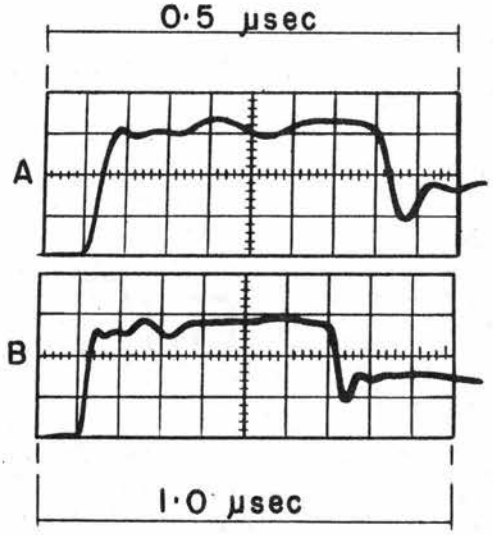

FIGURE 8.
"REFLECTED" MICROWAVE PULSE FROM THE 1 cm DISCHARGE CHAMBER.

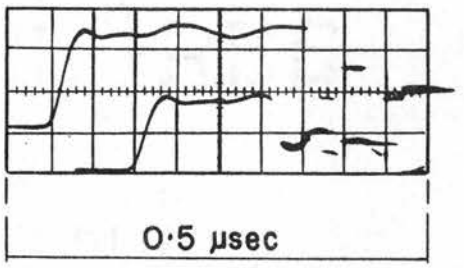

FIGURE 9.
"REFLECTED" MICROWAVE PULSE FROM THE 0·164 cm CONTOUR ASSEMBLY.

source. The horizontal scale on the photograph is 0.5 microsecond per square. The apparatus was changed slightly to obtain the transmitted microwave signal. The brass end plate on the chamber was replaced by a microwave window, followed by a slotted section of waveguide and then a stub tuner. The stub tuner was adjusted to place the voltage standing wave in the required location. The transmitted microwave signal was obtained from a probe inserted in the slotted-line. The purpose of recording the light pulse shape is to illustrate how rapidly the discharge reaches an equilibrium condition. Further reference to this point is made in Section 7a.

It was observed with the 1 cm discharge chamber that when the discharge first started the initial formative time was occasionally longer than the equilibrium value. However, for a given set of conditions the equilibrium value, which was attained after a period of several seconds, was always the same regardless of the initial value. A brief study was made of this point with the above chamber. It was visually observed that occasionally several discharges started simultaneously and, over a period of several seconds, all but one would slowly "die" out. This phenomena was accompanied with a longer

initial formative time which then reverted to its normal value (i.e. the equilibrium value) when there was only one discharge present.

Under certain conditions of gas pressure and microwave power, the reflected wave from the discharge sets up a large voltage standing wave with an antinode near the microwave window which produces a discharge across the window. Evidence of this was observed by the staining of the silver plating on the window flange.

A check was made with the final 1 cm chamber to determine the effects of possible impurities in the gas due to by-products from the gas discharge. A steady discharge was maintained under constant conditions for a period of 10 minutes and no change in the formative time of the discharge was observed. However, in order to minimize any long term effects the discharge chamber was pumped out and refilled every few minutes throughout the final experiment.

5c. Measurements to Determine $d\tau/dT$

The theory requires that the formative time of the discharge be measured as a function of the repetition rate of the microwave pulses at various pressures and microwave power levels. A range of

repetition rates of 250 to 450 pps was set by the operating conditions of the magnetron in the microwave power supply. The upper limit is within the range specified in Section 3d. A check was made to ensure that the shape of the microwave pulse was the same at all repetition rates; this then enabled the energy per pulse to be maintained at a constant value, when the repetition rate was varied, by varying the recorded power level in proportion to the repetition rate. All the data was taken using the 2.1 microsecond pulse length.

The required data were taken by setting the gas pressure and the repetition rate of the microwave pulses constant, then measuring the formative time of the steady state discharge as a function of power. The repetition rate was measured with the aid of a second oscilloscope. The data for the 1 cm chamber were repeated at least three times; the readings generally repeated to within about 3%. A certain amount of personal judgment was involved in measuring the formative time of the discharge. This is best illustrated by the photographs shown in Figure 8. The discharges were located in the 1 cm chamber; and the traces are for different power levels, a gas pressure of 10 mm Hg and a repetition rate of

400 pps. The horizontal scale is 0.05 microseconds per square on trace A, and 0.1 microseconds per square on trace B.

The necessary data to determine $d\tau/dT$ were also obtained with the contour assembly, using gap widths of 0.114, 0.164 and 0.214 centimeters. The data repeated to within about the same order of accuracy as for the 1 cm chamber but a lot more personal judgment was involved in determining the value of the formative time because of the variations in the formative time. This variation increased with the formative time. This point is illustrated in Figure 9 which shows two oscilloscope traces, at different power levels, taken with the 0.164 cm gap assembly and at a pressure of 12.5 mm Hg. The horizontal scale is 0.05 microseconds per square. The variation in the formative time of the longer pulse (i.e. the upper trace) is difficult to see because of the faint trace associated with the wide spread of the different oscilloscope sweeps.

6) RESULTS

6a. Experimental Results

With the 1 cm discharge chamber data were obtained at pressures of 4.9, 9.8, 15.1 and 19.6 mm Hg

(corrected to a temperature of 22°C), at repetition rates of 250 to 450 pps, in steps of 50 pps, and for formative times from 0.1 to 1.0 microseconds. A preliminary set of results for this experiment also included data obtained at higher gas pressures; reference to this will be made when required.

With the 0.114 cm gap assembly data were obtained at pressures of 4.9, 7.4, 14.7 and 19.6 mm Hg (corrected to a temperature of 22°C), at repetition rates of 250 to 450 pps and for formative times from 0.1 to about 0.5 microseconds. The variation in the formative time of the discharge prevented taking data for formative times larger than about 0.5 microseconds. A limited range of data was also taken with the 0.164 cm and the 0.214 cm gap assemblies, at pressures of 4.9, 7.4 and 12.5 mm Hg for the 0.164 cm gap, and 4.9 and 7.4 mm Hg for the 0.214 cm gap. Once again the large variation in the formative times limited the range of data that could be obtained.

A typical set of results of the formative time of the discharge versus the recorded microwave power is shown in Figure 10. The results are for the 1 cm chamber at 10 mm Hg pressure. Due to the shape of the microwave pulse it is necessary to correct the value of microwave power before evaluating $d\tau/dT$

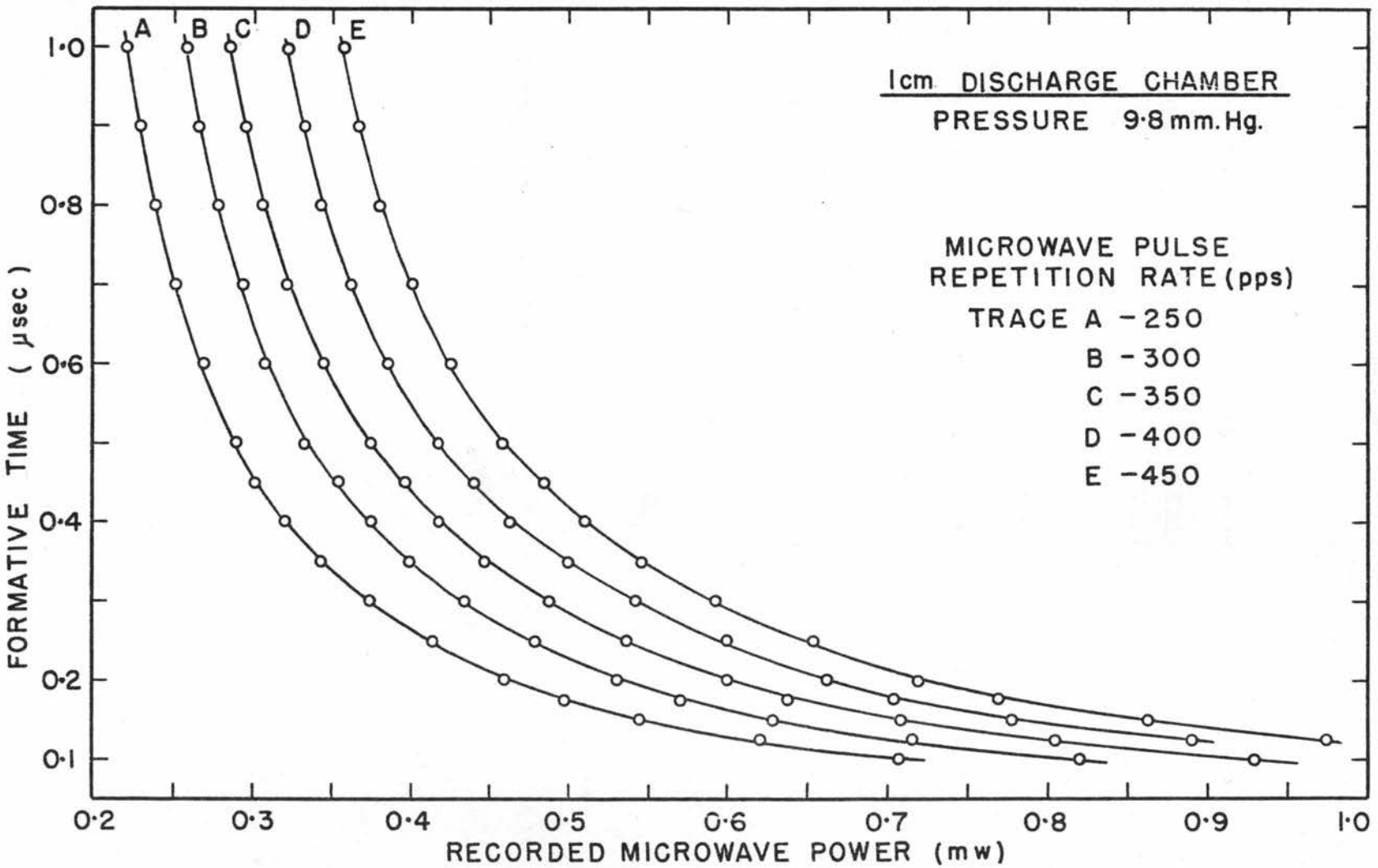

FIGURE 10. FORMATIVE TIME OF DISCHARGE - Vs - RECORDED MICROWAVE POWER

from the experimental results; this is described in detail in Section 6b. A plot of the corrected results from the above data is shown in Figure 11. From this type of graph a plot can be obtained of the formative time as function of the time between pulses, for a constant energy per pulse (see Figure 12). The power values to the right of the curves in Figure 12 are taken from the abscissa of Figure 11 for the data obtained at a repetition rate of 450 pps. In order to retain a constant energy per pulse the power values at the other repetition rates have to be reduced in proportion to the repetition rates. A complete set of graphs representing all the data for the formative time of the discharge versus the "corrected" recorded microwave power (such as Figure 11) is included in the appendix. Typical variations in the formative times are indicated by "error lines" on the graphs.

It can be seen from Figure 12 that the slope $d\tau/dT$ is very uniform and easily evaluated. However, at gas pressures above about 25 mm Hg the plots of τ versus T are definitely curved, particularly at the lower power levels and the lower repetition rates. The effect is shown in Figure 13; the plot is for 50 mm Hg pressure and is part of the preliminary data.

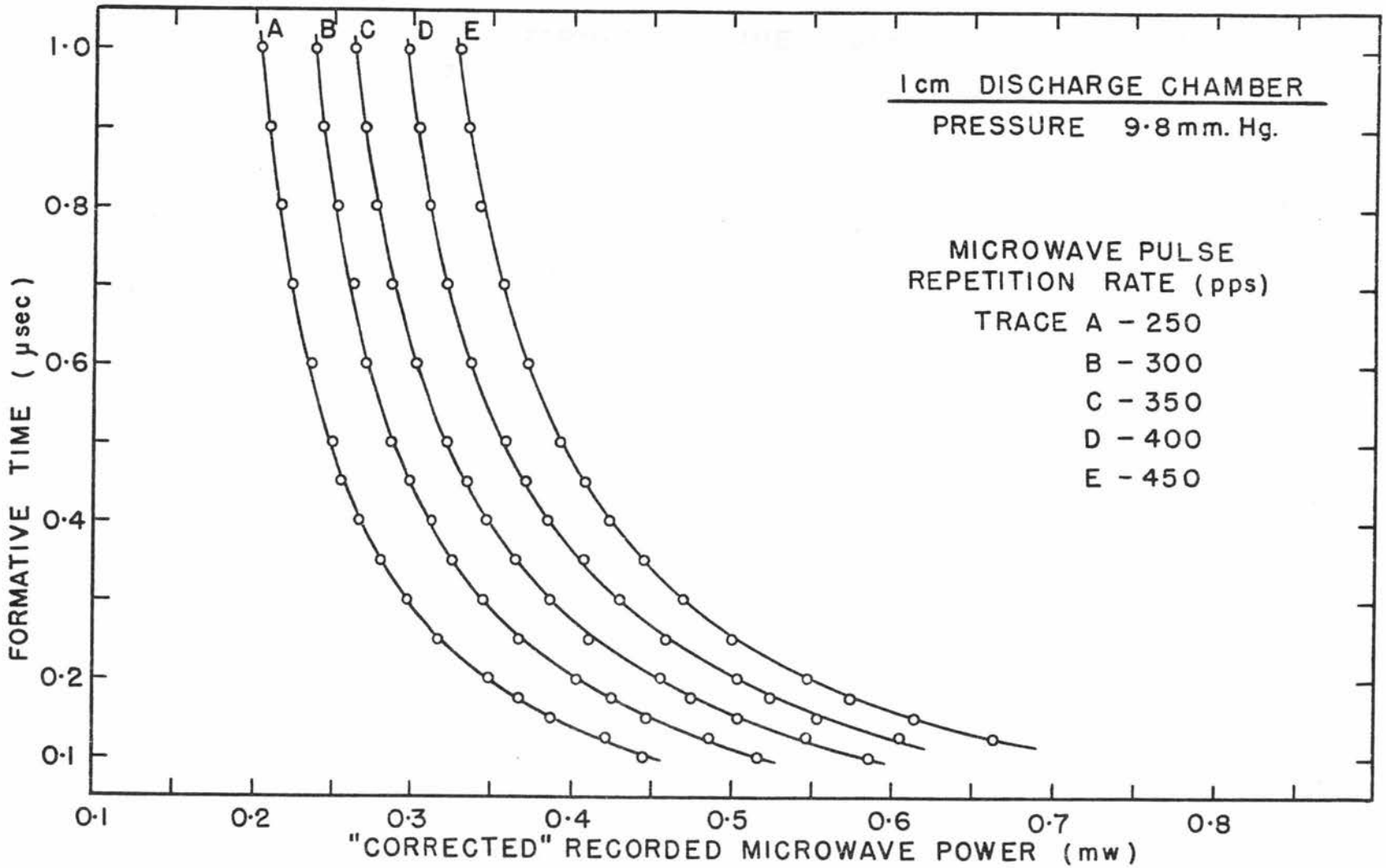

FIGURE II. FORMATIVE TIME OF DISCHARGE – Vs – "CORRECTED" RECORDED MICROWAVE POWER

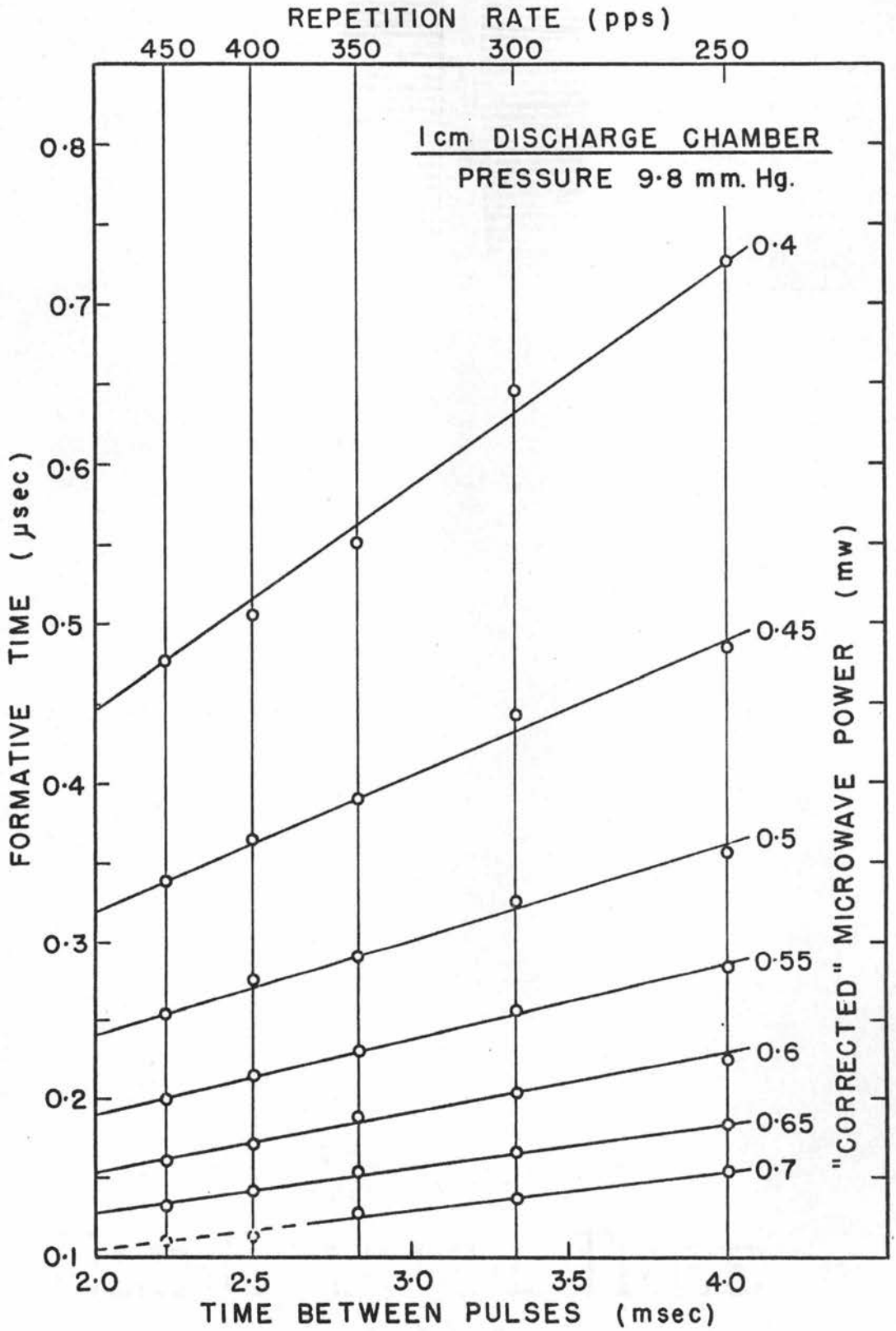

FIGURE 12. FORMATIVE TIME - Vs - TIME BETWEEN PULSES

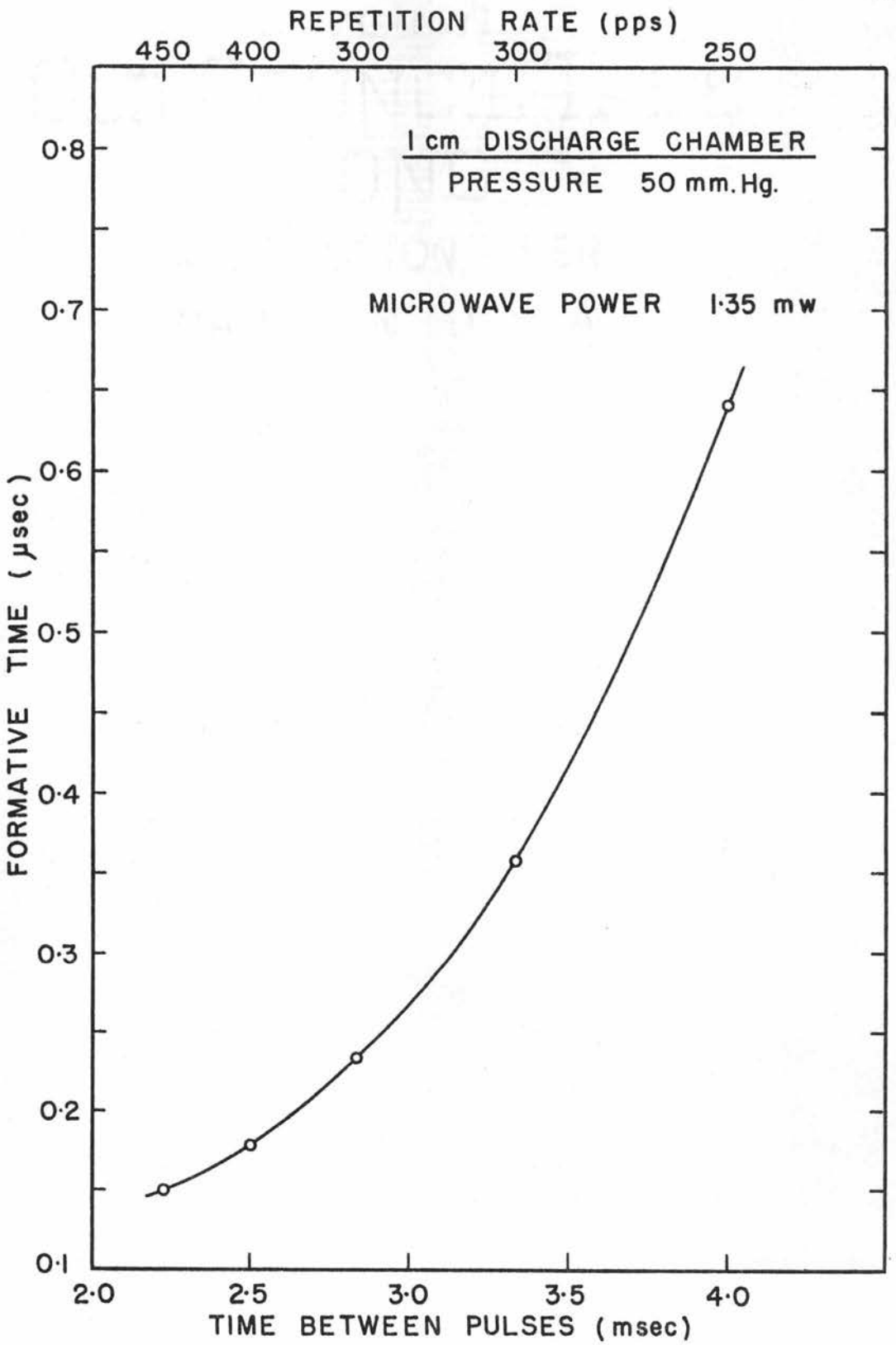

FIGURE 13. FORMATIVE TIME - Vs - TIME BETWEEN PULSES

A possible explanation for this type of result is that at the higher gas pressures there is a large electron loss by attachment, during the afterglow period, which will cause the electron density to decay rapidly. The diffusion coefficient may therefore start a transition from the ambipolar to the free-electron diffusion coefficient. As the value of the diffusion coefficient for the afterglow period increases, so will the value of the decay constant β . Likewise, a lower electron density at the beginning of the formation of the discharge may cause the diffusion coefficient to change from free-electron to ambipolar during this period. If the diffusion coefficients vary with time then so will the value of $d\tau/dT$ (see Equation 18). No results have been evaluated from this type of data.

With the value of $d\tau/dT$ obtained from plots such as Figure 12 the value of ν/p can then be obtained from Equation 19. This equation is used on the assumption that the diffusion losses are negligible at all times. A typical tabulation of the results is shown in Table 1.

TABLE 1

9.8 mm Hg - 1 cm discharge chamber

Power (mw)	$d\tau/dT$	$\frac{\beta/p^*}{d\tau/dT}$	$E_{m(sw)}$ volts/cm	$E_e/p^\#$ volts/ cm mm Hg
0.7	24×10^{-6}	2.88×10^6	1453	52.6
0.65	29.5×10^{-6}	2.34×10^6	1400	50.7
0.6	38×10^{-6}	1.82×10^6	1345	48.7
0.55	48×10^{-6}	1.44×10^6	1287	46.6
0.5	62×10^{-6}	1.11×10^6	1228	44.4
0.45	84×10^{-6}	0.82×10^6	1165	42.2
0.4	141×10^{-6}	0.49×10^6	1098	39.7

* $\frac{\beta}{p} = 69.1 \text{ (sec mm Hg)}^{-1}$ \# $\frac{E_e}{pE_{m(sw)}} = 0.0362 \text{(mm Hg)}^{-1}$

The first column marked "Power" is corrected recorded microwave power for a repetition rate of 450 pps (i.e. it is taken from the abscissa of graphs such as Figure 11). The second and third columns are self explanatory. The fourth column is the peak value of the electric field in the center of the discharge chamber, allowing for the standing wave (see Section 6c). The fifth column is the required coordinate for plotting the final results and it is obtained from the value of $E_{m(sw)}$ by the use of Equation 20.

The completed set of results for the 1 cm chamber is plotted on Figure 14; the expected error on the points not marked with error-lines is less than 10%. The value of $\frac{\nu}{p}$ obtained from the dc parameters (see Section 3f) is plotted on the same graph for comparison purposes. The results are discussed in Section 7g.

The results for the 0.114, 0.164 and 0.214 cm gap assemblies are given in Figures 15, 16 and 17 respectively, where the values of $69.1/(d\tau/dT)$ are plotted as a function of E_e/p. These results are discussed in detail in Section 7f.

6b. Correction Due to the Shape of the Microwave Pulse

An oscilloscope trace of the microwave pulse is shown in Figure 18; the horizontal scale is 0.25 microseconds per square. It is observed that the height of the pulse increases with time; therefore for small values of the discharge formative times (about 0.7 microseconds or less) the average microwave power present during the formation of the discharge is less than the average power throughout the pulse. Allowance must be made for this when determining the effective value of E_e/p.

The trace shown in Figure 18 was obtained using

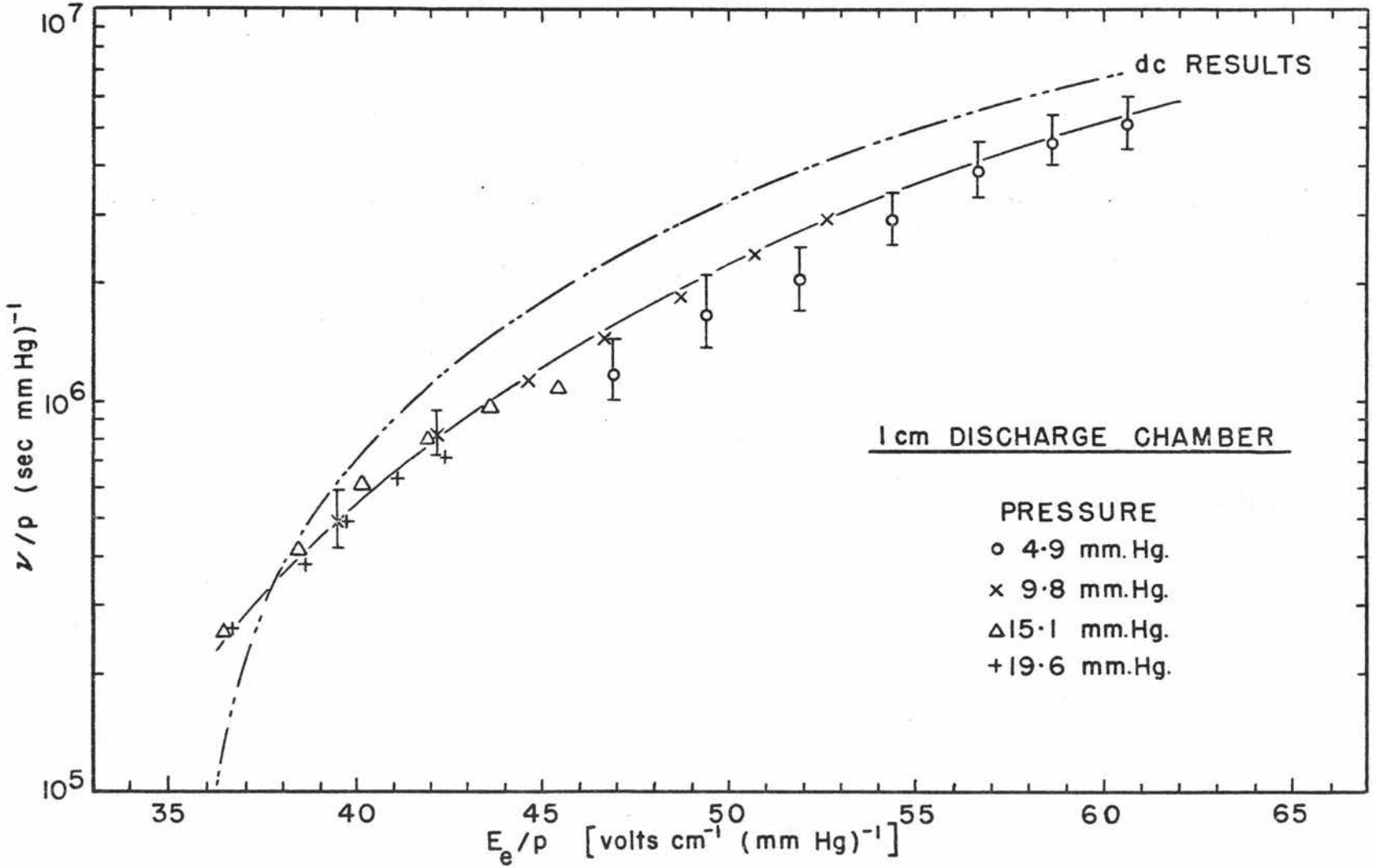

FIGURE 14. NET FREQUENCY OF IONIZATION – Vs – EFFECTIVE ELECTRIC FIELD

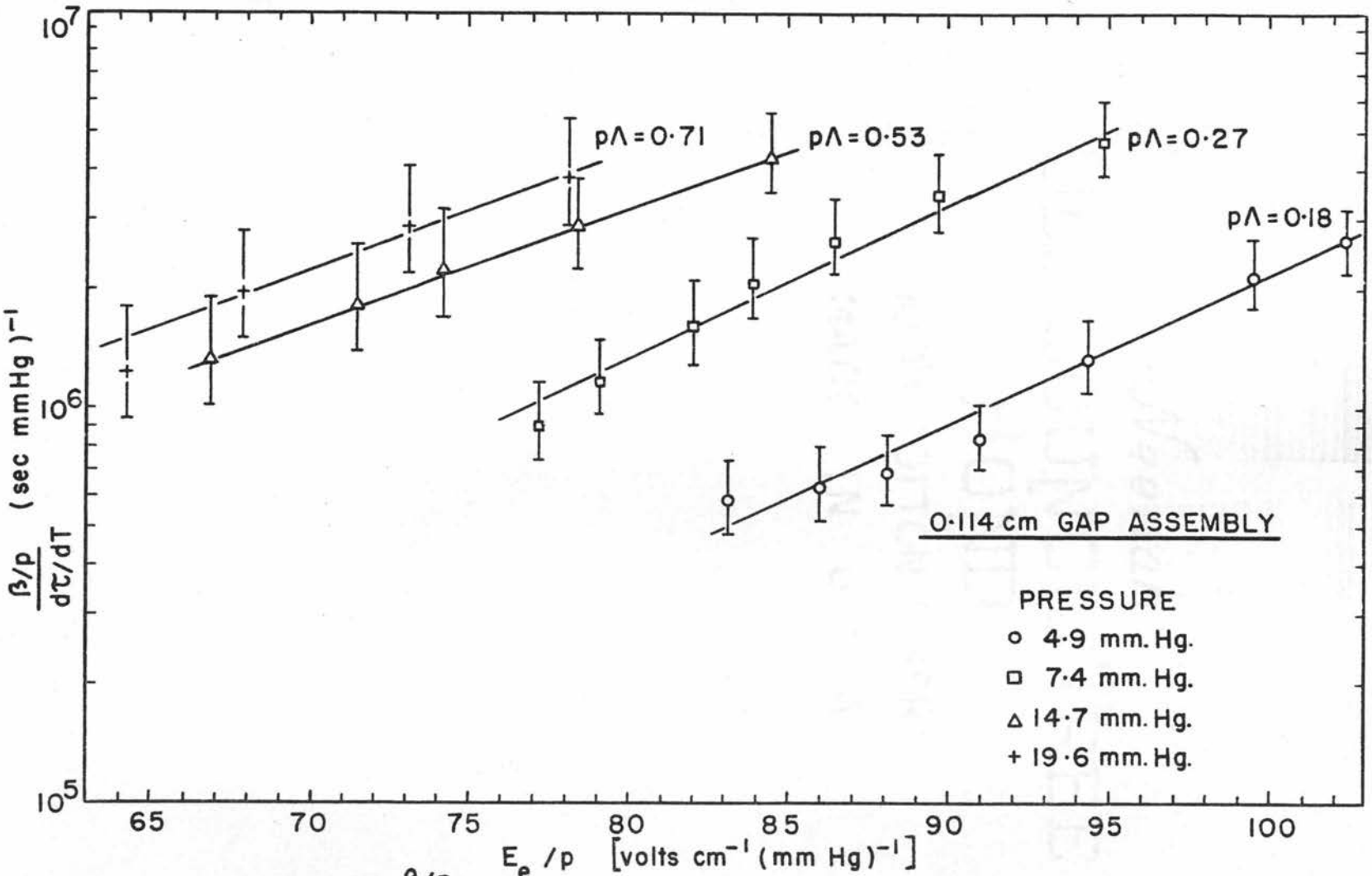

FIGURE 15. $\frac{\beta/p}{d\tau/dT}$ — Vs — EFFECTIVE ELECTRIC FIELD

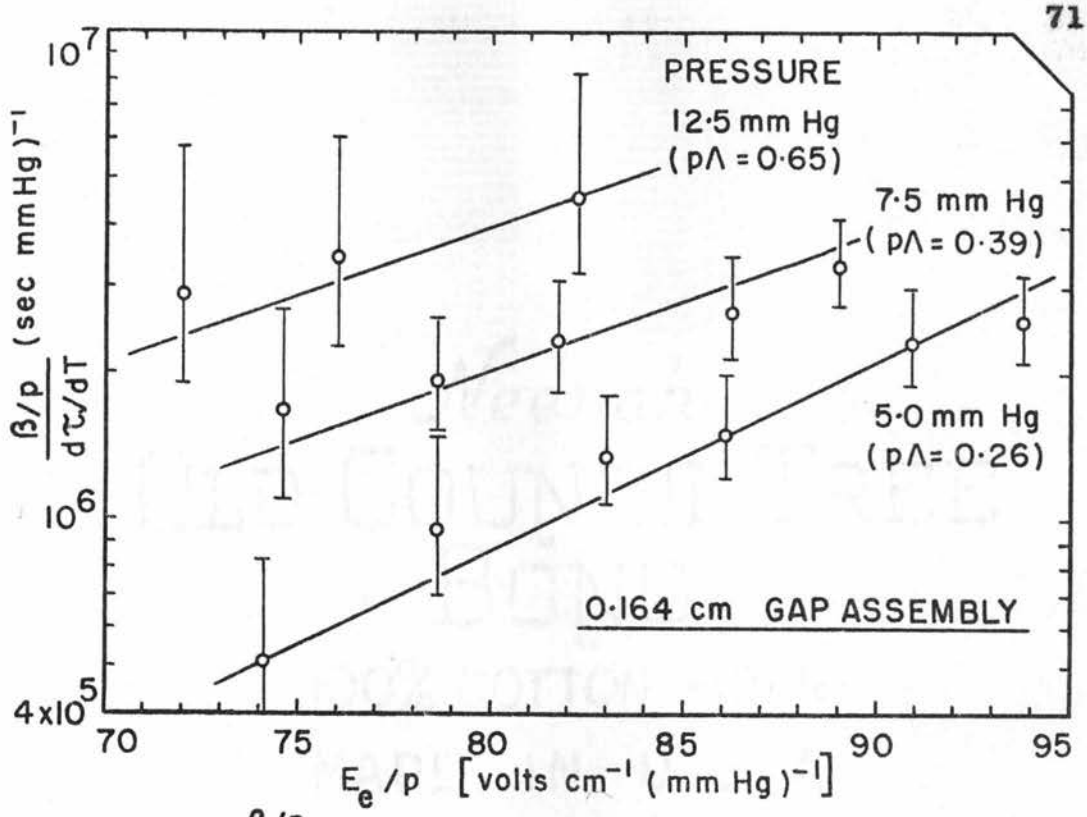

FIGURE 16. $\frac{\beta/p}{d\tau/dT}$ – Vs – EFFECTIVE ELECTRIC FIELD

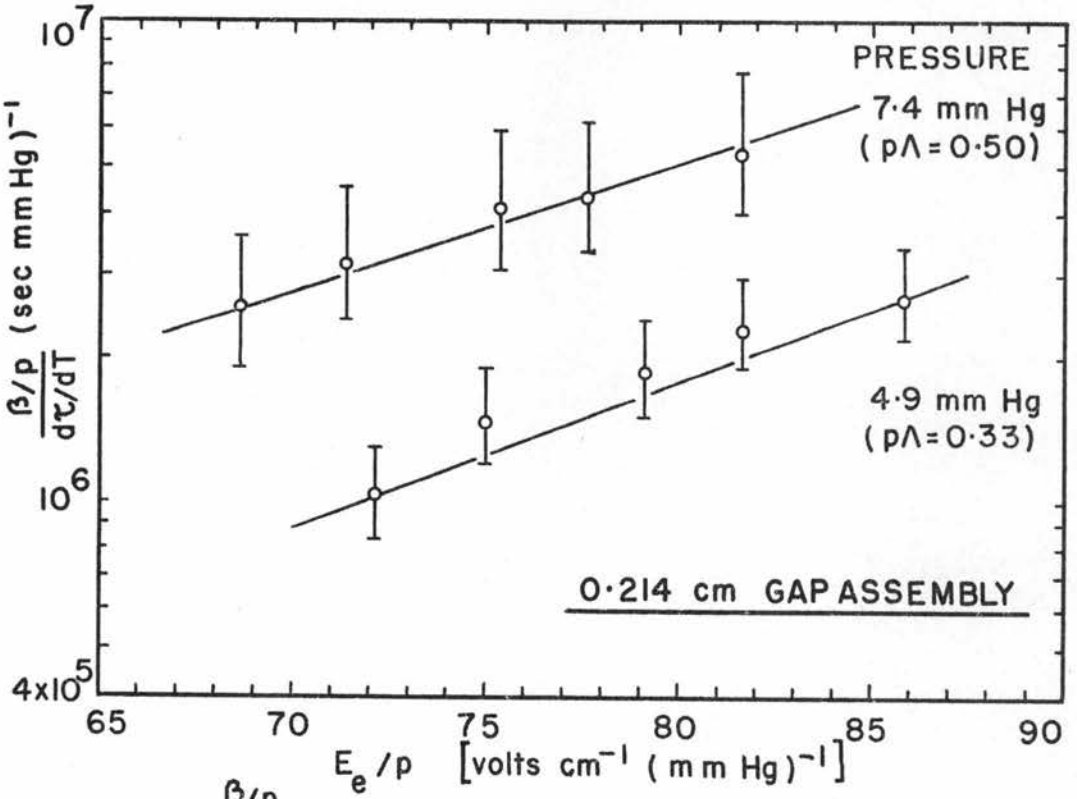

FIGURE 17. $\frac{\beta/p}{d\tau/dT}$ – Vs – EFFECTIVE ELECTRIC FIELD

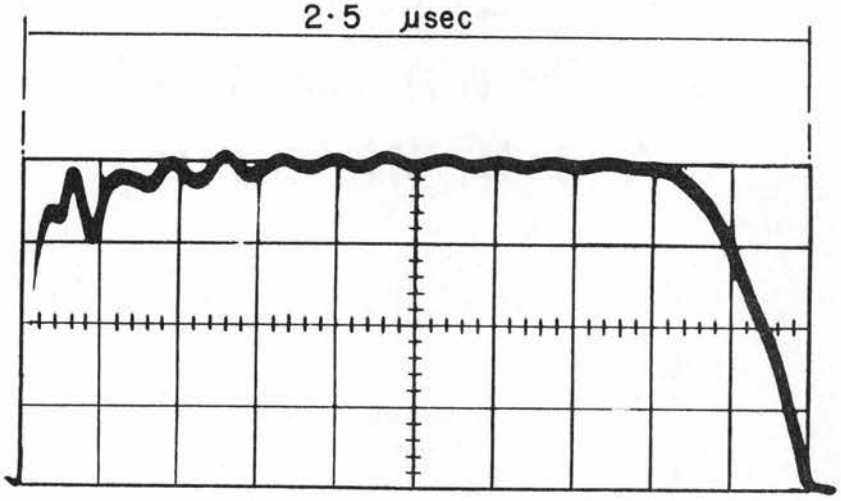

FIGURE 18. SHAPE OF THE MICROWAVE PULSE.

a 1N23 crystal with a 56 ohm resistor in parallel with it. The microwave power level was reduced to a low value so that the crystal response was linear. The voltage across the crystal was approximately 0.02 volts. The trace was viewed on a Tektronix Type 581 oscilloscope with a type B plug-in preamplifier and a type 81 plug-in adaptor. The rise time of the oscilloscope when using the 0.005 volts/cm vertical sensitivity scale is listed as 0.025 microseconds. With a 200 ohm resistor across the crystal, the pulse shape was almost identical except that the rise time was increased. There is some question as to whether the rise time of the pulse is limited by the microwave circuitry or the detection system. The rise time on the photographed trace is 0.06 microseconds. The manufacturer's specification sheet (44) for the type 725-A magnetron recommends that the voltage pulse for the magnetron have a rise time of 0.1 to 0.2 microseconds. It is therefore reasonable to assume that the rise time on the recorded trace is at least very close to the actual rise time of the microwave pulse.

The average power during the formation of the discharge is given by $(1/\tau) \int_0^{\tau} P \, dt = C \, P_m$ where τ

is the formative time of the discharge, P is the microwave power at time t, P_m is the maximum power (i.e. the top of the pulse shape) and C is a correction factor. Completing the left hand side of the equation by numerical integration for different values of τ , we obtain a tabulation of the power correction factor for different formative times (see Table 2). The correction factor is applied by multiplying the recorded average microwave power by C to obtain the effective average microwave power (referred to in the text as the "corrected microwave power").

TABLE 2

$\tau(\mu sec)$	C	$\tau(\mu sec)$	C	$\tau(\mu sec)$	C
0.05	0.447	0.35	0.816	0.75	0.896
0.1	0.632	0.4	0.832	0.8	0.902
0.125	0.681	0.45	0.844	0.9	0.913
0.15	0.713	0.5	0.860	1.0	0.922
0.175	0.747	0.55	0.864	1.2	0.934
0.2	0.762	0.6	0.876	1.4	0.944
0.25	0.767	0.65	0.884	1.6	0.952
0.3	0.794	0.7	0.891	2.0	0.961

6c. Calculation to Determine the Electric Field

The microwave power entering the discharge chamber is different from the recorded power because of the loss of power between the recording point and the discharge chamber, and due to the coupling factor between the main waveguide and the detector. The power loss was measured by placing an additional directional coupler, detector mount and power detector in place of the discharge chamber, and terminating the microwave circuit with a matched terminating load (Hewlett Packard Model X912A). The manufacturers calibration values were used for the coupling ratios in the directional couplers, and for the attenuation values in the fixed attenuators. The two power meters were calibrated according to the manufacturers specifications and the two gave identical readings when checked in a suitable microwave circuit. The results showed that the average microwave power entering the discharge chamber (or the contour assembly) was 817.4 times the recorded power reading.

It should be noted that the power meter measures an average power value whereas the microwave power is pulsed. The manufacturers specifications of the power meter states that power measurement of pulse

modulated signals is accurate down to a critical frequency which is below 100 pps for thermistor type detectors. The accuracy of the meter is listed as 5% of the full scale reading. The relation between pulse power in the discharge chamber and the recorded average power is obtained in the following manner:

Let P = recorded power meter reading in watts

P_{ave} = average power entering the discharge chamber = 817.4P

$$P_m = \text{pulse power} = \frac{P_{ave}}{\text{repetition rate x pulse length}}$$

The pulse length must be suitably defined. From Figure 18, if we define P_m to be the maximum height of the microwave pulse then the length of the pulse is given by $(1/P_m) \int P\,dt$ where the integral is taken over one microwave pulse. This yields a pulse length of 2.26 microseconds. The value of the repetition rate in the equation for P_m is 450 pps since all power values are referred to this value. With these values we obtained the relation

$$P_m = 80.37 \times 10^4 P$$

The relation between the pulse power and the peak electric field E_m, at the center of a rectangular waveguide operating in the dominant TE_{01} mode, is

obtained from the Poynting vector (38, p. 171). The power P_m transmitted through the waveguide is given by

$$P_m = 1/2 \epsilon \int E^2 \, dv \, u$$

where E is the peak value of the electric field, $1/2 \epsilon E^2 dv$ is the energy per volume element dv and u is the velocity of propagation of the microwave power in the waveguide. For the TE_{01} mode of propagation the electric field distribution across the guide is $E_m \sin (y \pi /b)$, where b is the width of the guide and y is the distance from one edge. The field is uniform in the x direction, which is across the shortest dimension of the waveguide. The height of the waveguide is given by a. Therefore the value of P_m is given by

$$P_m = 1/2 \epsilon E_m^2 \, u \, a \int_o^b \sin^2 (y \pi /b) \, dy = 1/4 \epsilon E_m^2 \, uab$$

Writing $u\epsilon = \dfrac{\epsilon}{(\mu\epsilon)^{1/2}} = (\epsilon/\mu)^{1/2}$

$$= \frac{(\epsilon/\epsilon_o)^{1/2}}{(\mu/\epsilon_o)^{1/2}} = \frac{\lambda_o/\lambda_g}{(\mu_o/\epsilon_o)^{1/2}}$$

where μ may be set equal to μ_o; $(\mu_o/\epsilon_o)^{1/2}$ is the resistivity of free space = 376.7 ohms, and λ_o and λ_g are the wavelengths of the microwaves in free

space and in the waveguide, respectively. These calculations yield the value

$$P_m = 6.63 \times 10^{-4} E_m^2 \, ab \, \frac{\lambda_o}{\lambda_g}$$

In this experiment the value of λ_o is 3.19 cm, as measured with a frequency meter placed in the power detector arm, and λ_g equals 4.46 cm.

The actual value of the peak electric field is greater than E_m because of the reflections within the discharge chamber. It is assumed that the signal is reflected 100% from the metal plate at the back of the chamber. A portion of the reflected signal is reflected back into the discharge chamber by the microwave components; this reflectivity was measured by replacing the discharge chamber with a slotted waveguide, a ferrite isolator and a klystron. With the magnetron turned off a voltage standing wave ratio of 1.57 was measured; this represents a power reflection of 4.8%. Therefore, the actual peak electric field $E_{m(sw)}$ equals 2.048 E_m.

For the 1 cm discharge chamber the values of a and b are 1.03 cm and 2.29 cm, respectively, therefore

$$E_{m(sw)} = 5.49 \times 10^4 \, (P \text{ watts})^{1/2}$$

where P is the recorded power meter reading in watts.

When using the contour assembly as a discharge chamber there is an additional loss factor due to the creation of non-transmittal modes at the points where the height of the waveguide decreases, i.e. at the contours (see part two). For the 0.114 cm gap assembly the loss in transmission is 10.6% whereas the reflection loss is less than 0.5%. For the 0.214 cm gap assembly the loss in transmission is 12%, with the same reflection loss. For simplicity the reflection loss has been ignored and it has been assumed that 50% of the transmission loss occurs on either side of the center line of the contour.

For all the contour assemblies the width b of the gap equals 2.29 cm. The values of a are 0.114, 0.164 and 0.214 cm. These values yield the following relations:

$E_{m(sw)} = 15.7 \times 10^4 \text{ (P watts)}^{1/2}$ for the 0.114 cm gap assembly

$E_{m(sw)} = 13.1 \times 10^4 \text{ (P watts)}^{1/2}$ for the 0.164 cm gap assembly

$E_{m(sw)} = 11.3 \times 10^4 \text{ (P watts)}^{1/2}$ for the 0.214 cm gap assembly

7. DISCUSSION

7a. Error Involved by Neglecting the Term d/dT (ln n_b/n_f)

An estimate of the maximum error involved by neglecting the term d/dT (ln n_b/n_f) may be obtained from energy considerations. We will assume that a negligible amount of the incident power is absorbed by the discharge before the critical electron density n_b is attained, and that a portion X of the incident power P goes into the production of electrons when the electron density exceeds n_b. It is also assumed that the final electron density n_f is determined by the absorbed power and is not limited by recombination, electron attachment or diffusion; therefore these calculations will place an upper limit on the error involved. Let the length of the microwave pulse be L = 2.26 microseconds (see Section 6c), then the value of n_f is given by

$$n_f = \frac{XP(L - \tau)}{12.57 \text{ ev}}$$

where the value 12.57 ev is the ionization energy of molecular oxygen. Now

$$d/dT \ (\ln n_b/n_f) = \frac{-d}{dT} (\ln n_f) = \frac{-1}{n_f} \frac{dn_f}{dT} = \frac{\frac{XP \ (d\tau/dT)}{12.57}}{\frac{XP \ (L - \tau)}{12.57}},$$

$$d/dT \ (\ln n_b/n_f) = \frac{d\tau/dT}{(L - \tau)}$$

Therefore if we include the term d/dT (ln n_b/n_f) in the calculations for ν/p then, neglecting the diffusion losses, from Equation 17 we have

$$p \frac{d\tau}{dT} \frac{\nu}{p} = \beta + d/dT \ (\ln n_b/n_f) = \beta + \frac{d\tau/dT}{(L - \tau)}$$

$$\text{therefore } \frac{\nu}{p} = \frac{\beta/p}{d\tau/dT} + \frac{1}{p\ (L - \tau)}$$

Since the value of τ varies from 0.1 to 0.5 microseconds, the value of $(L - \tau)$ is approximately 2.0 microseconds. Therefore the error involved by neglecting the term d/dT ln (n_b/n_f) is given by

$$\Delta \frac{\nu}{p} = \frac{10^6}{2p} \text{ (sec mm Hg)}^{-1}$$

At a pressure of p = 5 mm Hg, $\Delta (\nu/p)$ equals 10^5 (sec mm Hg)$^{-1}$ compared with the minimum experimental value of (ν/p) equal to 10^6 (sec mm Hg)$^{-1}$. At 20 mm Hg, $\Delta (\nu/p)$ equals 2.5×10^4 (sec mm Hg)$^{-1}$ compared with the minimum experimental value of (ν/p) equal to 2.6×10^5 (sec mm Hg)$^{-1}$.

The calculations show that within the approximations made in this experiment the error involved by neglecting the term d/dT ln (n_b/n_f) is negligible. One further piece of evidence on this matter is the shape of the light pulse emitted by the discharge

in the 1 cm dischamber (see Figure 8 and Section 5b). The light pulse attains an equilibrium level very rapidly thus suggesting that the electron density also attains an equilibrium value before the end of the microwave pulse. Therefore no change in the final electron density n_f would be expected for small variations in the formative time. (NOTE. Rose and Brown (46) used the intensity of the light emitted from a microwave discharge as an indication of the variation of the electron density).

7b. Criticism on the Decay Constant of the Electron Density

The value of the decay constant, of the electron density in the microwave afterglow, that is used to determine the net frequency of ionization was obtained from experiments by Sexton et al (51, vol. 1, p. IA94; 49, p. 493) using a microwave cavity. The discharge in their experiment was contained within a quartz bottle 1.5 cm diameter x 3.0 cm high, located in the center of a microwave cavity 2.1 cm diameter x 3.77 cm high (50). The Q of the cavity was 3100, and the pulsed microwave power used to produce the discharge was between 5 to 35 kw with a pulse length of one microsecond. Ignoring the presence of the quartz bottle these figures yield

values of E_e/p of from about 1,000 to 3,000 volts $(cm\ mm\ Hg)^{-1}$ at a gas pressure of 20 mm Hg.

It is explained in Section 3c that the decay rate of electrons in a microwave afterglow in oxygen is believed to be the result of a balance between attachment and detachment of electrons; the detachment resulting from collisions of the negative ions with vibrationally excited neutral molecules, which are formed during the microwave discharge. From this one might argue that the number of excited neutral molecules and the degree of excitation may depend on the value of E_e/p of the applied microwave signal, and consequently the value of the decay constant might vary with the value of E_e/p. Sexton et al states that "no change in the decay rate was found" over the values of power used. However, their published results indicate a tendency for the decay rate to increase slightly with decreasing E_e/p, amounting to about a 20% increase over the value used in this experiment at E_e/p equal to about 50 volts $(cm\ mm\ Hg)^{-1}$. The high values of E_e/p used in Sexton's experiment would only exist for a short period of time during the formation of the discharge because the Q of a cavity decreases as the electron density increases. This decrease in Q

would decrease the value of E_e/p. The limitations of the microwave cavity techniques have been studied by Persson (39) who has shown that at a gas pressure of about 16 mm Hg (i.e. when $\nu_c = w$) the Q of a cavity decreases to 10 or less when the electron density is greater than one-fifth of the critical electron density. At a Q value of 10 the above microwave power levels give values of E_e/p of 57 to 170 volts (cm mm Hg)$^{-1}$. These values would decrease further as the electron density approaches and exceeds the critical value. In addition, it is observed experimentally that when the electron density is less than the critical value then only a small portion of the incident power is absorbed by the electrons. Therefore one would not expect much energy to be absorbed during the period when the value of E_e/p is large.

The conclusion to be drawn from the above comments is that the value of the decay constant, of the electron density during the afterglow period, should not depend greatly upon the value of E_e/p of the incident microwave power. Therefore, we are justified in using the value obtained by Sexton *et al*.

7c. Increase in the "Effective" Electric Field due to the Electrons

In Section 3b, Equation 8 was obtained under the assumption that the net frequency of ionization ν was constant throughout the formation of the discharge. However, due to the presence of the electrons the effective electric field, and hence ν, increases as the electron density increases. The effect of this is to speed up the rate of production of electrons and decrease the formative time. Since the calculations for the net frequency of ionization depend on the rate of change of the formative time and not on the magnitude, then no error should be introduced since the process should be the same for a given power level. However, the correction in the value of the electric field, due to the shape of the microwave pulse, is dependent on the magnitude of the formative time and so an estimate of the error involved should be made.

The ratio between the electric field E_d in a homogeneous discharge medium and the electric field E_g in the gas-filled waveguide for a TE_{01} mode of electromagnetic propagation is given by (12) (see Section 6c)

$$(E_d/E_g)^2 = \gamma_g/\gamma_d = \lambda_d/\lambda_g$$

where γ is the phase constant, λ is the waveguide wavelength and the subscripts g and d denote the gas and discharge regions respectively. From Equation 2 we have the relation

$$\partial^2 E / \partial z^2 + K^2 E = 0$$

Let $K = \gamma + j\alpha$, then the solution to Equation 2 is

$$E = E \exp(jKz) = E \exp(-\alpha z + j\gamma z)$$
$$= E_o \exp(-\alpha z) + j(\gamma z - wt)$$

where α is the attenuation factor and γ is the phase constant. Therefore $K^2 = (\gamma + j\alpha)^2 = \frac{w^2}{u^2}\left[1 + \frac{j\sigma}{w\epsilon}\right]$, from Equation 3. Substituting for the conductivity σ, expanding the terms and equating the real and imaginary parts yields

$$\gamma^2 - \alpha^2 = \frac{w^2}{u^2}\left[1 - \frac{ne^2}{m\epsilon(\nu_c^2 + w^2)}\right] \quad \text{and}$$

$$2\alpha\gamma = \frac{w^2}{u^2}\left[\frac{ne^2\nu_c}{m\epsilon w(\nu_c^2 + w^2)}\right]$$

These are the same equations as obtained from Equation 4 where $\gamma = \eta w/u$ and $\alpha = \eta Xw/u$. In the discharge region the phase constant γ_d is given by the above value of $\gamma = \eta w/u$. In the discharge-free region the phase constant γ_g is given by $\gamma = w/u$ (i.e. $\eta = 1$). Therefore the required ratio E_d/E_g equals $\eta^{-1/2}$. Since a portion of the incident power is

reflected by the discharge then the correct value of E_d/E_g is given by $(1 - R)^{1/2} \eta^{-1/2}$, where R is the reflectivity of the discharge. The value of E_d/E_g is plotted as a function of the electron density ratio n/n_c in Figure 19.

In order to determine at what point of the discharge the electric field starts to increase, it is necessary to make a plot of the expected "reflected" microwave signal so that the approximate value of n_b may be determined. The detected microwave signal is the sum of the power reflected from the discharge and the transmitted power after it has passed through the discharge twice. The reflected power is given by R, and the transmitted power equals $(1 - R) \exp (8\pi \eta Xz/ \lambda g)$. The discharge length z is approximately 0.5 centimeters, as determined experimentally with the 1 cm discharge chamber with the window along one side. This yields that the "reflected" microwave signal is given by $R + (1 - R) \exp (-3 \eta X)$. A plot of this curve is given in Figure 19.

It is observed from Figure 19 that the theory predicts an increase in the electric field up to an electron density of about n_c, then it starts decreasing. One would expect the increase in the electric

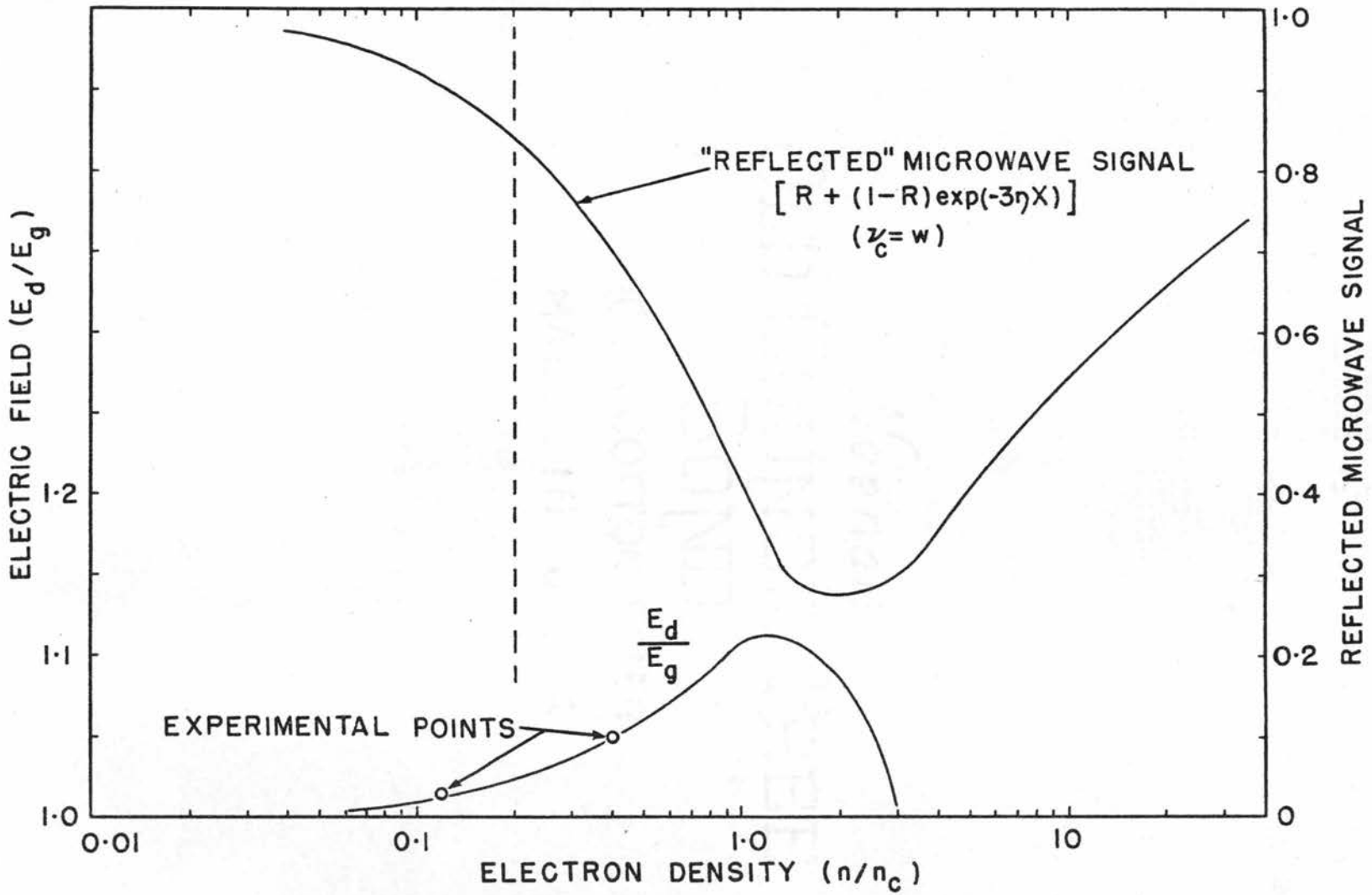

FIGURE 19. ELECTRIC FIELD — Vs — ELECTRON DENSITY

field due to the presence of the electrons to continue increasing with the electron density. This therefore places some doubt on the theory. The results show that the "effective" electric field E_d is about 1.01 E_g at an electron density of $0.1n_c$, and E_d = 1.1 E_g at the critical density n_c. Experimental results by Anderson and Goldstein (3) show that a waveguide wavelength of 5.64 cm is increased to 6.18 cm in the presence of a discharge having an electron density of $1.45 \times 10^{11}/cm^3$ and is increased to 5.79 cm at a density of $4.2 \times 10^{10}/cm^3$. Using Equation 5 to determine the value of n_c shows that at a density of 0.4 n_c the value of E_d equals 1.05 E_g, and at a density of 0.1 n_c the value of E_d equals 1.015 E_g. These values compare favorably with the graph on Figure 19, which tends to confirm the theory in the region of interest. Assuming that the formative time is measured up to the point when the electron density n_b = 0.2 n_c, then the "effective" electric field only increases about 1% at an electron density of n = 0.5 n_b, and a maximum of about 3% at n_b. Since the electron build-up is very rapid in this region it is considered that the small increase in the electric field due to the presence

of the electrons is negligible and may consequently be ignored.

It should be noted that experimentally the "reflected" microwave signal exhibits a much sharper demarcation point, when the discharge forms, than is shown by Figure 19. Assuming that the electron density builds up exponentially, then the abscissa scale represents a linear time scale. This may therefore be compared with the photographs of the microwave signal in Figure 7 which illustrates the relatively abrupt attenuation of the signal that is observed experimentally.

7d. Accuracy of Measurements

The recorded data on the graphs such as Figure 10 are the arithmetric average of the three or four sets of data. The calculations for the error in the value of the net frequency of ionization, due to errors in measurements, are based on the variation in the formative time τ of the discharge due to the limit of accuracy with which the microwave power meter and the gas pressure gauge can be read. The accuracy of the power meter readings, including the zero error, is about 1/4 division which corresponds to 0.0025 mw. The accuracy of the reproducibility

of the pressure gauge was measured to be 0.25 mm Hg (see Section 4c).

The procedure is to find the error in τ at repetition rates of 250 and 450 pps, due to the limit in accuracy of measuring the power and the pressure. This is obtained from plots of formative time versus microwave power at a constant gas pressure, such as Figure 10, and from plots of formative time versus pressure at a constant power level. The deviation in τ at a given repetition rate is then given by $\Delta\tau_{pps} = \sqrt{(\Delta\tau_1)^2 + (\Delta\tau_2)^2}$, where $\Delta\tau_1$ and $\Delta\tau_2$ are the errors in τ due to the accuracy of measuring the microwave power and the gas pressure, respectively. The variation in the value of $d\tau/dT$ is then determined by the slope of the lines which pass through the extremes of $\Delta\tau$ at the two repetition rates, that is

$$\pm\, \Delta\,(d\tau/dT) = \frac{\Delta\tau_{250} + \Delta\tau_{450}}{(1/250 - 1/450)}$$

The error in the value of the net frequency of ionization ν is then obtained from Equation 19 $\nu/p = (\beta/p)/(d\tau/dT)$, therefore

$$\Delta\,(\nu/p) = \frac{\beta/p}{m}\left[\frac{-\Delta m}{m} + \left(\frac{\Delta m}{m}\right)^2 - \left(\frac{\Delta m}{m}\right)^3 + \ldots\right]$$

where $m = d\tau/dT$ and $\Delta m = \pm \Delta (d\tau/dT)$. The expected deviations in the value of (ν/p) are given by the "error-lines" on the plots of ν/p versus E_e/p.

It should be noted here that there are large variations in the formative times of the discharges produced in the contour assembly which are very difficult to interpret in terms of variations in the value of the net frequency of ionization. One method of analysis would be to plot graphs for the value of τ measured to the beginning and to the end of the observed variations in τ. However, due to the uncertainties in the results it is considered that the time spent on such an analysis would not be justified.

7e. Gas Purity

The oxygen gas used in this experiment was tank oxygen supplied by the National Cylinder Gas Company. The listed purity value is 99.5% or better; the average tank analysis yields a value of 99.7%. The listed known impurities are 0.01% N_2 and the remainder is argon. The question of gas purity was considered by Prasad and Craggs (42, p. 385-398) in their measurement of the net ionization coefficient in oxygen. They use pre-dried tank oxygen of 99.5%

purity for their general experiments, and spectroscopically pure oxygen for a comparison experiment. The gas was dried further by passing it through a cold trap containing a mixture of solid CO_2 and acetone. No apparent differences were noted due to the different levels of impurities and the results of the experiments are in good agreement with those of other workers who used high purity gases. Since the vacuum system with which this present experiment was carried out was not designed as a high-vacuum system it was decided to run the experiment with tank oxygen. The vacuum system includes a cold trap containing a mixture of solid CO_2 and acetone and a second trap containing liquid nitrogen, to remove the water vapor from the gas. The impurity in the gas due to the base pressure of the mechanical vacuum pump amounts to 0.015% in the reservoir and 0.03%, at 10 mm Hg pressure, in the discharge chamber. However, by flushing out these systems the gas impurity levels were undoubtedly reduced. The gas impurity due to leaks in the reservoir amounts to about 10^{-5}% per minute and about 0.01% per minute in the discharge chamber when at a pressure of 10 mm Hg. The discharge chamber was flushed out

every three to four minutes during the experiment to avoid the possible accumulation of gas impurities due to by-products from the gas discharge.

The gas purity is therefore limited by the quality of the gas from the manufacturer. However, it is obvious that the vacuum system is not adequate to justify using high purity gas. In view of the results of Prasad and Craggs it is felt that the gas impurities in this experiment have little effect, if any, on the final results.

7f. The Results from the Contour Assembly

The values of $(\beta/p)/(d\tau/dT)$, with $\beta/p = 69.1$ (sec mm Hg)$^{-1}$, are plotted as a function of E_e/p for the 0.114 cm gap on Figure 15 and for the 0.164 cm gap and the 0.214 cm gap on Figures 16 and 17 respectively. It is quite evident from these results that in addition to the electron loss by attachment, given by the above numerical value of β/p, there are additional loss factors which are presumably loss by diffusion. If we include the diffusion loss during the formation period of the discharge and in the afterglow period, then from Equations 13 and 18 we obtain the equation

$$\frac{\nu}{p} = \frac{1}{d\tau/dT}\left[\frac{\nu_a}{p} + \frac{D'p}{(p\Lambda)^2}\right] + \frac{Dp}{(p\Lambda)^2}$$

where the "electron attachment" decay is given by $\nu_a/p = 69.1$ (sec mm Hg)$^{-1}$, and D' and D are the diffusion coefficients during the periods of the afterglow and discharge formation, respectively. To allow for the diffusion loss during the afterglow period the results in Figure 15, 16 and 17 must be multiplied by the factor

$$\frac{\nu_a/p + D' p/(p\Lambda)^2}{\nu_a/p}$$

To allow for the diffusion loss during the formation of the discharge a constant equal to $(Dp)/(p\Lambda)^2$ must be added to the results in Figures 15, 16 and 17. The only limitation that the experiment places on these two factors is that if the primary electron loss mechanism is by attachment, then at a value of $p\Lambda = 1.5$ cm mm Hg the value of $(D'p/(p\Lambda)^2$ must be small compared to ν_a/p (see Section 3h); that is we require

$$\frac{\nu_a}{p} = 69.1 \gg \frac{D' p}{1.5^2} ,$$

therefore $D' p \ll 155$ mm Hg cm^2/sec. The results for the 0.114 cm gap were used to determine the value of D' and D. About the best alignment that could be obtained from the results in Figure 10 is with the values of $D'p = 5$ mm Hg cm^2/sec and $Dp = 2 \times 10^5$ mm Hg cm^2/sec, the results are shown in Figure 20.

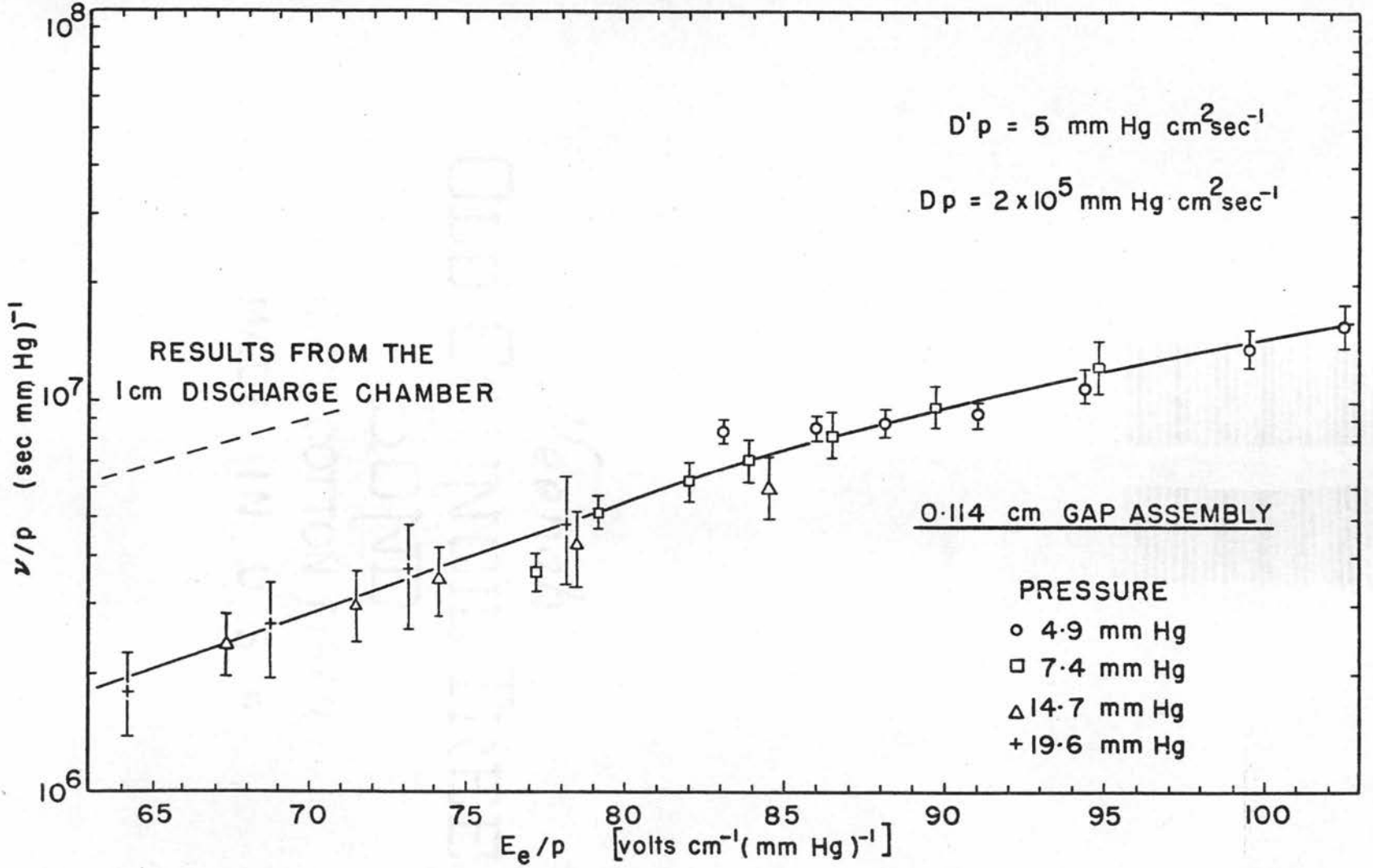

FIGURE 20. NET FREQUENCY OF IONIZATION - Vs - EFFECTIVE ELECTRIC FIELD.

These results were determined graphically by using different values of D'p and Dp. In general it is found that a larger value of D'p separates the results for $p\Lambda = 0.27$ and $p\Lambda = 0.18$. A larger value of Dp separately aligns the results for $p\Lambda = 0.27$ with those for $p\Lambda = 0.18$, also $p\Lambda = 0.72$ with $p\Lambda = 0.59$ but not all four values of $p\Lambda$; decreasing the value of Dp separates the results for $p\Lambda = 0.27$ and $p\Lambda = 0.18$. The results plotted in Figure 20 presumably have all the loss factors accounted for and the ordinate is labelled ν/p accordingly.

A comparison between Figures 14 and 20 shows that the values of ν/p obtained from the results of the contour assembly are only about one-third of those obtained from the results of the 1 cm discharge chamber. Furthermore, the above experimental values of the diffusion coefficients are not in agreement with those given in Section 3g. Assuming that ambipolar diffusion exists during the formation period then from Section 3g the value of Dp is between 1.3×10^4 to 8×10^4 mm Hg cm^2/sec, depending on whether one uses the theoretical value of $D_a = D_e/250$ or $D_a = D_e/40$ and if the value of $D_e p = 3.2 \times 10^6$ mm Hg cm^2/sec is used [value by Bröse

for E_e/p = 80 volts (cm mm Hg)$^{-1}$]. Assuming that ambipolar diffusion exists in the afterglow period then the value of D'p is between 33 to 66 mm Hg cm^2/sec, depending on whether the primary electron decay mechanism is electron attachment, so that many negative ions are formed, or by diffusion. If the predominant loss mechanism is electron attachment, then from Equation 13 we see that the value of ν_a/p should be very much larger than the value of $D'p/(p\Lambda)^2$. The maximum value of $(p\Lambda)^2$ is 0.5 (mm Hg cm)^2, therefore, using the minimum value of D'p equal to 33 mm Hg cm^2/sec we see that the loss by diffusion is equal to or greater than the loss by attachment. Under these circumstances the value of x in Equation 13 is equal to or greater than one-half, and the equation reduces to $D_a = 2D_+ = 66$ mm Hg cm^2/sec. The results for the three contour assemblies have been plotted on Figure 21 using the values of D'p = 66 and Dp = 8 x 10^4. The graph shows that even though there is a greater scattering of the data points there is much better agreement with the results of ν/p obtained from the 1 cm chamber. The scattering of the points may well be due to the inaccuracy of measuring the formation time of the discharge.

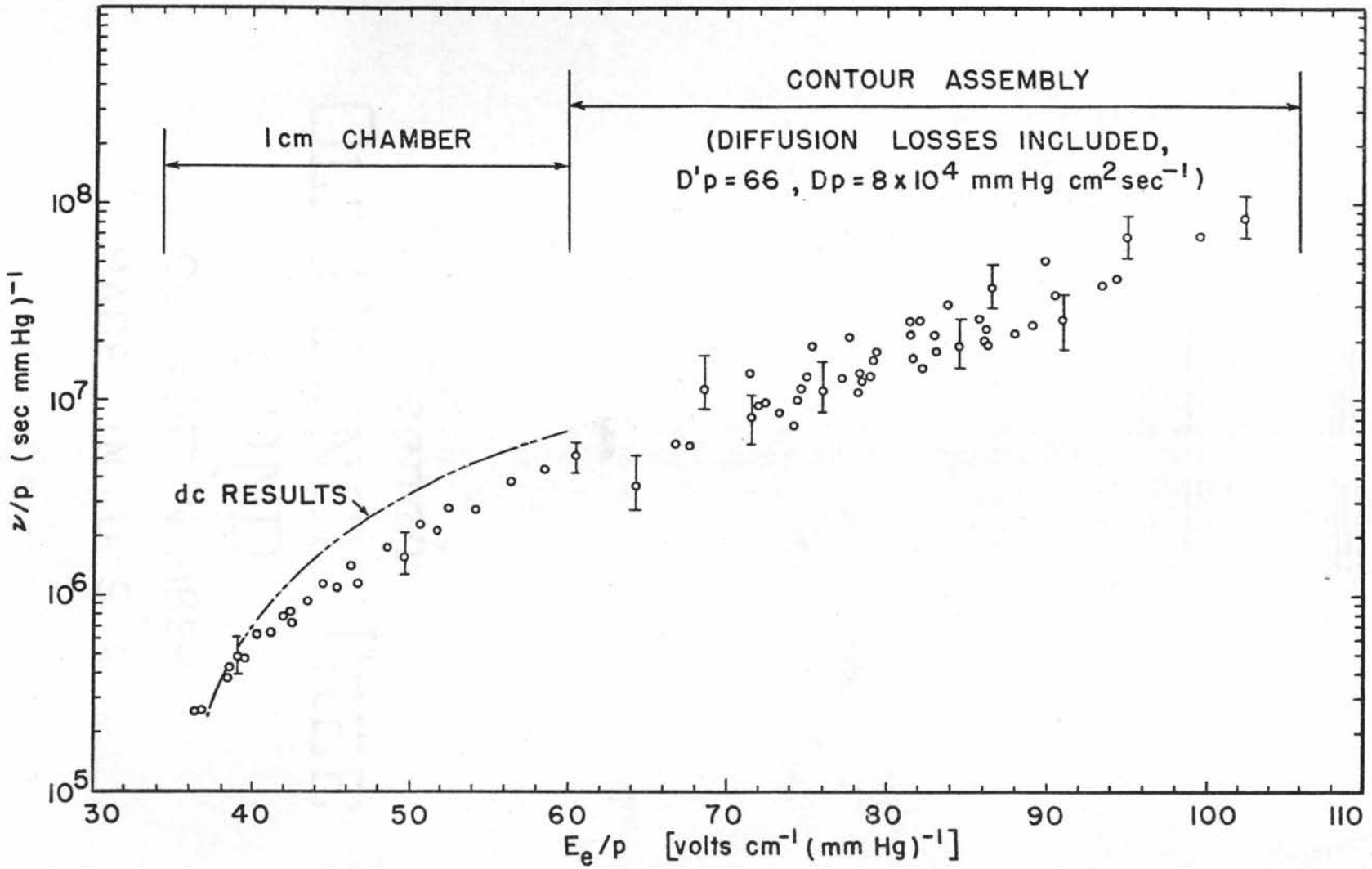

FIGURE 21. NET FREQUENCY OF IONIZATION — Vs — EFFECTIVE ELECTRIC FIELD

It is of interest to note that the value of the ambipolar diffusion coefficient for the afterglow period, given as 33 mm Hg cm^2/sec when the electron loss is by attachment only, does not agree with the experimental observation by Sexton *et al* that the value of D'p be very much less than 155 mm Hg cm^2/sec.

Summarizing the above results we may draw the following conclusions. The results obtained with the contour assembly are difficult to analyze because they contain two unknown diffusion coefficients, one pertaining to the formation period of the discharge and the other to the afterglow period. Using a value of Dp = 8 x 10^4 mm Hg cm^2/sec for the ambipolar diffusion coefficient during the formation period, it is found that the diffusion term has very little effect on the final results. Even using a value of $D_a = 0.1\ D_e$ (see Section 3h) only increases the value of ν/p by 0.6 x 10^7 (sec mm Hg)$^{-1}$ for the smallest value of $p\Lambda$. This suggests that the diffusion loss during the formation period of the discharge, in this region of E_e/p, is negligible. With reference to the afterglow period it is found that if a value of the ambipolar diffusion coefficient is used which satisfies the experimental observations of Sexton *et al*, that D'p $\ll$ 155 mm Hg cm^2/sec, the

experimental values of ν/p obtained with the results from the contour assembly are lower than that obtained with the 1 cm chamber. However, using the "theoretical" value of D'p = 66 mm Hg cm^2/sec, then much better agreement is obtained between the two sets of results. This discrepancy can only be resolved by measuring the electron decay rate in the same experimental arrangement that is used to determine the value of the net frequency of ionization.

At several points throughout this thesis reference has been made to the problems encountered with the contour assembly. It is convenient at this point to list these factors. Where noted further information is given in part two.

1) The formation time of the microwave discharge has a larger variation, for a given set of conditions, than is observed with the 1 cm chamber. It is very difficult to allow for this variation in the calculation of ν/p.
2) The data for the plots of τ versus T are not aligned as well as those for the 1 cm chamber. This means that the values of $d\tau/dT$ and hence ν/p are not so accurately defined.
3) There is a large loss (11%) of microwave power, in the contour assembly, which has been explained

as being due to the production of high frequency modes of propagation which are very rapidly attenuated within the waveguide. It is difficult to say what effects these modes may have on the properties and production of the microwave discharge under observation. For instance, it is observed that except for low microwave power levels there is always a discharge extending from the center of the contour assembly towards the microwave source. The length of the discharge may be several centimeters, depending on the power level (see part two). It is difficult to say how this may affect the discharge at the center of the contour assembly which is the one being examined.

4) It is found experimentally that when there is no discharge present the waveguide wavelength in the center of the contour is longer than that in the main waveguide (see part two). This is difficult to explain.

5) As mentioned before it is necessary to include two unknown parameters (D' and D) before the value of ν/p can be determined.

It is evident that the contour assembly is not a suitable discharge chamber for this experiment.

7g. Results from the 1 cm Discharge Chamber

The plot of ν/p versus E_e/p on Figure 14 show that the results obtained at the gas pressures of 9.8, 15.1 and 19.6 mm Hg have good agreement within themselves. The results for 4.9 mm Hg are lower than the other pressures, as expected, presumably because the loss of electrons by diffusion has been neglected. The experimental results are, however, only about 70% of the dc results obtained by using the net ionization coefficient evaluated by Harrison and Geballe (19), and the drift velocity by Bröse (8, p. 536-546).

It should be noted that all the parameters that have been neglected would all tend to increase the value of ν/p for a given value of E_e/p. Possibly the largest factor is that due to diffusion loss during the afterglow period. According to the experimental results of Sexton et al these losses should be negligible in this experimental arrangement for pressures above 10 mm Hg. However the "theoretical" value for this diffusion coefficient suggests the loss may be larger than expected. For example using a value of $\Lambda = 0.2$ cm for the higher values of E_e/p (the minimum value of Λ is 0.16 cm at the low values of E_e/p, see Section 3h) then

according to Equation 13 the decay rate is given by

$$\frac{\beta}{p} = \frac{\nu_a}{p} + \frac{D'p}{(p\Lambda)^2} \qquad (13)$$

where the "electron attachment" decay rate is given by $\nu_a/p = 69.1$ (sec mm Hg)$^{-1}$. Using the theoretical value of $D'p = 33$ mm Hg cm^2/sec and a gas pressure of 10 mm Hg then the value of ν/p would be 12% larger at the higher values of E_e/p (Figure 14). This would certainly give better agreement with the dc results. A similar argument would, however, increase the value of ν/p at low values of E_e/p above the dc results, and the microwave and dc results would then "cross-over". A similar phenomena is observed in the comparison between the microwave and the dc results obtained for the ionization coefficient for hydrogen by Varnerin and Brown (54).

7h. Suggestions for Future Experiments

In making suggestions for future experiments it is useful to first survey the criticisms of this experiment. These may be listed as follows:

1) The decay constant β/p is obtained from the results of other workers.
2) Corrections have to be made because of the shape of the microwave pulse.

3) It is assumed that the final electron density in the microwave discharge is independent of the repetition rate of the microwave pulses (i.e. it is assumed that the pulse length is long enough for the electron density to reach an equilibrium condition independent of the initial electron density).
4) The possible error due to the effective electric field increasing with increasing electron density is assumed to be small.
5) The gas impurities could be reduced.

The writer believes that the above criticisms have been satisfactorily answered within the limit of the equipment used to perform this experiment. It would, however, be advantageous to set up an experiment designed to eliminate these problems. The major suggested change is to use a microwave cavity, instead of the rectangular waveguide, as the discharge chamber. A cavity has the advantage that the density of the electrons within the cavity can be determined by measuring the resonant frequency of the cavity. The advantages of using a cavity are:

1) With the aid of a probing signal it would be possible to measure the electron decay rate

β/p in the period between the microwave pulses.

2) Due to the relatively high Q of a cavity it should be possible to use a klystron for the microwave power source, (i.e. a klystron is an inherently lower microwave power source than a magnetron but it may be operated under either "continuous wave" operation or the signal may be modulated with a suitable external circuit). With such a power source it should be possible to produce a fairly true rectangular microwave pulse, which would eliminate the need for the "pulse correction".

3) A klystron may be operated with a much longer duty-cycle and hence a longer microwave pulse may be used which would ensure that the electron density attained an equilibrium condition. However, by measuring the electron decay rate it will also be possible to measure the magnitude of the electron density which will then enable the effect of the term $d/dT\ (n_b/n_f)$ to be determined. This may eliminate the need for a long microwave pulse.

4) By measuring the formation time of the discharge up to the point where the presence of the electron density starts changing the electric

field (i.e. by measuring up to the time when a certain electron density is attained rather than using the "breakdown" point) the effect of the changing electric field may be eliminated.

5) By measuring the electron density decay rate at different pressures and characteristic diffusion lengths it should be possible to determine the electron diffusion coefficient in the afterglow period. It will then be possible to experimentally determine the electron diffusion coefficient for the formation period.

The purity of the gas can easily be improved by the use of a suitable high vacuum system and research grade oxygen.

8. CONCLUSIONS

A microwave method has been described for the determination of the net frequency of ionization of a gas. The experimental results obtained when using oxygen agree very well, within the limits of the experimental apparatus, with the results obtained using dc techniques and certain correspondence equations. The described method can be applied to any gas whose primary electron decay mechanism, in the afterglow of a microwave discharge, is either by

diffusion and/or electron attachment; the requirement being that the electron decay rate be exponential and that the decay rate be known. With due considerations to the remarks in Section 7g the final results of this experiment are shown in Figure 14 where the net frequency of ionization, divided by the pressure, is plotted as a function of the effective electric field, divided by the pressure.

PART TWO

1) PURPOSE

The object of this investigation is to study the dielectric breakdown of oxygen at microwave frequencies as a function of gas flow.

2) INTRODUCTION

In a stationary discharge electrons are continually being lost by attachment to atoms and molecules, recombination with positive ions, and diffusion from the discharge region. Another loss mechanism is added when the gas is caused to move out of the discharge region by means of a directed gas flow.

In a paper by Kelly and Margenau (25) the microwave breakdown property of the air surrounding the antenna of a high-speed vehicle is determined from a knowledge of the ambient electron concentration in the atmosphere and an electron "heating" time which depends on the mode of transmission. In the case of continuous wave (cw) transmission the "heating" time is given by the length of the radiator divided by its velocity. In the case of pulse transmission the "heating" time is given by the length of the pulse, providing it is less than the cw "heating" time.

This method of calculation implies that the preceding pulses, and the electron densities they produce, have no effect on the breakdown properties of future pulses. In other words, the effect of the electrons retained in the boundary layer of gas around the antenna is ignored. This is a reasonable assumption because of the relatively small change in the formation time of the discharge due to a variation in the initial electron density. However, since the change is a measureable amount (10% - 20%) and since the gas flow will affect the initial electron density it is felt that a study of the effect of the gas flow on a microwave discharge is warranted.

The experimental work involves a study of steady-state discharges produced by microwave pulses of about a microsecond in duration, and with maximum velocities of the order of 10^4 cm/sec. During the formation of the discharge the gas is displaced a distance of about 0.01 cm; therefore since the discharge region is of the order of 0.5 cm, it is assumed that the gas flow has a negligible effect during the formation of the discharge. The major effect of the gas flow is in the time period between the microwave pulses and will therefore affect the initial electron density at the beginning of each

discharge.

The theoretical results are obtained in the following manner: From the theory in part one it is assumed that at zero gas flow the electron density configuration is a cosine distribution across the height of the discharge region. The number of electrons which are swept out of the discharge region, and hence the electron density remaining at the arrival of the next microwave pulse, is then determined as a function of the gas velocity from the boundary layer theory of gas flow. The expected increase in the formative time of the discharge, due to the decrease in the initial electron density, is then evaluated for a constant power level and as a function of the gas velocity from the theory of the electron production in gases.

It should be noted that the desired agreement between the experimental results and the theory has not been achieved. One reason for this is that it was not possible to obtain a large change in the formation time of the discharge, as a function of the gas velocity, because of the large variation in the formative time for values greater than about 0.5 microseconds. A solution to this problem would be to

compare the power required to produce a given formative time (less than 0.5 microseconds) as a function of the gas velocity. This, however, requires a fairly accurate knowledge of the net frequency of ionization as a function of the microwave power. The values available from the dc data do not cover the range of E_e/p required for this investigation (values greater than 60 volts/cm mm Hg). It was because of this that part one of this thesis was carried out; but as recorded in part one, it was not possible to obtain sufficiently accurate results in the region of interest. One reason for recording this experimental work is to explain the difficulties encountered in producing an isolated discharge at a certain location in a tapered waveguide; another is to describe the unusual reflected microwave signals and light pulses associated with this discharge.

The general method of studying the breakdown is patterned after that of Posin (41, p. 496-509) and employs a constricted region in a standard X-band waveguide. This procedure lends itself to the possibility of obtaining high velocity gas flow while isolating the microwave discharge.

3) THEORY

The general theory of the production and decay of electrons in a microwave discharge is given in part one. In this section consideration is given to the gas flow.

3a. Gas Flow Considerations

The gas flow line consists of a length of standard X-band waveguide, referred to as the flow tube, attached to a special assembly, known as the contour assembly or the constricted region, in which the height of the waveguide is gradually reduced to a millimeter or so and then gradually opens up to the standard waveguide dimension again. The flow tube is used to damp-out the swirling action of the gas as it enters the waveguide, and the constricted region is where the discharge is produced. For convenience, all the contoured sections used to reduce the height of the waveguide are referred to by the distance from the narrowest part of the constriction to the point where it tapers out to the standard waveguide dimensions. A summary of the shapes of the different contours is given in appendix C.

The effect of the gas flow on the electron density configuration is a very complicated process

and it is necessary to make some rather simple assumptions before proceeding with the calculations. When the gas is flowing it is reasonable to assume that the positive and negative ions are swept out of the discharge region in the same manner as the neutral molecules. These ions and molecules have a random motion, due to their thermal energy, superimposed on the uniform motion of the gas flow; for simplicity the random motion will be ignored. It is assumed that the electrons are swept out of the discharge region with the same velocity as the gas molecules under a combined action of the electrostatic force between the positive ions and the electrons, and the numerous collisions between the electrons and the gas molecules. Due to the velocity profile across the height of the discharge chamber, the center layer of ions and electrons will be swept out first; this will cause the electrons to diffuse in two directions across the height of the discharge region instead of just to the walls. This complicated process is simplified by assuming that the diffusion loss and the loss of electrons due to the gas flow act separately. First it is assumed that after the cessation of the discharge, the electron density

configuration decays to that which exists with zero gas flow. The central portion of the configuration is then swept out by the gas flow, and finally the remaining electrons diffuse across the chamber to form a uniform density configuration.

In order to make the above calculations it is necessary that the gas flow be laminar in the region of interest, and that the velocity profile be known.

3b. Laminar Gas Flow

Two conditions are necessary in order for laminar flow to exist in the discharge region. One is that the Reynolds number for the gas flow must be less than a certain critical value, and the other is that the swirling action of the gas as it enters the flow tube must be damped out.

The Reynolds number R is defined by (47, p. 35) $R = \rho \bar{U} d/\mu$, where ρ is the gas density = $1.75 \times 10^{-6} p$ grams/cm^3 for oxygen at 20°C (28, Sec. 2, p. 197-201), p is the gas pressure in mm Hg, $\bar{U}$ is the average gas velocity in cm/sec, d is a characteristic length (cm) depending on the use of R, and μ is the coefficient of viscosity of the gas = 2.03×10^{-4} poises for oxygen at 20°C and 760 mm Hg (26, Sec. 2, p. 201-210). [NOTE. The coefficient of viscosity

is independent of pressure, to a first approximation, for pressures less than one atmosphere (43, p. 41; 27, p. 295).] Numerous experiments indicate that for values of R less than about 2000 the gas flow remains laminar even in the presence of a very strong disturbance (47, p. 376).

In the case of gas flowing in a circular tube the characteristic length d is the diameter of the tube; in the case of a rectangular tube it is the diameter of a circular tube with the same cross-sectional area. In the constriction region the minimum gap opening is 0.114 cm x 2.29 cm, and the maximum value of $p\bar{U}$ is approximately 2×10^5 mm Hg cm/sec. Hence the maximum value of the Reynolds number at this point is 1000. In the flow tube the maximum value of R is about 320. Therefore all parts of the flow line satisfy the Reynolds number criterion.

The problem of the decay of the swirl component of velocity of a gas flowing in a circular tube has been studied by Talbot (53). The velocity of the swirl may be given by

$$V(r,z) = V(r,0) \exp(-\beta z)$$

with the boundary conditions $V(0,z) = V(a,z) = 0$,

where a is the radius of the tube and z is the position along the length of the tube measured in terms of tube radii. The decay constant β, as determined by Talbot, is given by $\beta R = 22.2$ for z greater than 40, and $\beta R = 74.3$ for z less than 15 where R is the Reynolds number. If we consider the flow tube as a circular tube of radius 0.85 cm (which has the same cross-sectional area as the rectangular tube) with the gas entering the flow tube through an aperture with an area of 0.9 cm^2 (a measured value) then the average value of the swirl velocity at the entrance is given approximately by

$$\bar{V} = \bar{U} \times \frac{\text{area of flow tube}}{\text{area of entry}} = 2.5\ \bar{U}$$

where $\bar{U}$ is the average velocity in the flow tube. Calculations for maximum flow conditions, when the decay rate is a minimum, show that the swirl velocity at the end of a flow tube 55 cm long is only about 2% of the average axial velocity. Since the flow tube is rectangular and not circular the swirl component will probably be less than this value. In the constriction region the axial velocity is about 10 times that in the flow tube, hence the radial velocity will be less than 0.2% of the average axial

velocity. Therefore with a flow tube of length 55 cm the swirling action of the gas may be considered to be damped out before the gas enters the constriction region.

3c. Gas Velocity Profile

In order to determine the velocity profile across the discharge region it is necessary to know what the boundary conditions are at the wall of the tube. To a first approximation the gas layer next to the wall may be considered to be stationary providing the mean free path of the gas molecules is small compared to the dimensions of the object. However, since the discharge region is comparatively short (about 0.5 cm), a small velocity at the surface will play an important role in the removal of the electrons from the discharge region and must therefore be considered. The velocity of the gas layer at the surface of the wall is given by (18, vol. 3, p. 718)

$$U(0) = \frac{2 - \sigma}{\sigma} \, l' \left(\partial U / \partial y \right)_0$$

where σ is the "reflection coefficient" which is equal to 1 for a machined brass surface (18, vol. 3, P. 695), l' is the mean free path of the gas molecules

and $(\partial U/\partial y)_0$ is the gradient of the velocity distribution evaluated at the surface. Since the mean free path of the gas (equal to 3×10^{-4} cm at a pressure of 15 mm Hg) is small compared to the dimensions of the discharge region, the surface velocity of the gas may be considered to be zero as far as its effect on the shape of the velocity profile is concerned.

We are concerned with the velocity profile in the constriction region where the width of the tube is very much larger than the height. The velocity distribution across the width of the tube may be considered to be uniform because the boundary layers at the surfaces will be small compared to the width of the tube. In any case the discharge does not extend across the full width of the tube so the boundary layers at the side walls will have no effect.

If the constriction region were very long the velocity profile would eventually become parabolic, assuming the gas layer at the surface is stationary, and the flow would be "fully developed". The velocity profile is then given by

$$U(y) = U_m (4y/a)(1 - y/a)$$

where y is measured from the wall of the tube, a is the separation between the walls (i.e. the height

of the gap) and U_m is the gas velocity at the center of the gap. The average velocity $\bar{U}$ for a parabolic flow in a rectangular tube equals $(2/3)U_m$.

The tapered section leading into the constriction region consists of two curved surfaces, see Appendix C, and the calculations for the velocity distribution of a gas flow in such a geometry is very complex. In the regions where the taper is relatively steep (10 degrees included angle) the contour section may be represented as a convergent channel with straight walls; a fairly complete derivation for the gas flow in such a geometry has been given by Millsaps and Pohlhausen (36). However, for the contour section of interest, the 2.5 inch contour, the height of the gap varies by only 10% over a length of 0.5 cm on either side of the center-line of the contour for the 0.114 cm gap assembly, and by only 10% over a length of 0.75 cm for the 0.214 cm gap assembly. If a gas enters a straight wall parallel channel with a uniform velocity $\bar{U}$, the flow becomes approximately fully developed after travelling a distance z given by

$$z = 0.004\, a^2 \bar{U} \rho / \mu = 3 \times 10^{-4} a^2 p \bar{U} \text{ for oxygen}$$

where a is the width of the channel, and ρ and μ are the density and viscosity respectively. In the

problem at hand the flow will at least be partly developed by the time it enters the constriction region because of the long flow tube. If we assume that the contour section is parallel for the lengths given above then the flow will be approximately fully developed by the time it reaches the center of the contour for velocities less than the value given by

$p\bar{U} = 1.3 \times 10^5$ mm Hg cm/sec for the 0.114 cm gap,

and

$p\bar{U} = 0.4 \times 10^5$ mm Hg cm/sec for the 0.214 cm gap.

Since the maximum experimental value of $p\bar{U}$ is about 2×10^5 mm Hg cm/sec for the 0.114 cm gap, and about 1×10^5 mm Hg cm/sec for the 0.214 cm gap then to a first approximation we may consider the velocity profile as parabolic. It should be noted that the maximum deviation from a parabolic velocity profile will be at the center region and not in the boundary layers.

With a parabolic velocity distribution, the velocity of the gas layer next to a machined brass surface is therefore given by $U(0) = 4\,l'\,U_m/a$. The effect of the slip at the boundary may be included in the calculations by assuming there is a net velocity given by $U'(y)$ equal to $U(y)$ plus the slip velocity; that is $U'(y) = (4U_m/a)(y - y^2/a + l')$. Using this

velocity profile and following the assumptions given in section 3a we may calculate the electron density $n_o(U_m)$ remaining in the discharge region after a time T. A plot of $n_o(U_m)/n_o(0)$ is given in Figure 22 for a discharge region of length 0.5 cm and a decay period T equal to 1/300 sec. A brief summary of the calculations is given in appendix B.

4) APPARATUS

The microwave circuit is the same as that shown in Figure 4, Part One, with the exception that the constricted waveguide assembly is mounted in place of the discharge chamber.

The gas circulating system was designed so that the gas being examined could be circulated in a closed system, if desired. The system is shown schematically in Figure 23. In this particular experiment the gas is obtained from a standard high-pressure gas cylinder and the exhaust from the system is ejected into the atmosphere. The gas is passed through a solid CO_2 and acetone trap to remove the water content. It then flows into a reservoir which is maintained at a constant pressure with the aid of a mercury manometer and a photocell which operates an electro-magnetic valve. The gas then flows through

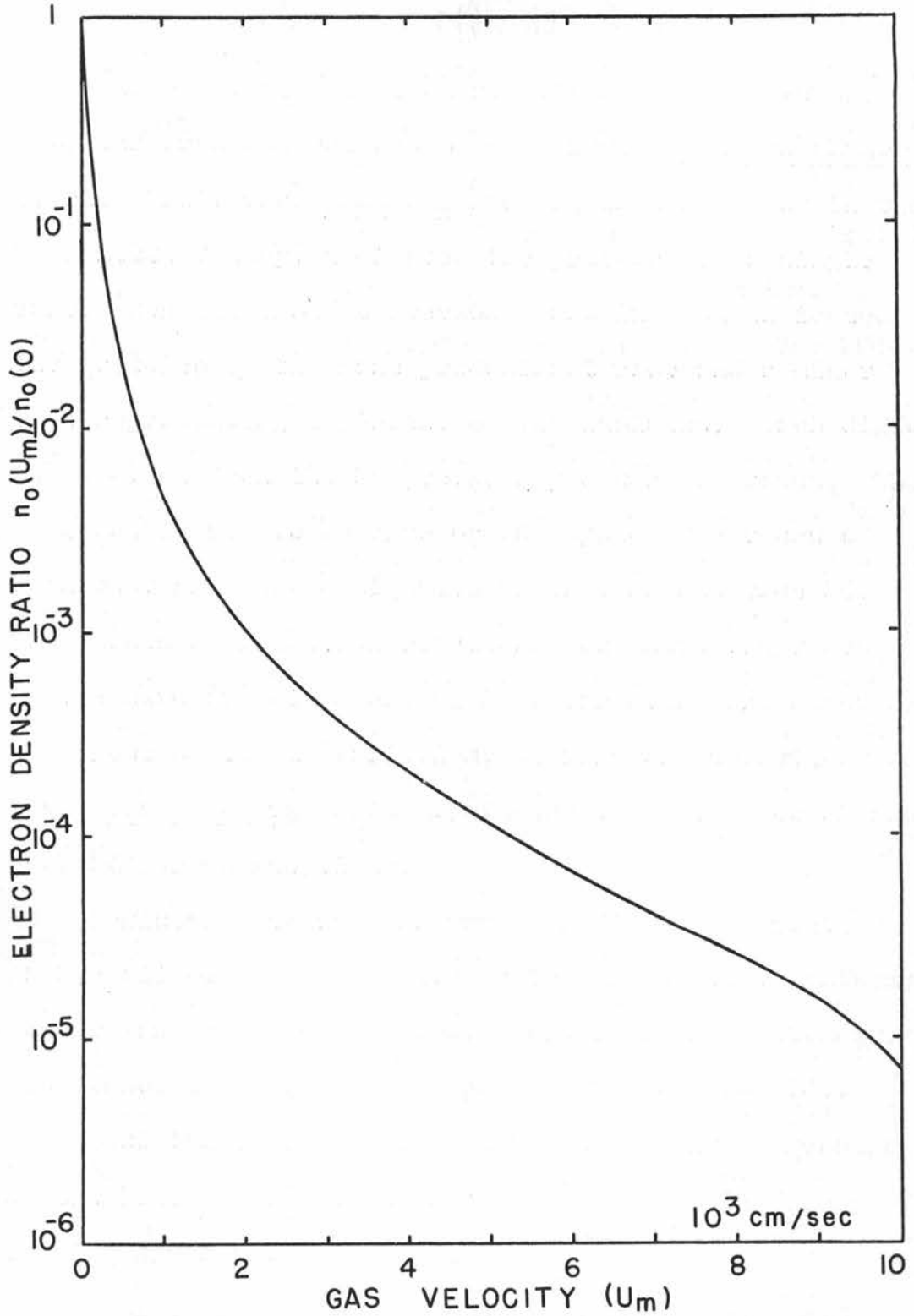

FIGURE 22. $n_o(U_m)/n_o(0)$ - Vs - GAS VELOCITY(U_m)

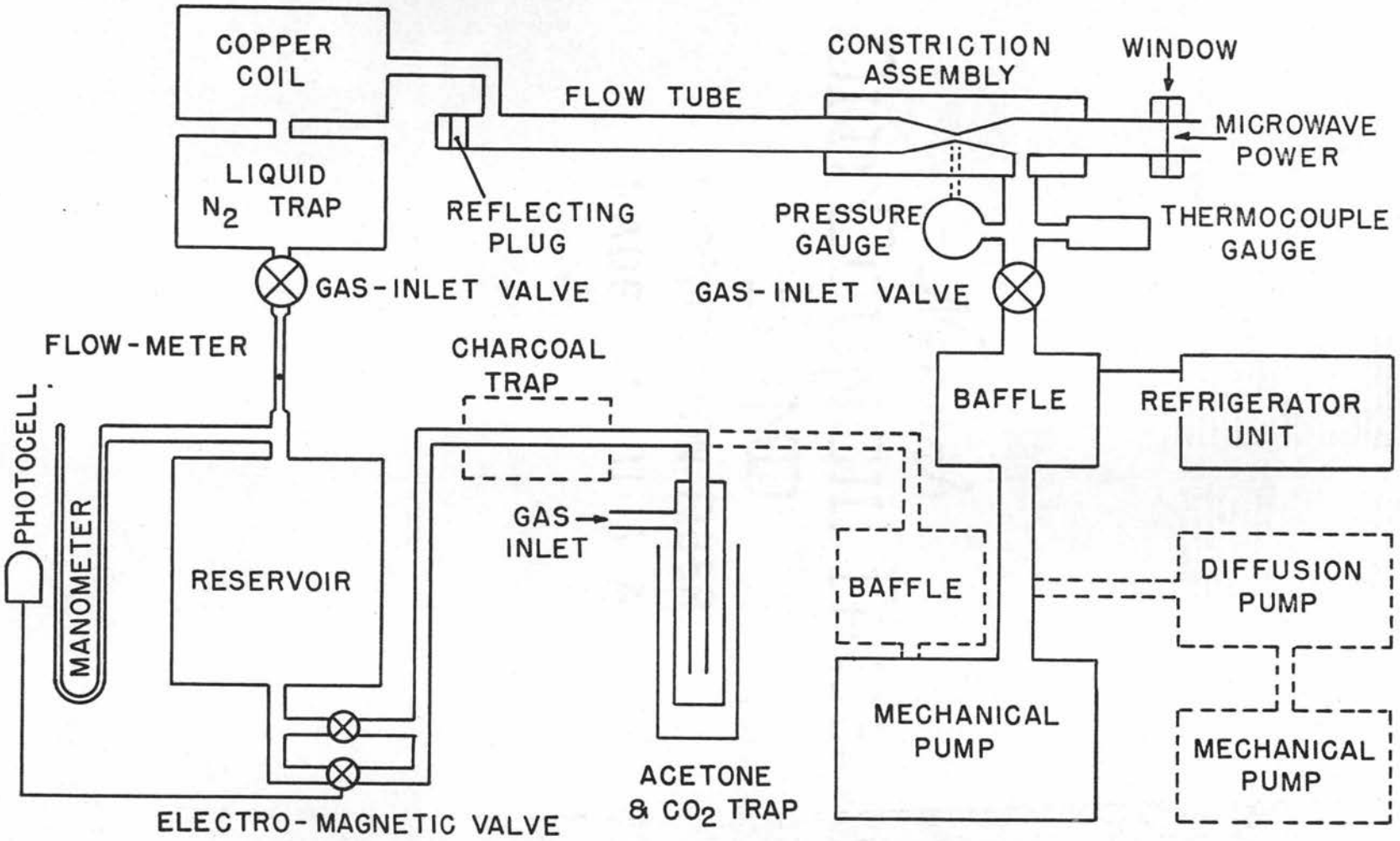

FIGURE 23. GAS CIRCULATING SYSTEM

a float-type flow meter (Matheson model 205, maximum flow rate of 9.1 liters per minute of air at 1 atmosphere pressure and 70°F) which is followed by a liquid nitrogen trap, to further dry the gas, then a copper coil, to bring the gas to room temperature, and then into the flow tube and the constriction region. The gas is pumped through the system with a large mechanical pump (Edward's model ISC-450B) located near the outlet of the constricted waveguide. The flow tube is sealed off at one end with a metal plate, and the contour assembly is vacuum sealed from the atmosphere with a microwave window. A valve at each end of the waveguide flow assembly controls the velocity of the gas in the waveguide and also the gas pressure. The resevoir is maintained at a pressure of 215 mm Hg to facilitate the control of the gas flow. It was found necessary to use a precision valve for the gas-inlet control valve (Veeco model R62ST) in order to maintain a constant gas flow. The outlet valve (Veeco model R62S) was modified by adding a small plug to the plunger which controls the size of the pump-out aperture; this improved the control of the gas flow at low flow rates. The charcoal trap, the second refrigerated baffle unit and the auxialiary diffusion

and mechanical pumps (all shown dotted-in on Figure 23) were partially included in the system so that it could be easily converted into a closed system when required.

The flow meter is supplied with a calibration chart for use with air at atmospheric pressure and 70°F; also the information necessary to make a theoretical calibration for other operating conditions. The theoretical calibration was checked experimentally by attaching a second indentical flow meter to the outlet of the mechanical pump where the conditions are approximately equal to those given above. The exhaust gas from the pump was refrigerated to remove the oil vapour, and passed through a long copper coil to return the gas to room temperature. The experimental calibration was about 5% lower than the theoretical values at the maximum flow rate (20 meter divisions), 8% lower at 10 divisions and about 10% lower at 4 divisions. The theoretical calibration of the flow meter is given in Table 3 where the flow rate is expressed in cm^3/sec for oxygen, at a pressure of 215 mm Hg and at a temperature of 20°C.

The velocity of the gas in the constriction

region may be evaluated directly from Table 3 if the gas pressure at the constriction and the area of the constriction is known, providing it is assumed that the temperature of the gas in the constriction is the same as that in the flow meter (i.e. no adiabatic expansions). This assumption is questionable at the

TABLE 3

Flow Meter	Flow Rate
2 div	4.1 cm^3/sec
3	9.9
4	19.2
5	29.7
6	41.6
7	54.0
8	67.5
10	95.0
12	123.1
14	151.2
16	178.2
18	210.6
20	241.4

entrance of the constriction region where the gas flow is laminar and where there is a pressure gradient along the length of the contour. Assuming that the flow is adiabatic in this region then if we define the quantity Q as the product of the average gas velocity, the cross-sectional area and the gas pressure then the quantity Q_c in the constriction region is given by $Q_c = (p/p_c)^{1/\gamma - 1}$, where p is the gas pressure and γ is the ratio of the specific heats C_p/C_v. The ratios Q_c/Q as determined from

experimental values of the gas pressures measured in the 2.5 inch contour with a 0.114 cm gap are given in Table 4. The problem of Q changing slightly with

TABLE 4

Flow Rate (meter divisions)	Pressure (at constriction)	Q_c/Q
12	10 mm Hg	0.95
	15	0.98
	20	0.98
16	10	0.91
	15	0.95
	20	0.97
20	10	0.86
	15	0.92
	20	0.96

gas flow was not pursued further since it is not a limiting factor in the analysis of the results. It is assumed that Q is constant and the velocity of the gas in the constriction region is obtained directly from Table 3.

The pressure in the center of the constriction is maintained at a constant value at all gas velocities. This is achieved by first using a dummy constriction assembly with a hole in the center and calibrating the pressure at the outlet as a function of the pressure at the constriction and the gas flow velocity. When the final contour is used, a constant pressure is then maintained at the center by setting the outlet pressure to suit the flow rate in accord with the calibration chart.

5) CONSTRICTION ASSEMBLY

As mentioned earlier, the general design of the discharge region is based on that used by Posin (41) for the study of the electrical breakdown of air at microwave frequencies. Posin used a constricted waveguide section in which the tapered section, from the constriction to the full width waveguide, was approximately 6 inches long. The minimum gap width was 0.038 inches. The minimum gas pressure used was about 5 mm Hg.

The first contour assembly used for this investigation had two 5 inch contours, placed symmetrically about the center-line,with a minimum gap width of 1 mm. The assembly was made of brass. It was made in two sections, which were soldered together, with the contours as an integral part of the main body. The preliminary investigation of the discharge employed running-waves in the microwave field, and the microwave circuit was terminated with a matched load instead of the metal plate shown in Figure 4, part one. The end of the flow tube was vacuum sealed with a microwave window, and a directional coupler was mounted between the window and the terminating load so that the transmitted microwave signal could be observed.

The first experimental results yielded a reflected microwave signal such as that shown in Figure 6, part one. It was later observed, however, that the discharge was occurring not in the constricted region but across the first microwave window. This problem was corrected by using microwave windows with a larger aperture (Microwave Associates type MA1430). As explained in Section 5a, part one, the reflected signal observed with the "window discharge" was very simple and easily explained. Apart from the abrupt increase in the reflection and decrease in transmission that occurred when the discharge was initiated, the contour of the pulse was very similar to that of the incident microwave pulse. With the microwave power producing breakdown in the constricted region, the results were very complicated and could not be readily explained. The results were different from those obtained with the "window discharge" in two respects. While a formative time could be inferred, the shape of the reflected and transmitted signals were complicated and power dependent. Furthermore, the formative time of the discharge decreased for a range of increasing gas flow; this was contrary to expectations. These

points are individually dealt with in the following sections.

5a. Reflected and Transmitted Pulse Shapes

An idea of the different pulse shapes that were observed may be obtained from the upper traces in Figures 24 and 25 (portions of the traces have been dotted-in because of the difficulty of reproduction). There were two particularly unusual features about the reflected pulse. One was that the reflection would decrease to almost zero at certain points even though there was a discharge present. The other was that a series of dips would appear at the tail of the reflected and transmitted pulse and would travel along to the front of the pulse as the power level was increased. The first point may be observed in trace A of Figure 25, the second point in trace C of Figures 24 and 25. These results were tentatively explained by assuming that a series of discharges were formed in the constriction. Calculations showed that assuming about 70% reflection from the primary discharge then the resultant standing wave could sufficiently increase the electric field at a distance of a quarter of a wavelength away to initiate another discharge. The two reflecting

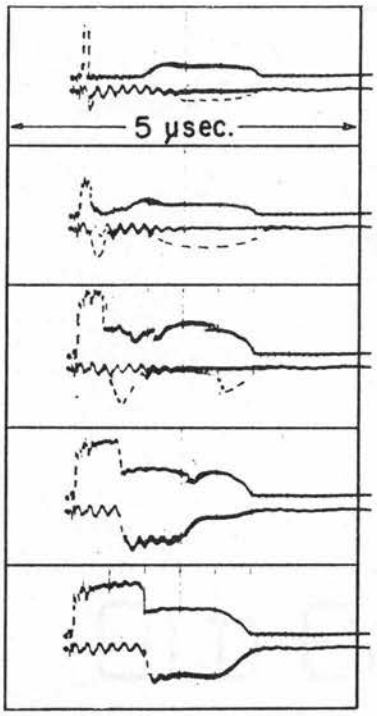

TRACE	VERTICAL SCALE (MICROWAVE PULSE)	RELATIVE POWER
A	10	6·7
B	10	2·5
C	4	1·5
D	4	1·2
E	4	1

ALL LIGHT PULSE TRACES ON SAME SCALE

FIGURE 24. TRANSMITTED MICROWAVE PULSE (2·1μs. AT 300 p.p.s)

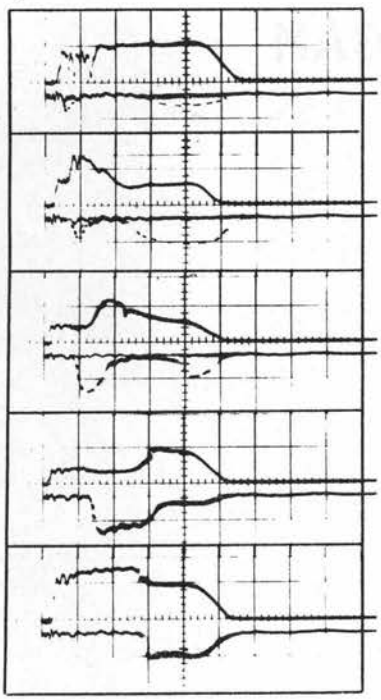

TRACE	VERTICAL SCALE (MICROWAVE PULSE)	RELATIVE POWER
A	10	6·7
B	4	2·5
C	4	1·5
D	4	1·2
E	1	1

ALL LIGHT PULSE TRACES ON SAME SCALE

FIGURE 25 REFLECTED MICROWAVE PULSE (2·1μs. AT 300 p.p.s)

planes separated by a distance of a quarter of a wavelength would produce an interference filter and would explain the low value of reflection observed at certain points.

In order to examine the problem more thoroughly, a new constriction assembly was made which had a 1/16" wide plastic strip along the length of the contour. The new design also simplified the manufacture of the contours and enabled them to be more readily interchanged, see Figure 26. A photocell was mounted on a carriage above the plastic strip so that the light pulse from different areas of the discharge region could be examined. The pressure in the constriction was measured through a hole in the center of the lower contour.

Four contours of different lengths were made. The longest was 5 inches and was the same as that used in the original constriction assembly. The shortest was 1.6 inches long and was made to obtain a single discharge in the constriction. The other two were 2.5 inches and 3.5 inches long. Ideally the shortest contour should be a quarter of a wavelength long (about 0.5 inches) so that the antinode of the standing wave would be in the main waveguide, where

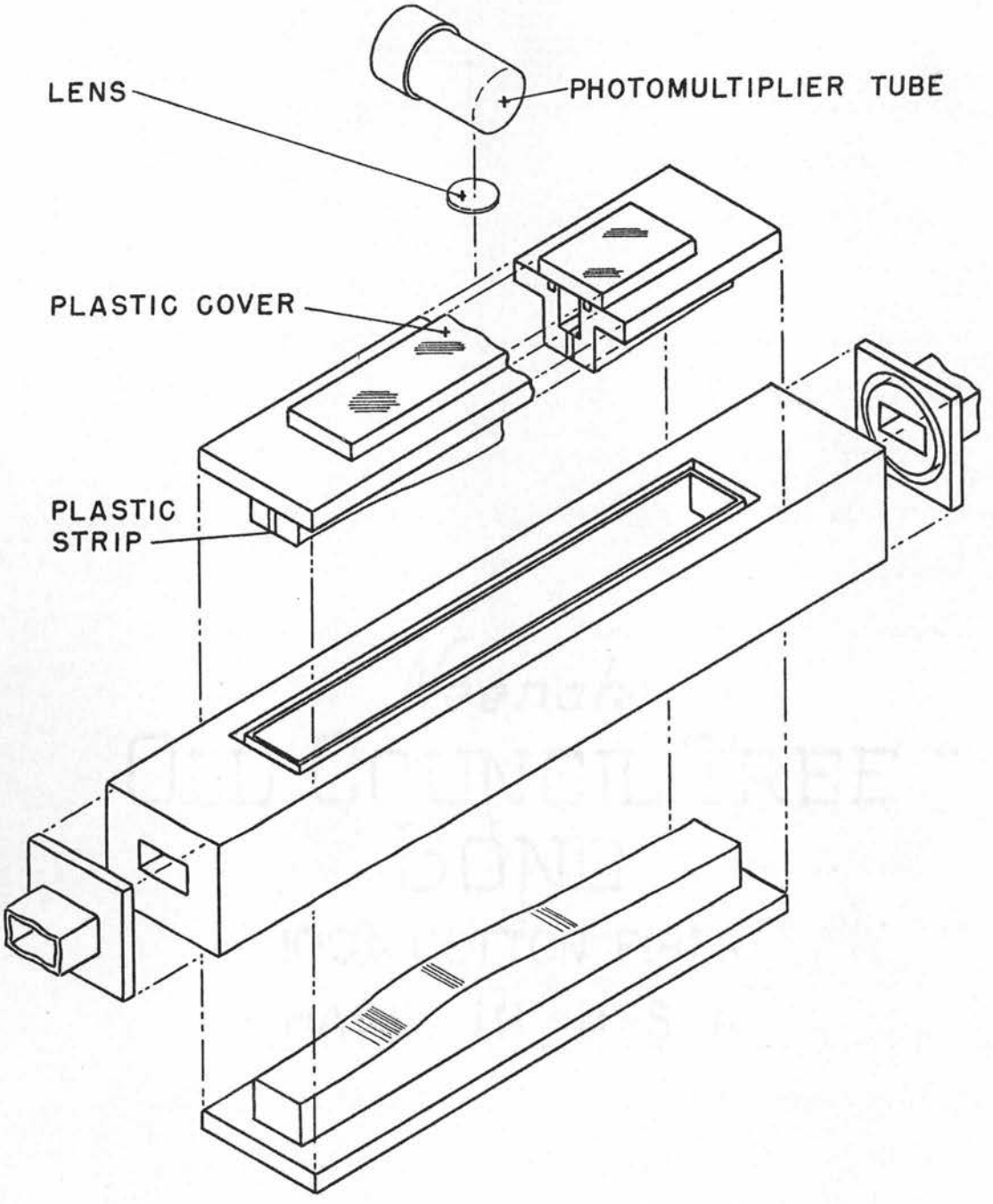

FIGURE 26 CONSTRICTION ASSEMBLY.

the electric field is a minimum. However, such a steep contour would itself produce large standing waves and would also introduce gas flow problems. By increasing the waveguide wavelength the antinode is moved out farther and a flatter contour may be used. For this reason a contour width of 0.643 inches (λ_g = 16 cms) was tried. Widths of 0.770 and 0.900 inches were also investigated, the latter being the standard waveguide size. In all cases the gap width was 0.04 inches.

The new constriction assembly clearly showed that several discharges were formed along the length of the contour. With aid of the photocell it was observed that in the 1.6 inch contour the off-center discharges started later than the center discharge, see Figure 27.

Considerable difficulty was encountered in trying to obtain a single discharge in the constriction. It is believed this may have been due to the "metallic" reflections from the tapered width producing large standing waves in the main waveguide. A single discharge was obtained with the 5 inch by 0.643 inch width contour, so the quest was pushed no farther. The traces shown in Figures 24 and 25 were taken with the 5 inch by 0.643 inch width contour and show

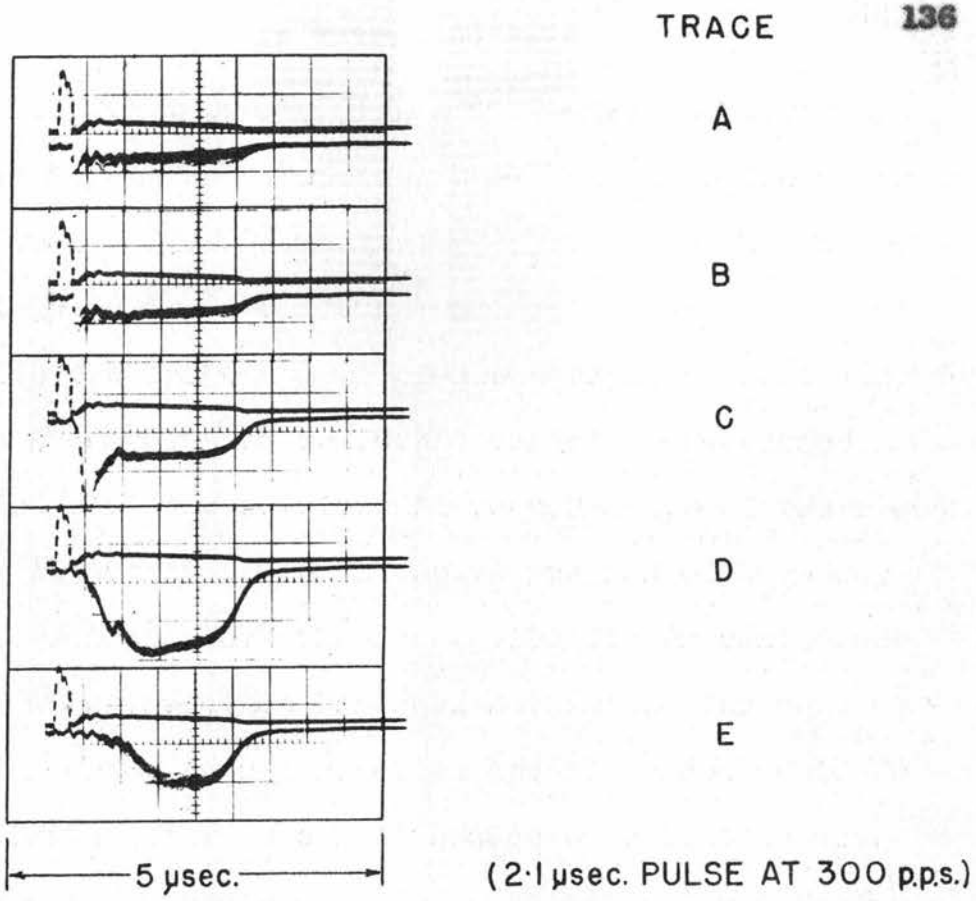

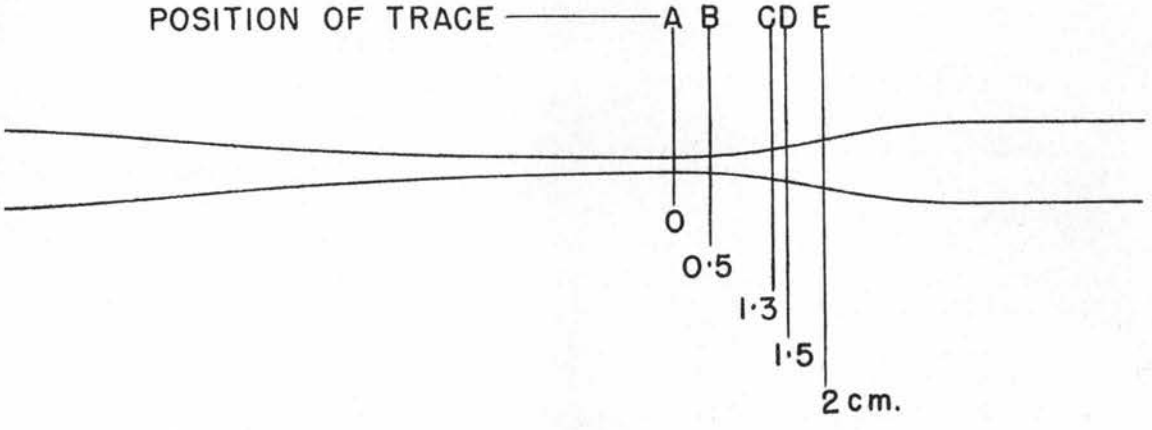

SHAPE OF LIGHT PULSE-VS-POSITION IN CONTOUR

FIGURE 27

the transmitted and reflected microwave pulses (upper traces) and the associated light pulse (lower traces). (NOTE. The light trace is inverted.) The power is a maximum for trace A and decreases toward trace E. The change from a single to a multiple discharge is clearly seen. Trace E, in each case, shows a single light pulse signifying a single discharge; this was verified by visual observation. The transmitted pulse is very similar to that observed with the window discharge. The reflected pulse is also similar except that the net reflection at the time of the discharge is less than the metallic reflection. This is possibly due to an interference between the reflection from the discharge and that from the contour assembly, and shows the large metallic reflection that was mentioned earlier. Trace D shows that a secondary discharge has just started, (i.e. the light pulse from the primary discharge is decreased when the secondary discharge is formed because of the power loss in transmission through the secondary discharge). The microwave pulses show a corresponding charge, in particular the transmitted signal shows one of the dips which is observed to "run" along the length of the pulse as the power is varied.

At the higher power levels it is observed, from traces A, B, and C, that the light pulse is either partly or completely extinguished in the middle of the microwave pulse (i.e. the primary discharge starts twice during the period of a single microwave pulse). This fact is explained as follows. The first peak is due to the primary discharge being initiated. This then sets up a standing wave which initiates the secondary discharges. The power transmission through several discharges is very small, so the primary discharge is extinguished. Since the secondary discharges rely on the reflection from the primary discharge for their existence then they also collapse, which enables full power to be transmitted to the center of the constriction where the primary discharge is again initiated.

It should be noted that the single discharge could only be obtained over a power range of 30% compared to a range of at least a factor of three required for the experiment (an experimental value). Also the position of the primary discharge in the 5 inch contour varied with the microwave power level, trace E in Figures 24 and 25 being recorded at a distance of 1 inch from the center of the contour. The length of the primary discharge was about 8 mm.

The above results showed that it would not be possible to work with a single discharge, over the required power range, with the present method of investigation. However, in order for the experimental results to have any meaning it is necessary for the primary discharge to be formed at the center of the constriction, where the gap width is known, and that it starts sooner than, or at least as soon as, any other discharge so that its formative time will not be masked by that of another discharge. An examination of the above mentioned contours showed that only the 1.6 inch by 0.900 inch width contour completely satisfied these requirements. The 2.5 inch by 0.900 inch contour generally satisfied these requirements but it was observed that discharges off-center would occasionally start before the center discharge. Because of the gas flow problems described in Section 5b, it was considered necessary to use a contour which was no steeper than the 2.5 inch contour. It was therefore decided to use a standing wave in the applied electric field to help localize the discharge in the center of the constriction.

The standing wave was set-up by producing a 100% reflection from an adjustable plug located at

the gas-inlet end of the flow tube. The position of the plug was set by two methods. (1) By removing the plastic strip and the window from the slotted contour, the standing wave could be detected by means of a suitable probe inserted in the slot. Although the detected standing wave pattern was very distorted, because the depth of penetration of the probe varied as it was moved along the contour, it was possible to position the plug to within a millimeter of the required location by adjusting its position until the detected standing wave was symmetrical about the center line of the constriction region. It should be noted that the waveguide wavelength at the center of the constriction was measured as 5 cm compared to about 4.5 cm in the standard X-band waveguide; this is difficult to explain. (2) The second method consisted of measuring the position of the standing waves when the microwave power was reflected from a metal plug (aluminum foil) placed at the center of the constriction. This was accomplished by mounting a slotted waveguide at the gas-inlet end of the flow tube, and feeding the microwave power into the slotted line (the reflecting plug having been removed). The positions of the antinodes in the slotted line were recorded. The reflecting plug

was then replaced in the flow tube with its "reflecting-surface" at a convenient number of anti-nodes from the positions measured in the slotted waveguide. The two methods agreed to within a millimeter. The effect of the standing wave is to produce a much more distinct discharge at the center of the constriction, and to increase the probability of it starting at the center.

5b. Effect of Gas Flow

From the theoretical considerations in Section 3 the power necessary to produce a discharge in a given formative time should at first increase with increasing gas velocity, and then gradually level off. The preliminary results, which were obtained before a standing wave in the applied electric field was employed, did not behave in this manner. With all other factors constant the formative time either decreased or remained relatively constant with increasing gas flow. The discovery of the multiple discharges explained this however. The gas flow was initially in the same direction as the incident radiation, (i.e. from the side of the constriction where the standing waves initiated the secondary discharges)and it could sweep electrons from the

nearby secondary discharge into the region of the primary discharge. With aid of the photocell it was observed that there were negligible discharges formed on the far side of the constriction (i.e. away from the microwave source). This suggested that by flowing the gas in the opposite direction to the incident radiation the necessary information of the effect of a gas flow could be obtained.

Reversing the direction of the gas flow produced an increasing formative time with increasing gas flow up to a certain velocity but at higher velocities the results deviated from what was expected. Generally the results were as per Figure 28 where the power required to form the discharge in a given formative time is plotted as a function of the gas flow rate. Figure 29 shows a set of experimental results obtained for a pressure at the constriction of 15 mm Hg with a 2.1 μsec microwave pulse at a repetition rate of 160 pps. The velocity $\bar{U}_1$ is that where the data deviates from a smooth rising curve. The velocity $\bar{U}_2$ is that where the peak of the experimental curve occurs. The degree in the decrease of power beyond velocity $\bar{U}_1$ varied with pressure, the microwave pulse repetition rate and the power level. Generally the curves were

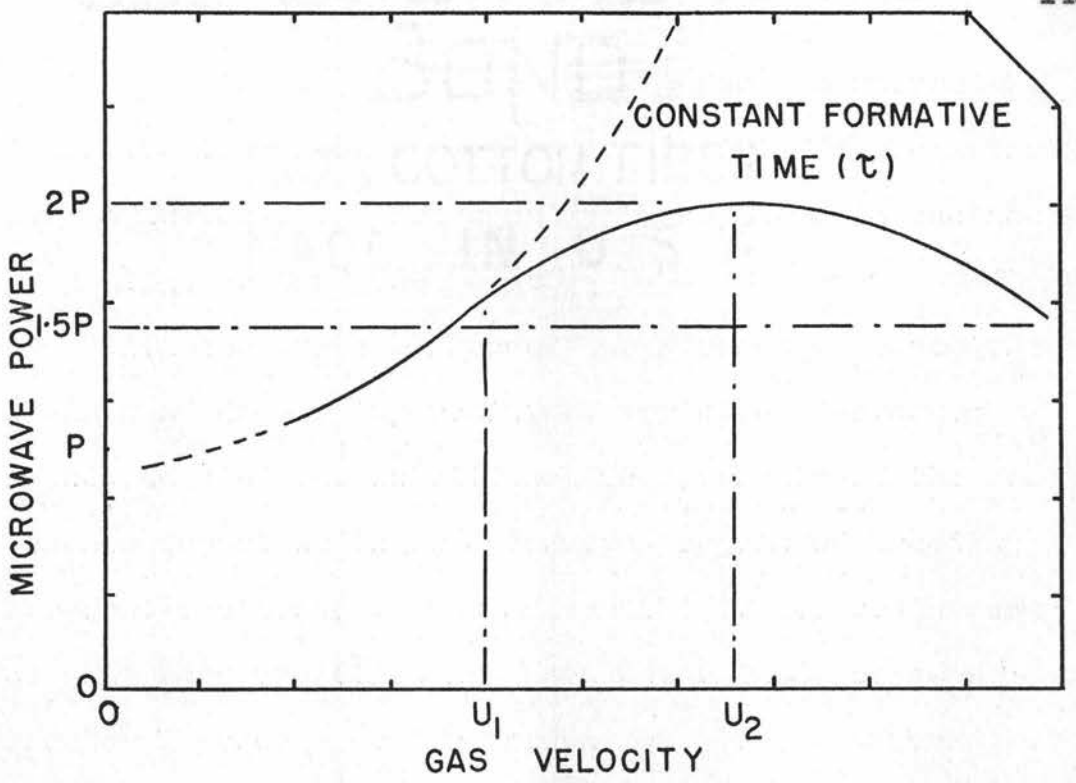

FIGURE 28. MICROWAVE POWER - Vs - GAS VELOCITY

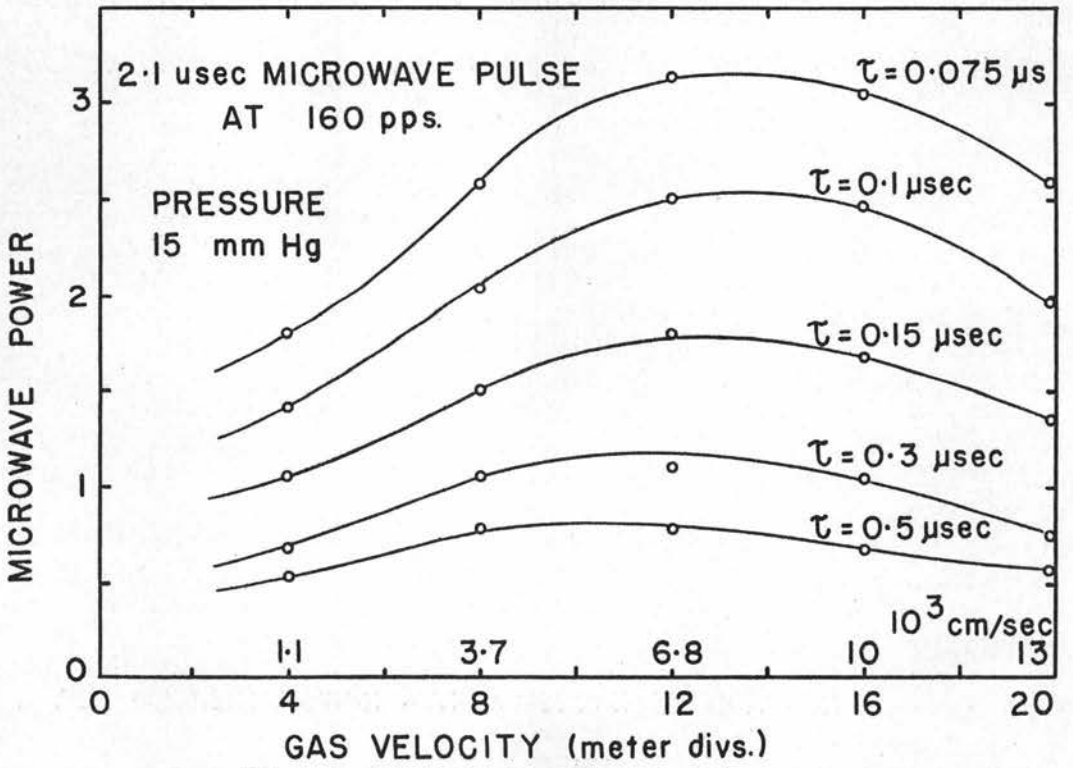

FIGURE 29. MICROWAVE POWER - Vs - GAS VELOCITY

flatter at the higher power levels, (i.e. shorter formative times), and the higher repetition rates. The value of $\bar{U}_1$ for the 1.6 inch contour was less than that obtained with the 2.5 inch contour, suggesting that the shape of the contour may influence the results. Another general observation was that the statistical variation in the formative time of the discharge decreased at the higher gas velocities, when the required power decreased.

The observed results could be explained if it were possible for the gas flow to retain electrons in the contriction gap, at the higher flow rates, rather than removing them. There is a phenomena in hydrodynamics known as "back-flow" which occurs when a fast moving gas stream flows through a diverging channel. The phenomena is due to the inability of the gas to expand laterally as rapidly as the diverging walls, with the result that the gas stream adheres to one of the divergent walls which then creates a low pressure region on the opposite wall. Gas is then caused to "flow-backwards" to fill up the void. Calculations with the 2.5 inch contour (see appendix D) show that at the experimental values of $p\bar{U}_1$ and $p\bar{U}_2$, this flow-back phenomena starts about 1.5 to 2.0 cm from the center of the contour.

An experimental study with fine wires (0.003 inches diameter) freely mounted in the contour showed that the wires started oscillating rapidly at approximately the value of $p\bar{U}_2$. An investigation with the photocell showed that at the high velocity gas flow, the discharge region out to a distance of about 1.8 cm started as soon as the discharge in the center of the constriction, whereas at the low velocity this region only extended out to about 1.1 cm from the center.

When the standing wave was set up in the constriction region, to help localize the discharge, it was found that the power required to produce a discharge in a given formative time did not decrease at the high flow rates (see Section 6). This is in agreement with the back flow phenomena because if there is an antinode at the center of the constriction, the electric field at a distance of 1.5 cm from the center will be very small and the increase in the electron density, due to back flow, will have little effect.

While it is difficult to directly connect the observed gas turbulence with the results of the "power versus flow" experiment, it is felt that the evidence is sufficient to at least relate the two.

Other parameters were considered which could possibly affect the gas flow results but these were either dismissed because of the result of experimentation or because their affect, if any, would be very small. The parameters considered included a possible change in the gas temperature caused by the gas flow (checked by preheating the gas before it entered the constriction region), increased molecular velocity due to the gas flow (a negligible effect), pressure variation across the height of the gap (the theory indicates that the affect, if any, would be opposite to that observed), a variation in the power attenuation caused by the electrons remaining in the gap (ruled out by observation), electrons being swept into the discharge region from an "upstream" discharge (could not observe any discharges in the flow-section prior to the center of the constriction).

The results discussed in this section indicate the difficulties involved in producing an isolated discharge in a given location in the waveguide. With the 3.5 and the 5 inch contour it was impossible to produce a discharge at the center of the constriction in the pressure range of interest (about 5 to 25 mm Hg). This is in conflict with Posin's results (41), for these pressures, if one assumes that he

used the minimum gap width to determine the breakdown electric field from the breakdown power values. The phenomena is explained, however, by the fact that the electron loss by diffusion is very large when the gap width is small. At a slightly larger gap width the electric field is smaller but this is more than compensated for by the decrease in the loss of electrons by diffusion (10, p. 186).

As a result of this experimentation it was decided to use the 2.5 inch contour, for future experiments, as a compromise between the conditions required to minimize back-flow and those required to produce a discharge at the center of the constriction.

6) RESULTS

All the results in this investigation were obtained with oxygen gas. This gas was used instead of a noble gas because the presence of a small quantity of oxygen due to air leaks in the gas system (see Section 7e, part one) would seriously affect the breakdown properties of the noble gas. This is because of the electron affinity of oxygen. By using oxygen as the gas to be examined the small air leaks in the gas system have a negligible effect.

The results to be reported in this section were obtained with the 2.1 microsecond microwave pulse and a repetition rate of 300 pps. A standing wave in the applied electric field was employed with an antinode of the wave located at the center of the constriction. The final data were obtained using the 2.5 inch by 0.90 inch width contour assembly with minimum gap heights of 0.114 cm and 0.214 cm.

A typical set of results is shown in Figure 30 where the power required to produce a steady state pulsed discharge in a given formative time is plotted as a function of the average gas velocity in the constriction region. The results shown are for a gas pressure of 10 mm Hg, and a constriction gap of 0.214 cm. The power is expressed in terms of the recorded microwave power and the power level for a given formative time has been corrected to allow for the shape of the microwave pulse (see Section 6b, part one). The tabulated power may be expressed in terms of an effective electric field from the information given in Sections 3e and 6c, part one.

Despite the precautions taken to avoid the effect of the back-flow phenomena, it was still observed that the variation in the formative time of the discharge decreased at the higher flow rate. The

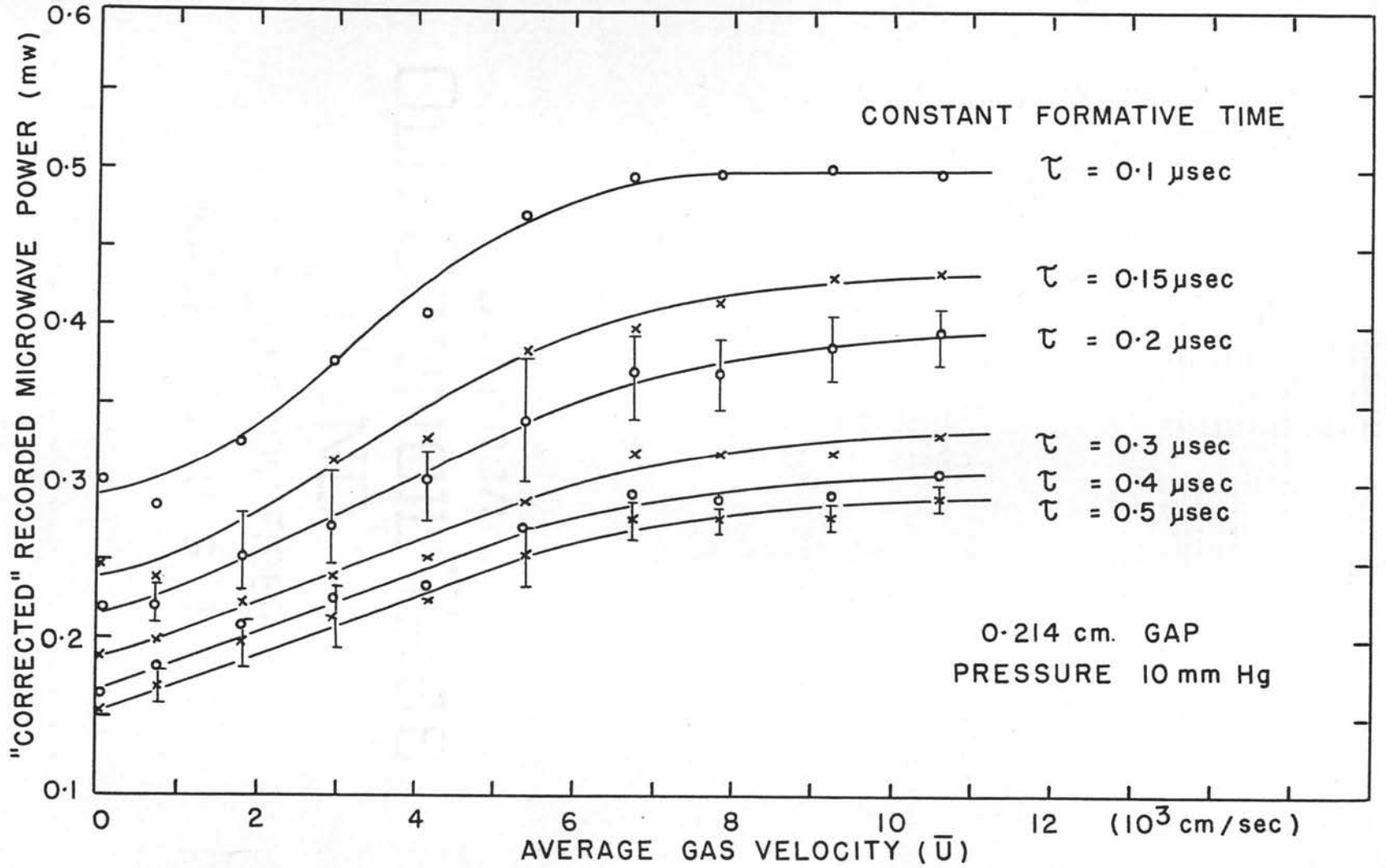

FIGURE 30 . "CORRECTED" RECORDED MICROWAVE POWER - Vs - GAS VELOCITY.

power values at the high flow rates in both the 0.114 cm and the 0.214 cm gap assemblies are about the same as those required to produce a discharge with the same formative time in the standard size waveguide (determined from the results of part one). This indicates that at the higher power levels a discharge is forming in the main waveguide; therefore the available range of the data is limited by the power that can be transmitted in the main waveguide without producing a discharge. An observation made with the aid of a photocell showed that the discharge was still formed at the center of the constriction even at the high flow rates, so presumably the discharge in the main waveguide must form on the side of the constriction farthest away from the microwave source.

The range of the data is also limited by the large variation in the formative time. Even at the low flow rates it was impossible to obtain readings for formative times longer than about 0.5 microseconds.

The experimental results and the theory may be compared either by considering the power necessary to produce the discharge in a given formative time or by considering the change in the formative time for a given power level, both as a function of the gas

velocity. Since it has not been possible to obtain an accurate knowledge of the net frequency of ionization as a function of E_e/p, and hence power, the latter method will be used. However, as mentioned earlier the available range of the formative time is very limited. From the theory of the production of electrons in a gas (see part one), the change in the formative time of a discharge due to a change in the initial electron density, from n_1 to n_2, is given by

$$\Delta\tau = \frac{\ln (n_1/n_2}{p\left[\frac{\nu}{p} - \frac{Dp}{(p\Lambda)^2}\right]}$$

where ν is the net frequency of ionization, D is the electron diffusion coefficient, Λ is the characteristic diffusion length, and p is the gas pressure. In this problem the value of (n_1/n_2) is given by $n_o(O)/n_o(U_m)$ as determined in Section 3. Assuming that the value of D is constant, then the change in the formative time as a function of the gas velocity is given by

$$\Delta\tau\,(U_m) = C\ln\left[\, n_o(O)/n_o(U_m)\,\right]$$

where U_m is the velocity in the center of the constriction gap (i.e. equal to 1.5 times the average velocity), and C is a constant. The theoretical

values of $\Delta\tau$ are obtained from the results given in Figure 22, and the experimental values are obtained from Figure 30. The values of $\Delta\tau$ as a function of gas velocity are given in Figure 31. In order to obtain the theoretical values of $\Delta\tau$ it was necessary to measure the length of the center discharge and assume that this was the length of the discharge region. The measurement was made with aid of the contour which has a plastic strip along its length. The length was approximately 5 mm and this value was used to obtain the theoretical results given in Figure 22.

Several theoretical plots are given in Figure 31 for different values of the constant C. Experimental plots are given for corrected recorded power levels of 0.27 mw, 0.22 mw and 0.19 mw. The experimental curve for the high power level is limited by the discharge forming in the main waveguide. The curves for the lower power levels are limited by the large variation in the formative times. The results for the high power level are in disagreement with the theory by quite a large margin; the difference is in such a direction as to suggest that the electrons are not removed from the discharge region as rapidly as the theory predicts, particularly

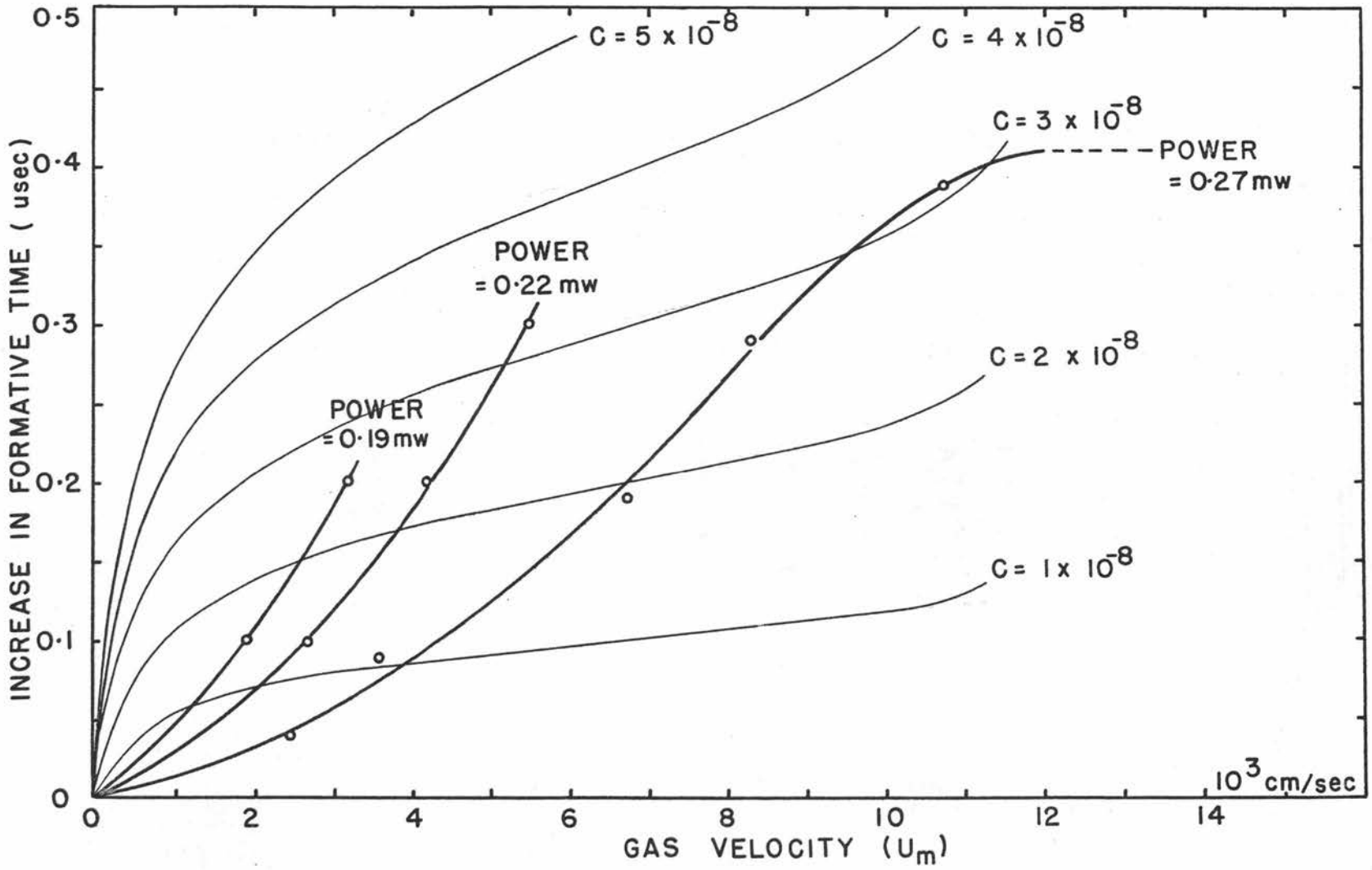

FIGURE 31 INCREASE IN FORMATIVE TIME - Vs - GAS VELOCITY (U_m)

at the low flow rates. The results for the low power level give better general agreement with the theory but the results are too limited to make a true comparison.

A possible explanation for this discrepancy is that the value of the electron diffusion coefficient D may not be a constant throughout the range of the electron densities being considered. If the electron density $n_o(U_m)$ at the beginning of the formation of the discharge is very large, then the value of D would be less than the free electron diffusion coefficient. As the value of $n_o(U_m)$ decreased the value of D would increase. This would make the value of the "constant" C increase with increasing gas velocity. Such a result would be in a agreement with the experimental results.

The experimental results for the different microwave power levels are in general agreement with the theory; that is, as the power level is decreased the value of the net frequency of ionization decreases and the value of C increases.

It is necessary to show that the values of C given in Figure 31 are at least of the correct order of magnitude. At a microwave power of 0.3 mw, with the 2.1 microsecond pulse and a repetition rate of

300 pps, the peak value of the electric field in the center of the 0.214 cm gap is 2400 volt/cm. At a gas pressure of 10 mm Hg, the value of E_e/p is 82 volts (cm mm Hg)$^{-1}$. The free electron diffusion coefficient for this value of E_e/p is given by $Dp = 3.3 \times 10^6$ mm Hg cm^2/sec (see Section 3g, part one). An approximate value of the net frequency of ionization, divided by the pressure, for this value of E_e/p is 1.5×10^7 (sec mm Hg)$^{-1}$. With these values, the value of the constant C is 1.2×10^{-8} sec. This is of the same order of magnitude as the values plotted on Figure 31.

If the initial breakdown of the gas is caused by a large number of electrons being produced by a single microwave pulse, then the theory indicates that the gas flow should have no effect on the power required to produce the initial breakdown of the gas because of the short periods of time involved. An experimental investigation was made to confirm this. A one-millicurie Cobalt 60 radioactive source was placed next to the contour assembly to produce a copious supply of primary electrons in the discharge region. The experimental procedure was to set the microwave power level at a constant value and then wait to see whether breakdown occured. With the

radioactive source present, the breakdown power is quite a distinct value. For example, with the 0.114 cm gap at 20 mm Hg pressure and zero gas flow, the discharge "flicks" on and off every few seconds at a power level of 0.155 mw but stays "on" continuously at a power level of 0.165 mw. Without the radioactive source the statistical variation in the required power is very large. The power required to produce breakdown without the radioactive source is about four or five times that required when the source is present.

The results of the above experiment showed that when using pulsed microwave power, the power required to produce the initial breakdown increased with increasing gas flow. At first this appears to be in conflict with the theory but care must be exercised when interpreting the results of this experiment. In order to determine the true effect of the gas flow during the formation of the discharge it is necessary to use a single microwave pulse, otherwise the effect of the gas flow is to change the electron density remaining from the preceding pulses and not to change the rate of build-up of the electron density during the formation of the discharge. When the dielectric breakdown of a gas by pulsed power is being considered

it is reasonable to consider the accumulative effect of the gas flow, whether the effect be during the formation of the discharge or during the period between the microwave pulses. From the time the pulsed power is first applied to the discharge region the electron density is continually building up in the duration of the microwave pulse, and decaying in the period between the pulses until finally the critical electron density for breakdown is attained. When a gas flow is present the decay rate of the electron density is increased and must be compensated for, if breakdown is to occur, by increasing the rate of formation. This is accomplished by increasing the applied field and hence the net frequency of ionization. The above experiment showed that the initial breakdown power, with the radioactive source present, is approximately the same as the "extinction power", which is defined as the power necessary to just maintain a steady state discharge. This is reasonable since in both cases the power must be sufficient to just form the discharge in the duration of the microwave pulse. The general shape of the curves of the "breakdown power - versus - gas flow" are similar to those shown in Figure 30. Once again the power values at the higher flow rates are

limited by the breakdown in the main waveguide. A set of results of the initial breakdown power (or extinction power), expressed in terms of E_e/p, as a function of the average gas velocity in the constriction region is shown in Figure 32. The results are for the 0.114 cm gap at a gas pressure of 20 mm Hg, and for the 2.1 microsecond pulse at a repetition rate of 300 pps.

7) CONCLUSIONS

It has been demonstrated that a directed gas flow has a pronounced effect on the dielectric breakdown of oxygen when using pulsed microwave power. It appears evident that the effect is due to the removal of electrons from the discharge region in the period between the microwave pulses. There is a discrepancy between the theory, developed for this investigation, and the experimental results which can be explained if the value of the effective electron diffusion coefficient increases with increasing gas flow. Such a variation would be caused by the decrease in the electron density, and could be verified if the value of the electron density could be determined. Another explanation for the discrepancy is that the electrons may not be removed from the discharge region at the low gas flow as

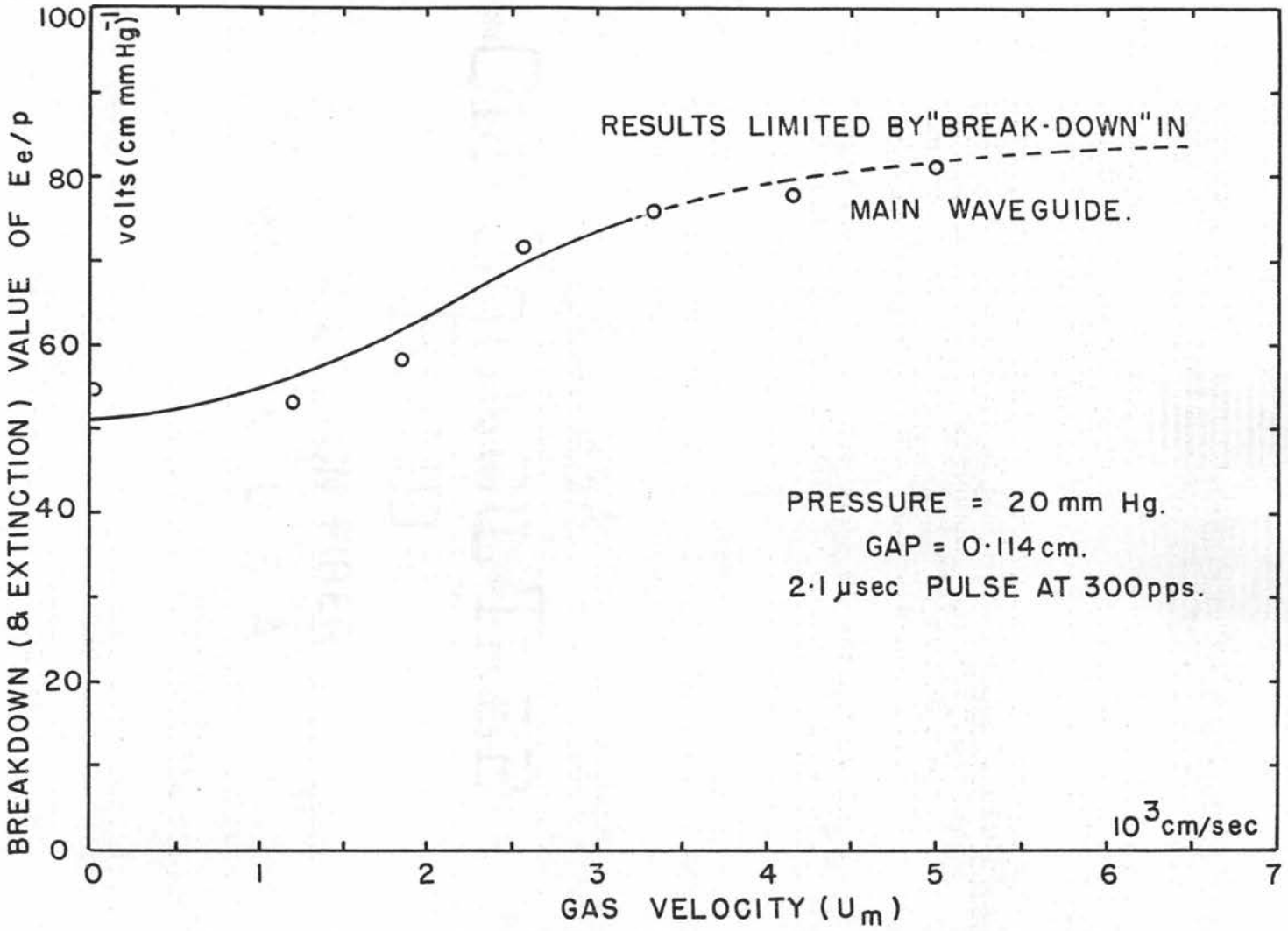

FIGURE 32. BREAKDOWN VALUE OF E_e/p – Vs – GAS VELOCITY (U_m)

rapidly as expected. The theory has been developed on some very simple assumptions and it is quite evident that a much more sophisticated theory is needed.

In Section 2 the question was raised as to whether electrons produced by discharges from preceding microwave pulses would be retained in the boundary layer around the antenna of a high-speed vehicle. The experimental results of this investigation show that even at moderately low velocities there is quite a large change in the initial breakdown power; this suggests that the gas flow must almost completely remove the electrons from the discharge region. Therefore, in the case of a high-speed vehicle the electrons from preceding discharges will most certainly be removed by the air flow. The initial electron density, for any discharge that may form, will therefore be the ambient density in the atmosphere or that produced by the friction between the vehicle and the atmosphere.

The results from the investigation of the reflected and transmitted microwave pulses and the associated light pulses connected with the discharge formed in the constriction region show that care must be taken when interpreting the shape of these pulses.

In particular the shape of the light pulse is very dependent on the presence of "unknown" discharges that may be formed between the discharge being examined and the microwave source.

The difficulties encountered in producing a single discharge at the center of the constriction region suggest that the results of Posin's experiment (41, p. 496-509) may be in error for the values at the low gas pressures.

Many of the experimental difficulties encountered in this investigation are the result of flowing the gas through the same tube as the microwave power is transmitted. These difficulties would be removed if the discharge could be isolated to a given section of the flow tube without the use of a constricted waveguide. This would be possible if the discharge were formed inside of a cavity. The experimental arrangement would be to flow the gas in a quartz tube which passes through the cavity. A cavity could also be used to measure the electron density in the gas stream. Such a measurement would give an indication as to whether the electron diffusion coefficient is likely to change with increasing gas flow (i.e. due to the decrease in the electron density). A similar arrangement has been used by

Benson (4) to measure the electron densities in a stream of ionized nitrogen. An idealized theory for the effect of a gas flow on a steady state continuous discharge in a cavity has already been given by Romig (45) and could be applied to this problem.

BIBLIOGRAPHY

1. Allis, W. P. Motion of ions and electrons. In: Encyclopedia of Physics, vol. 21. Berlin, Springer-Verlag, 1956. p 383-444.

2. Allis, W. P. and David J. Rose. The transition from free to ambipolar diffusion. Physical Review 93: 84-93. 1954.

3. Anderson, J. M. and L. Goldstein. Interaction of electromagnetic waves of radio-frequency in isothermal plasmas: Collision cross section of helium atoms and ions for electrons. Physical Review 100:1037-1046. 1955.

4. Benson, James M. Measurement of the physical properties of active nitrogen. Journal of Applied Physics 23:757-763. 1952.

5. Biondi, Manfred A. Attachment of thermal electrons in oxygen. (Abstract). Physical Review 84:1072. 1951.

6. Biondi, Manfred A. Electron attachment and collision frequencies in oxygen and nitrogen. In: Ionization phenomena of gases, Proceedings of the Fourth International Conference, Uppsala 1959. vol. 1. Amsterdam, North-Holland Publishing Company, 1960. IA 72 - IA 78.

7. Born, Max and Emil Wolf. Principles of optics. New York, Pergamon Press, 1959. 803p.

8. Bröse, H. L. The motion of electrons in oxygen. Philosophical Magazine, 6th ser. 50:536-546. September 1925.

9. Brown, Sanborn C. Breakdown in gases:Alternating and high-frequency fields. In: Encyclopedia of Physics, vol. 22. Berlin, Springer-Verlag, 1956. p 531-575.

10. Brown, Sanborn C. Basic data of plasma physics. Cambridge, Mass., Technology Press of the Massachusetts Institute of Technology, 1959. 336p.

11. Burch, David S. and Ronald Geballe. Ionic drift velocities and electron attachment coefficients in oxygen. Physical Review 106:183-187. 1957.

12. Chen, C. L., C. C. Leiby and L. Goldstein. Electron temperature dependence of the recombination coefficient in pure helium. Physical Review 121: 1391-1400. 1961.

13. Craggs, J. D. Some experiments on negative ions in gases. In: Ionization phenomena in gases, Proceedings of the Third International Conference, Venice 1957. Venice, Giorgio Cini, 1957. p 203-214.

14. Craggs, J. D., R. Thorburn and B. A. Tozer. Attachment of slow electrons in oxygen. Proceedings of the Royal Society, London, Series A, 240:473-483. July 16, 1957.

15. Desloge, Edward A., Steven W. Matthysse and Henry Margenau. Conductivity of plasmas to microwaves. Physical Review 112:1437-1440. 1958.

16. Goodwin, J. D. Ph.D. Thesis University of Birmingham. Cited in: Craggs, J. D., R. Thorburn and B. A. Tozer. Attachment of slow electrons in oxygen. Proceedings of the Royal Society, London, Series A, 240:473-483. July 16, 1957.

17. Gould, Lawrence and Louis W. Roberts. Breakdown of air at microwave frequencies. Journal of Applied Physics 27:1162-1170. 1956.

18. Emmons, Howard W. (ed.). High speed aerodynamics and jet propulsion. vol. 3. Fundamentals of gas dynamics. Princeton, New Jersey. Princeton University Press, 1958. 749p.

19. Harrison, Melvin A. and Ronald Geballe. Simultaneous measurement of ionization and attachment coefficients. Physical Review 91:1-7. 1953.

20. Healey, R. H. and J. W. Reed. The behaviour of slow electrons in gases. Sydney, Amalgamated Wireless (Australasia) Limited, 1941. 179p.

21. Herlin, Melvin A. and Sanborn C. Brown. Breakdown of a gas at microwave frequencies. Physical Review 74:291-296. 1948.

22. Herlin, Melvin A. and Sanborn C. Brown. Electrical breakdown of a gas between coaxial cylinders at microwave frequencies. Physical Review 74:910-913. 1948.

23. Herlin, Melvin A. and Sanborn C. Brown. Microwave breakdown of a gas in a cylindrical cavity of arbitrary length. Physical Review 74:1650-1656. 1948.

24. Herreng, Pierre. Drift velocity of electrons in oxygen. Cahiers de Physique 38:6-16. 1952.

25. Kelly, Donald and Henry Margenau. High-frequency breakdown of air. Journal of Applied Physics 31:1617-1620. 1960.

26. Kestin, J. Viscosity of gases. In: American Institute of Physics Handbook. New York, McGraw-Hill, 1957. Section 2, p 201-210.

27. Kuethe, A. M. and J. D. Schetzer. Foundations of aerodynamics. New York, Wiley, 1950. 374p.

28. Lindsay, Robert. Density of gases at standard temperature and pressure. In: American Institute of Physics Handbook. New York, McGraw-Hill, 1957. Section 2, p 197-201.

29. Loeb, Leonard B. Basic processes of gaseous electronics. Berkeley, University of California, 1955. 1012p.

30. MacDonald, A. D. High frequency breakdown in air at high altitudes. Proceedings of the Institute of Radio Engineers 47:436-441. 1959.

31. MacDonald, A. D. and Sanborn C. Brown. High-frequency gas discharge breakdown in helium. Physical Review 75:411-418. 1949.

32. MacDonald, A. D. and Sanborn C. Brown. High-frequency gas discharge breakdown in hydrogen. Physical Review 76:1634-1639. 1949.

33. MacDonald, A. D. and J. H. Matthews. High-frequency ionization coefficient in neon-argon mixtures. Physical Review 98:1070-1073. 1955.

34. Madan, M. P. et al. Determination of the coefficient of diffusion and frequency of ionization in microwave discharges. Physical Review 106:839-843. 1957.

35. Margenau, Henry. Theory of high-frequency gas discharges. IV. Note on the similarity principle. Physical Review 73:326-328. 1948.

36. Millsaps, Knox and Karl Pohlhausen. Thermal distribution in Jeffery-Hamel flows between non-parallel plane walls. Journal of Aeronautical Sciences 20:187-196. 1953.

37. Oskam, H. J. High-frequency gas discharge breakdown in neon-argon mixtures. Journal of Applied Physics 27:848-853. 1956.

38. Panofsky, Wolfgang K. H. and Melba Phillips. Classical electricity and magnetism. Reading, Mass., Addison-Wesley, 1955. 400p.

39. Persson, K. B. Limitations of the microwave cavity method of measuring electron densities in a plasma. Physical Review 106:191-195. 1957.

40. Platzman, Philip M. and Elsa Huber Solt. Microwave breakdown of air in nonuniform electric field. Physical Review 119:1143-1149. 1960.

41. Posin, D. Q. The microwave spark. Physical Review 73:496-509. 1948.

42. Prasad, A. N. and J. D. Craggs. Measurement of Townsend's ionization coefficients and attachment coefficients in oxygen. Proceedings of the Physical Society, London, 77(2):385-398. February 1, 1961.

43. Present, R. D. Kinetic theory of gases. New York, McGraw-Hill, 1958. 280p.

44. Raytheon Company. Raytheon Technical Information. Type 725-A pulsed-type magnetron oscillator. Waltham, Mass. 1958. 5p.

45. Romig, Mary F. Steady state solutions of the radio frequency discharge with flow. The Physics of Fluids 3:129-133. 1960.

46. Rose, David J. and Sanborn C. Brown. High-frequency gas discharge plasma in hydrogen. Physical Review 98:310-316. 1955.

47. Schlichting, Hermann. Boundary layer theory. Translated by J. Kestin. 4th ed. New York, McGraw-Hill, 1960. 647p.

48. Schlumbohm, Hans. A method for determining the ionization coefficient by the statistics of avalanches. In: Ionization phenomena in gases, Proceedings of the Fourth International Conference, Uppsala 1959. vol. 1. Amsterdam, North-Holland Publishing Company, 1960. IB 127-IB 130.

49. Sexton, M. C. and J. D. Craggs. Recombination in the afterglows of argon and helium using microwave techniques. Journal of Electronics and Control, London 4(6):493-502. June 1958.

50. Sexton, M. C., J. J. Lennon and M. J. Mulcahy. Microwave method of investigating the afterglow of pulsed gaseous discharges. British Journal of Applied Physics 10:356-359. August 1959.

51. Sexton, M. C., M. J. Mulcahy and J. J. Lennon. Electron removal processes in the afterglows of microwave discharges in argon and oxygen. In: Ionization phenomena in gases, Proceedings of the Fourth International Conference, Uppsala 1959. Vol. 1. Amsterdam, North-Holland Publishing Company, 1960. IA 94-IA 98.

52. Spitzer, Lyman. Physics of fully ionized gases. New York, Interscience Publishers, 1956. 105p.

53. Talbot, L. Laminar swirling pipe flow. Journal of Applied Mechanics 21:1-7. 1954.

54. Varnerin, Lawrence J. Jr. and Sanborn C. Brown. Microwave determinations of average electron energies and the first Townsend coefficient in hydrogen. Physical Review 79:946-951. 1950.

55. Varney, Robert N. Drift velocity of ions in oxygen, nitrogen and carbon monoxide. Physical Review 89:708-711. 1953.

APPENDIX

Appendix A

EXPERIMENTAL PLOTS OF THE "FORMATIVE TIME -VS-MICROWAVE POWER" FOR DIFFERENT REPETITION RATES.

(Figures 33 to 44)

This data is referred to in part-one (see page 62) and was used to evaluate the net frequency of ionization of oxygen. The dimension and pressure given in the upper right hand corner of each graph is the height of the discharge chamber and the pressure at which the experiment was performed. The curves on a given figure are for different microwave pulse repetition rates and the letters A, B, C, D and E are for repetition rates of 250, 300, 350, 400 and 450 pps respectively.

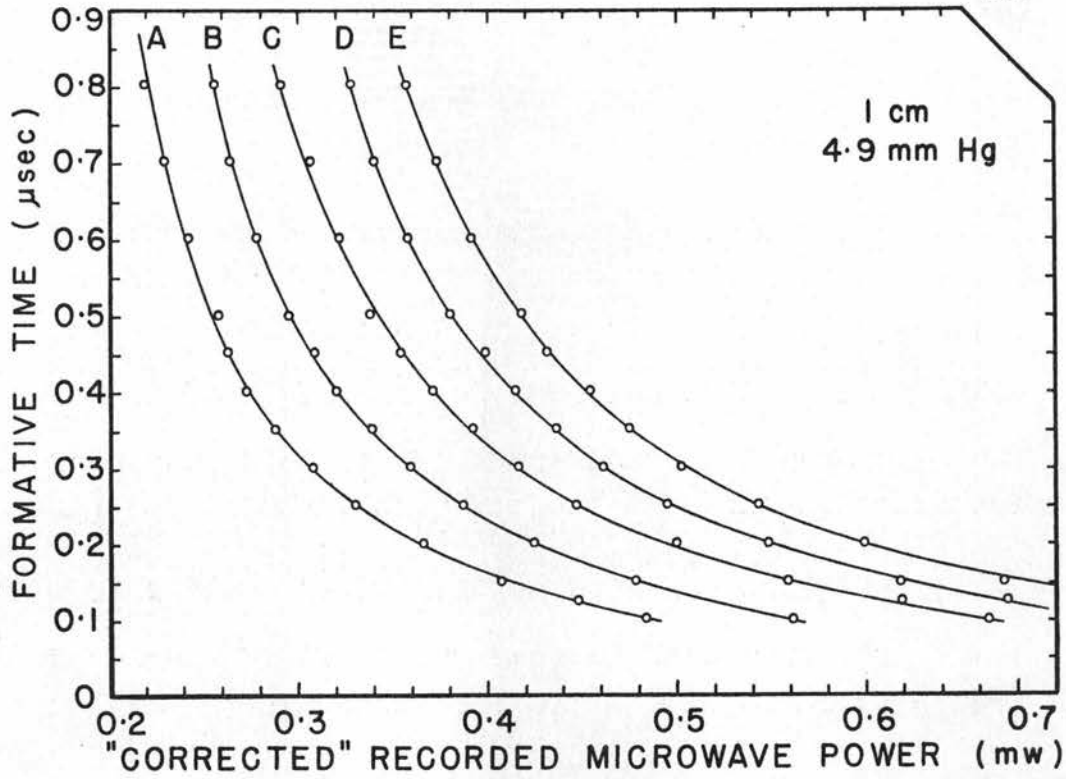

FIGURE 33

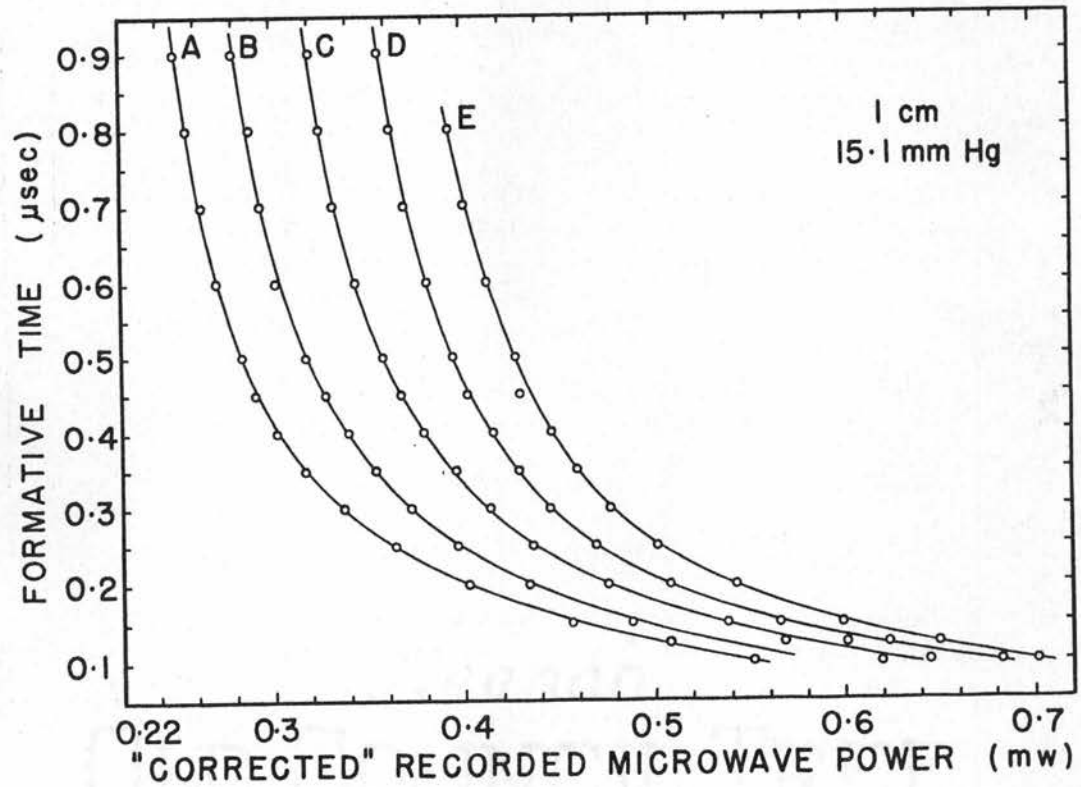

FIGURE 34

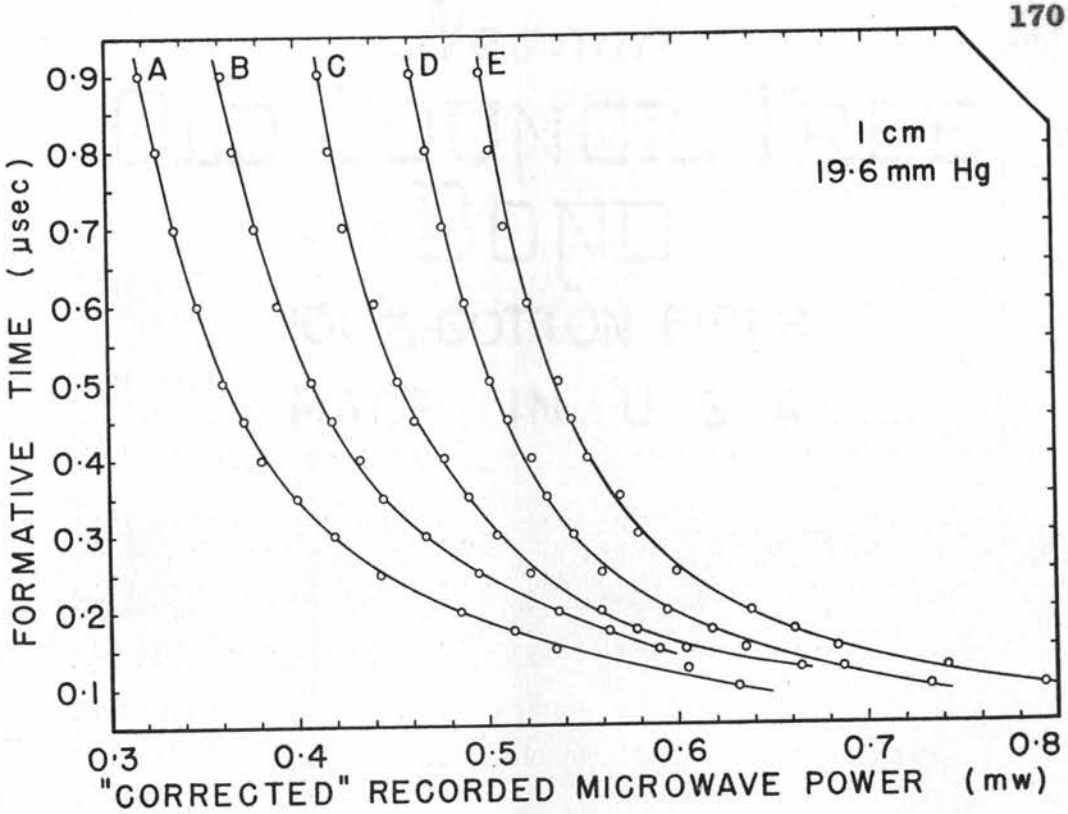

FIGURE 35

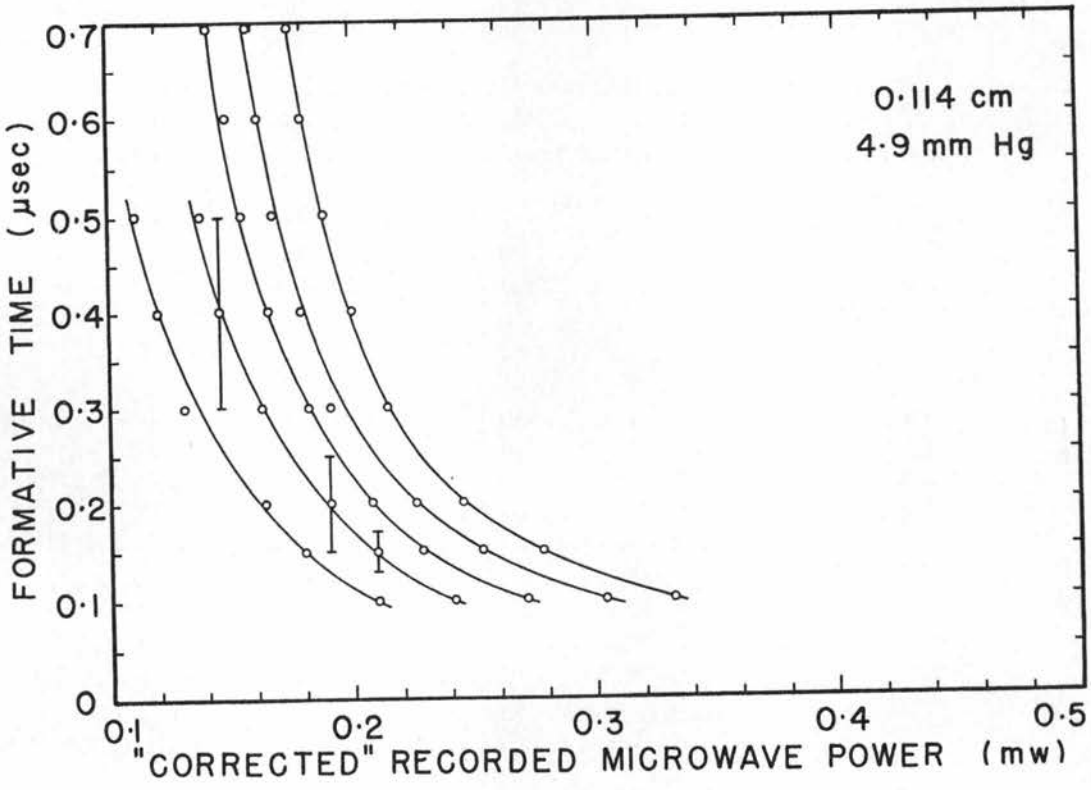

FIGURE 36

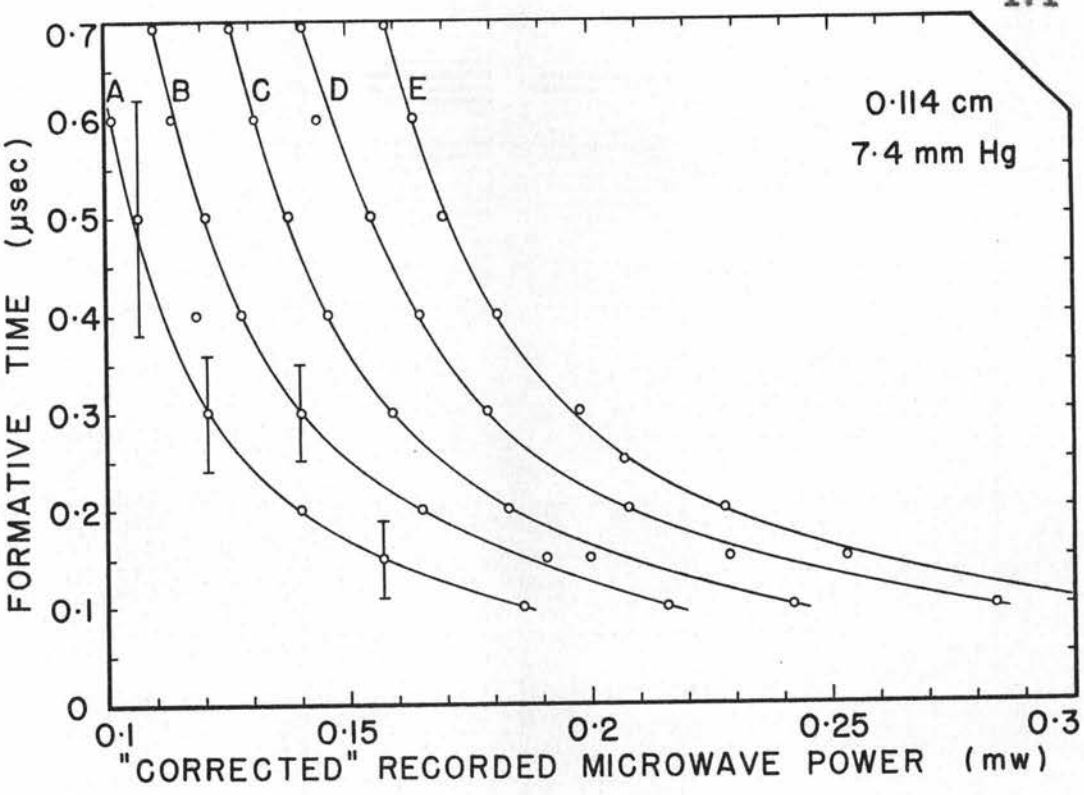

FIGURE 37

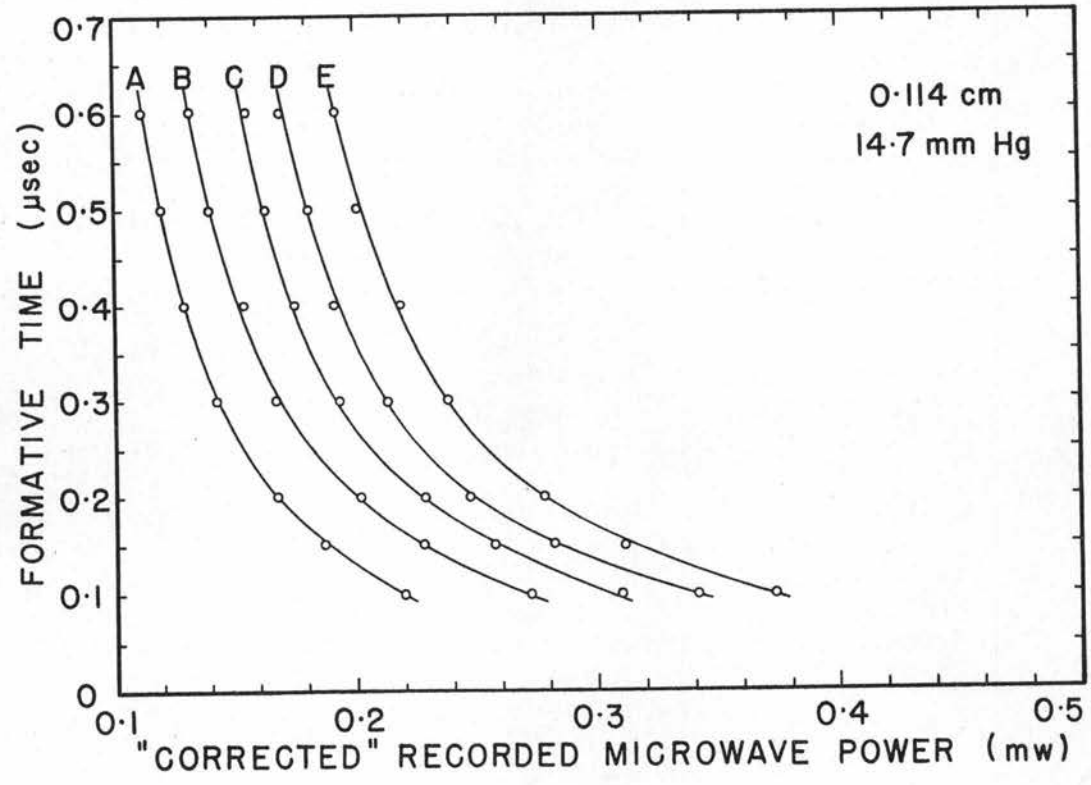

FIGURE 38

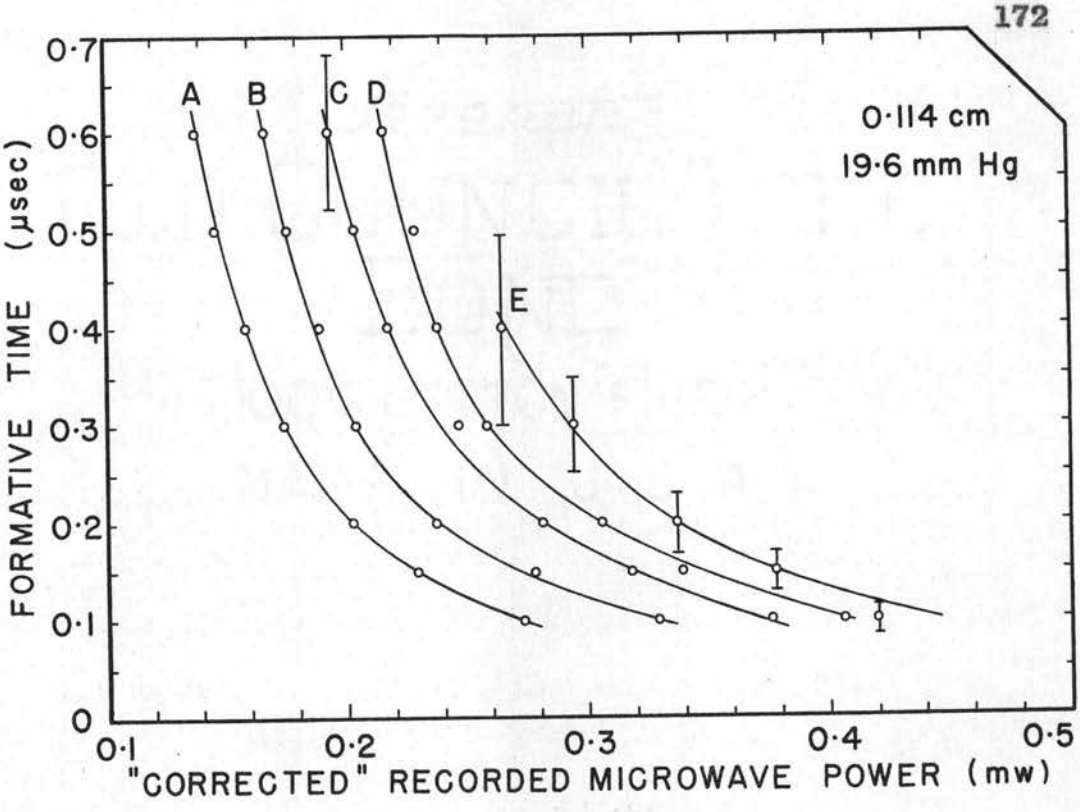

FIGURE 39

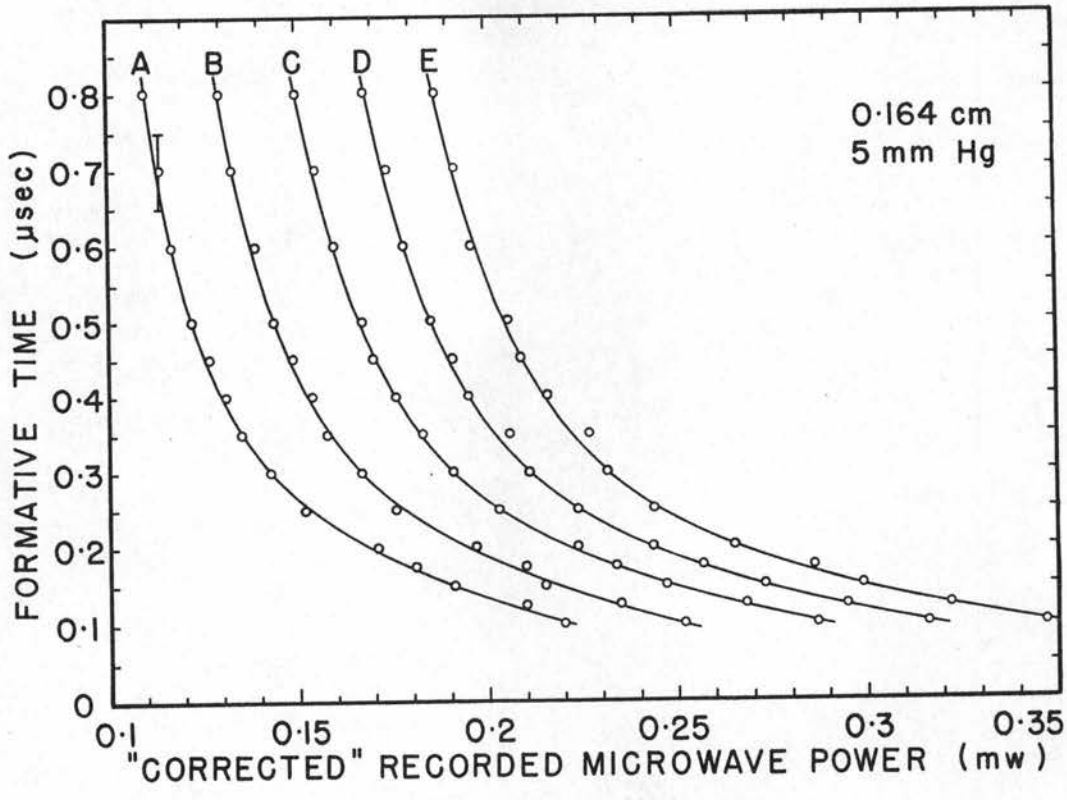

FIGURE 40

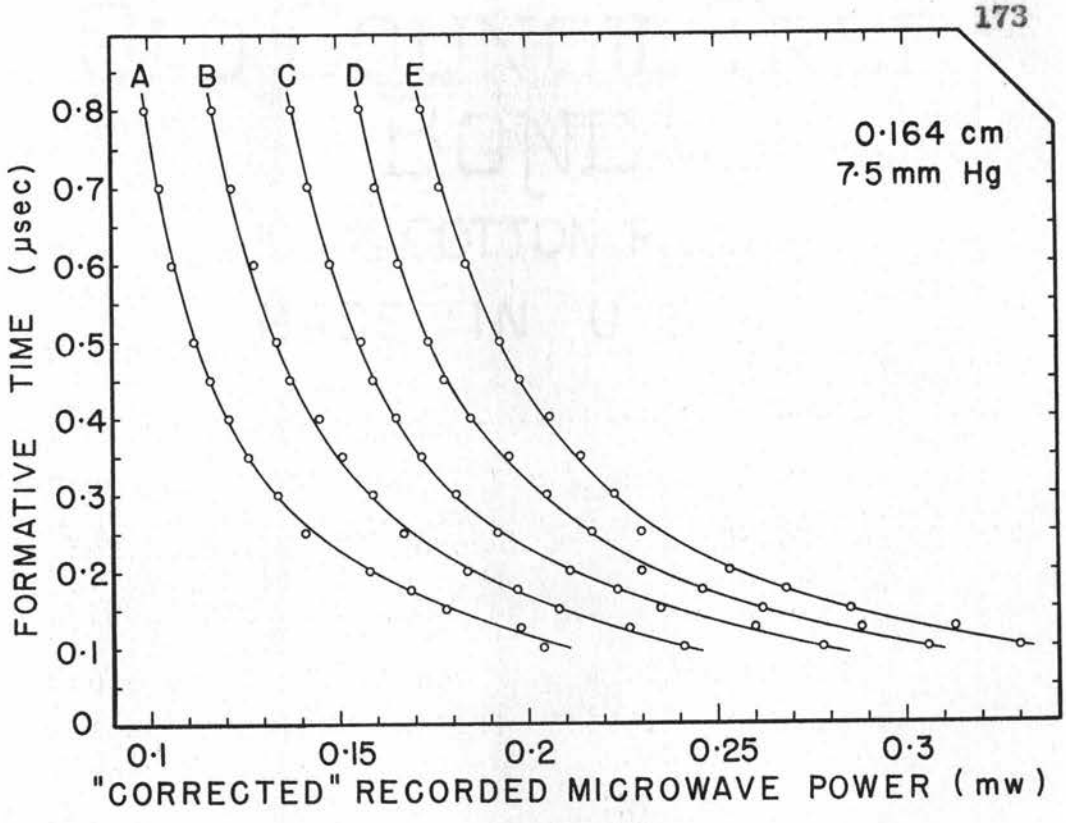

FIGURE 41

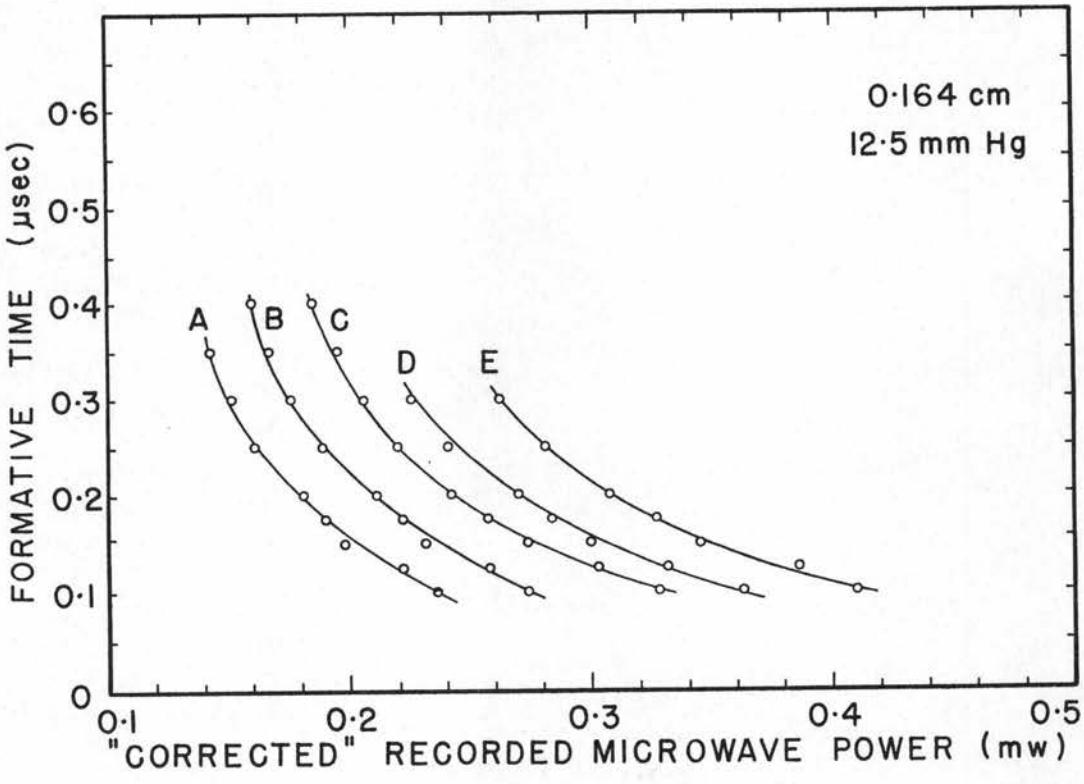

FIGURE 42

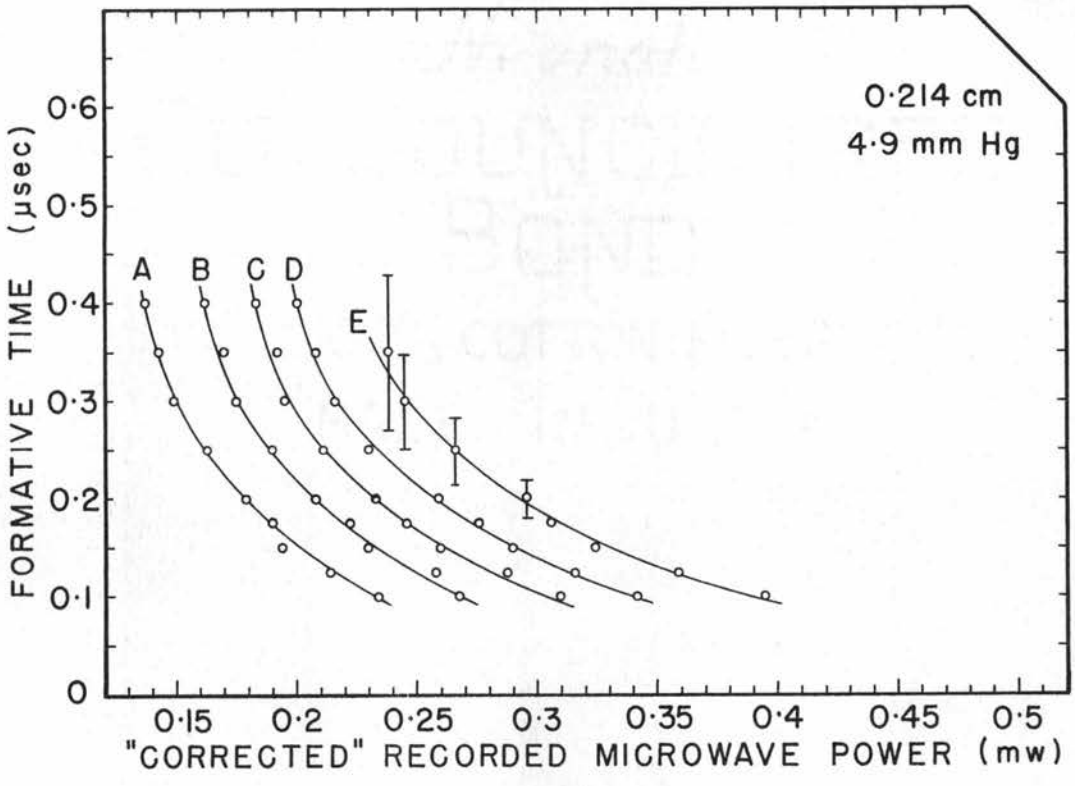

FIGURE 43

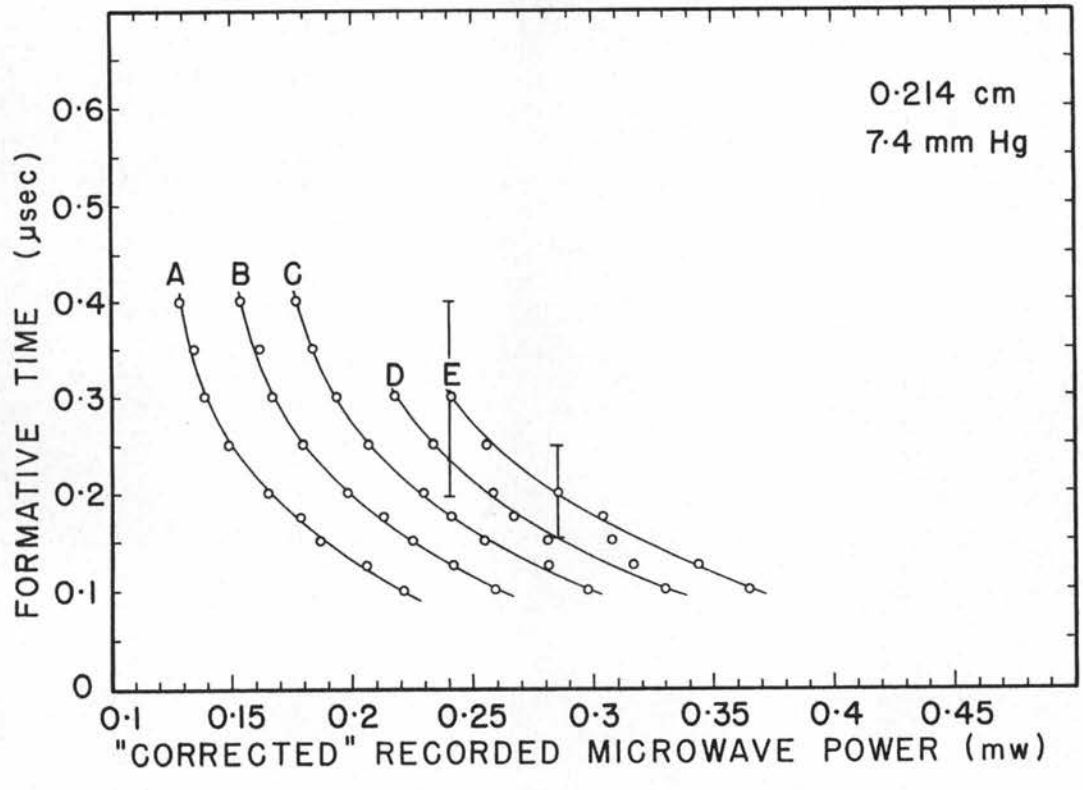

FIGURE 44

Appendix B

CALCULATIONS FOR THE VALUE OF $n_o(U_m)/n_o(O)$

The calculations are based on three assumptions. First it is assumed that the electron density decays to a cosine distribution across the constriction gap with a maximum value of $n_o(O)$ at the center. Then it is assumed that the center region of the electron density configuration is removed by the gas flow. Finally, it is assumed that the remaining electrons diffuse across the constriction gap to produce a uniform distribution $n_o(U_m)$.

Let L be the length of the discharge region and T be the time between the microwave pulses. The velocity distribution of the gas flow is given by

$$U'(y) = (4U_m/a)\ (y - y^2/a + l')$$

where l' is the mean free path of the gas, a is the height of the constriction gap and y is a distance measured from the wall of the chamber. The velocity necessary to sweep the electrons out of the discharge region is given by $U(T) = L/T$. The maximum thickness of the electron sheath d after time T is given by

$$2d/a = 1 - (1 - U(T)/U_m + 4\ l'/a)^{1/2}$$

The length z of the electron sheath at a position y is given by $z = L - U'(y)T$. Therefore, the number of electrons N remaining in each sheath of electrons is

$$N = n_o(0)\ (db) \int_o^d \sin\ (y\pi/a).(L - U'(y)T).dy$$

where (db) is the width of an elementary strip of the electron sheath. Dividing this quantity by the volume (db) La/2 we obtain the required density $n_o(U_m)$. Evaluating this integral and including terms up to $\left[U(T)/U_m \right]^3$ we obtain

$$\frac{n_o(U_m)}{n_o(0)} = \frac{U(T)^3}{U_m^3} + \frac{2U(T)^2}{U_m^2} - 8\ \frac{U(T)}{U_m}\ \frac{1'}{a} - 32\ \frac{1'^2}{a^2}$$

A plot of this function for the values L = 0.5 cm, T = 1/300 sec, a = 0.214 cm and for a gas pressure of 10 mm Hg is given in Figure 22.

Appendix C

SHAPE OF THE CONTOURS

The different contours have been referred to in this dissertation by their length from the narrowest part of the constriction out to the point where the full width of the waveguide is attained. A brief description of the shape of the contour is given here. The equation for the shape of each curve is given under each heading; all the dimensions are in inches. A graphical representation of the curves is given in Figure 45.

5 inch contour by 0.04 inch gap. This was designed to have a maximum slope of 0.1. The equation for the curve is

$$y = 0.02 + 0.0081\ (e^{x} - 1)$$

3.5 inch contour by 0.04 inch gap.

$$y = 0.02 + 0.0294\ x^{2}$$

2.5 inch contour by 0.04 inch gap (final gap size=0.114cm).

$$y = 0.02 + 0.0576\ x^{2}$$

2.5 inch contour by 0.06 inch gap (final gap size=0.164cm). Used one of the 0.04 inch and one of the 0.08 inch contours.

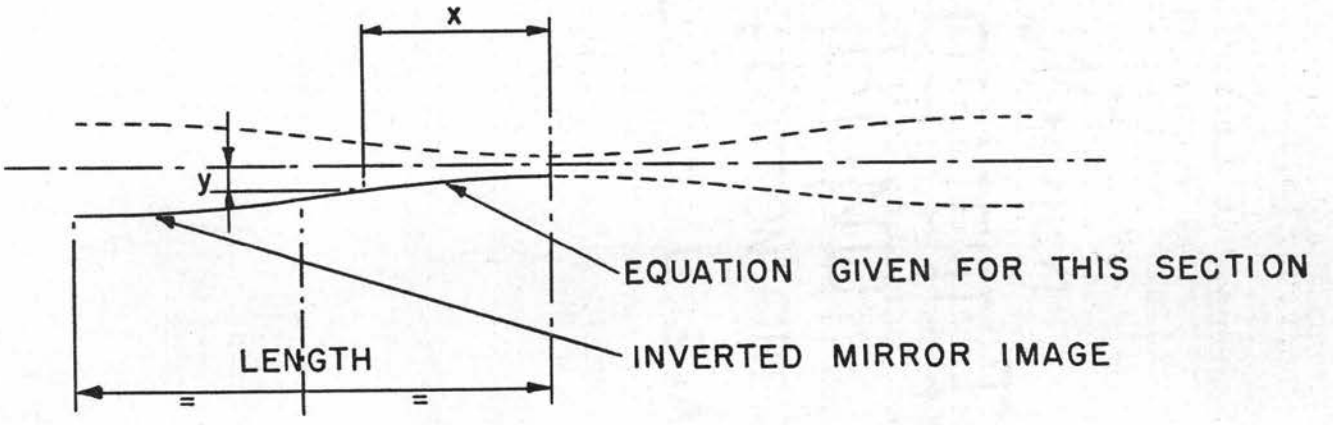

FIGURE 45 SHAPE OF CONTOUR

2.5 inch contour by 0.08 inch gap (final gap size=0.214cm).

$$y = 0.04 + 0.0512\ x^2$$

1.6 inch contour by 0.04 inch gap.

$$y = 0.02 + 0.1411\ x^2$$

The contours were made by first machining a prescribed series of steps (each about 0.002 inches deep), removing the steps with a fine file and then finishing the surface with a 400-grit carborundum powder. The width of the contours was made to be a push-fit into the constriction assembly (see Figure 27).

Appendix D

BACK-FLOW PHENOMENA

The velocity profile of a gas flow in a divergent straight-wall channel has been determined in general terms by Millsaps and Pohlhausen (36). Their results show that in a divergent channel with an included angle of 10^{o} the velocity profile "breaks down" at a critical Reynolds number of 1340, and the gas velocity at one of the walls of the channel reverses its direction. (Theoretically it should occur at both walls simultaneously). As before the Reynolds number is given by $R = \rho U_m d/\mu$ where in this case U_m is the gas velocity at the center of the cone (i.e. the maximum velocity of the profile) and the characteristic length d is the distance from the point of the cone (i.e. where the two walls originate from) to the point of interest.

At a distance of 2 cm from the center-line of the constriction region, the 2.5 inch contour with the 0.114 cm gap may be represented as a divergent channel of 10^{o} with the point of the "cone" being 0.5 cm from the center-line of the constriction. Using the relation $\bar{U} = U_m\ 2/3$ and the values for ρ and μ as given in Section 3b, we obtain the relation $R = 0.013\ p\bar{U}d$. Therefore, from the

above critical value of R we see that "back-flow" will occur at a value given by

$$p\bar{U}d = 1 \times 10^5 \text{ mm Hg cm}^2/\text{sec}$$

The average experimental values of $p\bar{U}_1$ and $p\bar{U}_2$ are 7×10^4 and 1×10^5 mm Hg cm/sec, respectively. At these values of $p\bar{U}$ the theory indicates that the back-flow phenomena should occur at a value of d = 1 to 1.5 cm; or about 1.5 to 2.0 cm from the center of the constriction. The theory indicates that the back-flow phenomena will occur at a smaller value of $p\bar{U}$ for a more divergent channel (i.e. such as in a steeper, and hence shorter, contour).